

Award Number: W81XWH-08-2-0061

TITLE: Advanced MRI in Blast-related TBI

PRINCIPAL INVESTIGATOR: David L. Brody

CONTRACTING ORGANIZATION: Washington University
St. Louis, Mo 63110

REPORT DATE: July 2012

TYPE OF REPORT: Revised Final

PREPARED FOR: U.S. Army Medical Research and Materiel Command
Fort Detrick, Maryland 21702-5012

DISTRIBUTION STATEMENT: Approved for Public Release;
Distribution Unlimited

The views, opinions and/or findings contained in this report are those of the author(s) and should not be construed as an official Department of the Army position, policy or decision unless so designated by other documentation.

REPORT DOCUMENTATION PAGE			<i>Form Approved</i> <i>OMB No. 0704-0188</i>		
Public reporting burden for this collection of information is estimated to average 1 hour per response, including the time for reviewing instructions, searching existing data sources, gathering and maintaining the data needed, and completing and reviewing this collection of information. Send comments regarding this burden estimate or any other aspect of this collection of information, including suggestions for reducing this burden to Department of Defense, Washington Headquarters Services, Directorate for Information Operations and Reports (0704-0188), 1215 Jefferson Davis Highway, Suite 1204, Arlington, VA 22202-4302. Respondents should be aware that notwithstanding any other provision of law, no person shall be subject to any penalty for failing to comply with a collection of information if it does not display a currently valid OMB control number. PLEASE DO NOT RETURN YOUR FORM TO THE ABOVE ADDRESS.					
1. REPORT DATE July 2012		2. REPORT TYPE Revised Final		3. DATES COVERED 1 September 2008- 30 June 2012	
4. TITLE AND SUBTITLE Advanced MRI in Blast-related TBI			5a. CONTRACT NUMBER		
			5b. GRANT NUMBER W81XWH-08-2-0061		
			5c. PROGRAM ELEMENT NUMBER		
6. AUTHOR(S) David L. Brody			5d. PROJECT NUMBER		
			5e. TASK NUMBER		
			5f. WORK UNIT NUMBER		
7. PERFORMING ORGANIZATION NAME(S) AND ADDRESS(ES) Washington University St. Louis, Mo 63110			8. PERFORMING ORGANIZATION REPORT NUMBER		
9. SPONSORING / MONITORING AGENCY NAME(S) AND ADDRESS(ES) U.S. Army Medical Research and Materiel Command Fort Detrick, Maryland 21702-5012			10. SPONSOR/MONITOR'S ACRONYM(S)		
			11. SPONSOR/MONITOR'S REPORT NUMBER(S)		
12. DISTRIBUTION / AVAILABILITY STATEMENT Approved for Public Release; Distribution Unlimited					
13. SUPPLEMENTARY NOTES					
14. ABSTRACT The purpose of the research effort was to test two advanced MRI methods, DTI and resting-state fMRI, in active-duty military blast-related TBI patients acutely after injury and correlate findings with TBI-related clinical outcomes 6-12 months later. The goal was to determine whether these methods may add clinically useful predictive information following traumatic brain injury that could be of assistance in standardizing diagnostic criteria for TBI, making return-to-duty triage decisions, guiding post-injury rehabilitation, and developing novel therapeutics. The overarching hypothesis guiding this project is that traumatic axonal injury is a principal cause of impaired brain function following blast-related TBI.					
15. SUBJECT TERMS- none provided					
16. SECURITY CLASSIFICATION OF:			17. LIMITATION OF ABSTRACT UU	18. NUMBER OF PAGES	19a. NAME OF RESPONSIBLE PERSON USAMRMC
a. REPORT U	b. ABSTRACT U	c. THIS PAGE U			19b. TELEPHONE NUMBER (include area code)

Table of Contents

	<u>Page</u>
Introduction.....	4
Body.....	4
Reportable Outcomes.....	17
Personnel Supported.....	17
Conclusion.....	17
Appendicies.....	18

Introduction:

The purpose of the research effort was to test two advanced MRI methods, DTI and resting-state fMRI, in active-duty military blast-related TBI patients acutely after injury and correlate findings with TBI-related clinical outcomes 6-12 months later. The goal was to determine whether these methods may add clinically useful predictive information following traumatic brain injury that could be of assistance in standardizing diagnostic criteria for TBI, making return-to-duty triage decisions, guiding post-injury rehabilitation, and developing novel therapeutics. The overarching hypothesis guiding this project is that traumatic axonal injury is a principal cause of impaired brain function following blast-related TBI.

Body:

Overall the study was successful from a logistical and scientific perspective.

The major technical and logistical accomplishments were as follows:

- 1) We obtained all required IRB approvals.
- 2) We enrolled a total of 104 US military personnel with blast-related TBI and 21 controls with other injuries and illness at Landstuhl regional medical center. Prior to starting the study, there were concerns raised about whether US military personnel would be willing to participate. These proved unfounded.
- 3) We performed all scans at 1.5T safely an average of 14 days after injury with no adverse clinical events. Prior to starting the study, there were concerns raised regarding the safety of MRI in subjects with combat exposure and potential metal shrapnel. We screened for MRI safety contraindications successfully using clinical history, exam, and a hand-held ferromagnetic detector. These methods have subsequently been implemented in Afghanistan.
- 4) We initially did all of the work ourselves at LRMC, but later trained clinical coordinators and MRI technologists at Landstuhl regional medical center to enroll subjects and perform scans.
- 5) We performed telephone-based monthly clinical assessments, and began scheduling in-person follow-up evaluations in St Louis.
- 6) We successfully worked with 4 different site principle investigators at LRMC: Dr Steve Flaherty, Dr. Ray Fang, Dr. John Oh, and Dr. David Zonies. This went smoothly.
- 7) We performed annual site visits to LRMC to audit performance. No concerns were raised.
- 8) We successfully arranged base leave and travel to St Louis for the purposes of performing in-person clinical follow-up assessments and repeat scans on 78 subjects with TBI and 18 controls.
- 9) We extensively analyzed DTI, resting-state fMRI, and clinical data.

The major scientific findings were as follows:

- 1) No abnormalities attributable to TBI were detected using CT or conventional MRI in these “mild” TBI subjects.
- 2) There were DTI abnormalities in US military personnel with blast-related TBI consistent with traumatic axonal injury in several brain regions not typically affected by civilian TBI.
 - a. Specifically, the middle cerebellar peduncle, the orbitofrontal white matter, and the cingulum were the most commonly affected regions in blast-related TBI, whereas there were few abnormalities in regions such as the corpus callosum that are commonly injured in civilian TBI.
 - b. In this initial cohort, 18/63 blast-related TBI subjects had DTI abnormalities in 2 or more brain regions.
 - c. However, most blast-related TBI subjects had normal DTI scans. Thus lack of abnormalities on DTI cannot exclude TBI, and TBI remains a clinical diagnosis.
 - d. DTI abnormalities were still present 6-12 months after injury, though their signal characteristics had evolved.
- 3) A manuscript describing these findings was published in *The New England Journal of Medicine* last year. It received widespread attention in the scientific and popular press. This manuscript and the supplementary appendix were attached to the annual report in 2011.
- 4) Resting-state fMRI did not strongly distinguish between TBI and control subjects. A substantial number (22/63) of resting-state fMRI scans in TBI subjects were degraded by motion artifact and therefore difficult to interpret. Resting-state fMRI may be less robust than DTI in this setting.

- 5) Overall outcomes using the Glasgow Outcome Scale –Extended, were worse in the subjects with blast-related TBI compared to controls, but both groups had relatively poor overall outcomes.
- 6) There were no abnormalities in cognitive performance in the subjects with blast-related TBI compared to controls or age-matched norms.
- 7) There were no focal neurological deficits in the subjects with blast-related TBI.
- 8) PTSD and depression severity were worse in the subjects with blast-related TBI compared to controls.
- 9) While initial analyses suggested that at early times after injury specific DTI and resting state fMRI abnormalities predict the severity of later PTSD, an attempt to validate these predictions in an additional cohort of subjects was unsuccessful. This may have been due to overfitting of the data, or to changes in the clinical features of the subjects from the first cohort (2008-2009) to the additional cohort (2010-2011). While this result was disappointing, our approach employed a very high standard of scientific rigor. By not publishing the results without validation using an independent cohort, we likely avoided confusion in the literature and premature scientific conclusions.
- 10) Because the cognitive performance and neurological function was generally normal, we did not attempt to perform clinical –radiological correlations for these parameters as they would be of limited clinical utility.

Supporting Data, Organized by SOW

Task 1) to obtain DTI, resting-state fMRI and conventional MRI scans acutely after injury at Landstuhl Regional Medical Center (LRMC) on a total of 100 military personnel, 80 who have sustained blast-related TBI and 20 who have sustained other injuries, but have no evidence of TBI.

Result: We obtained good quality scans in 124 US military personnel at LRMC: 64 with acute blast-related TBI and 21 controls with blast exposure and other injuries or illnesses but no TBI in the first phase, then 40 additional subjects with blast-related TBI in the second phase.

Please see the attached manuscripts for details:

Mac Donald et al *NEJM* 2011

Han et al 2013 *In preparation*

Task 2) to collect detailed clinical information on TBI-related outcomes 6-12 months after injury on the same participants recruited for Task 1. This will include global outcome assessments, neuropsychological testing for memory, attention and executive function deficits, motor performance measures, and clinician administered rating scales for depression and post-traumatic stress disorder. Repeat DTI, resting-state fMRI and conventional MRI will be performed to track the evolution of the injuries.

Result: We obtained complete follow-up data in 97 subjects 6-18 months after injury: 47 with blast-related TBI and 18 controls from the first phase and 31 with blast-related TBI in the second phase. Loss to follow-up was 22%.

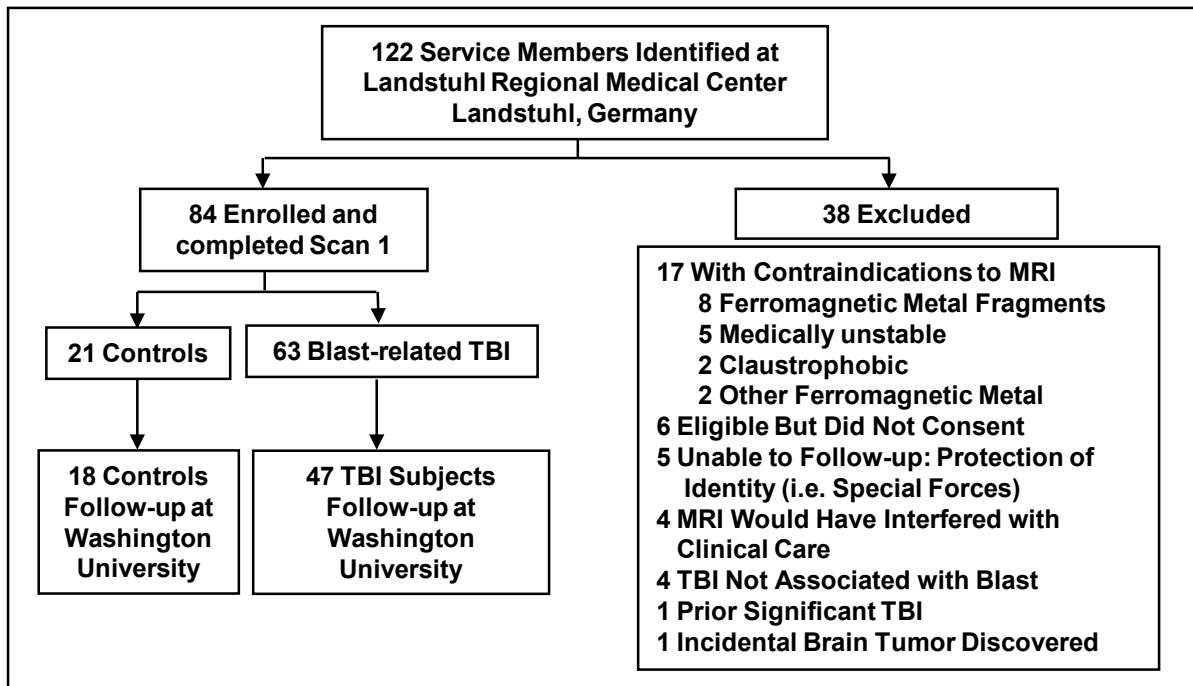


Figure 1: Screening, enrollment, and exclusion characteristics of the study participants.

Table 1. Characteristics of Study Participants

Characteristic	Control (n=21)	Control Follow-up (n=18)	TBI (n=63)	TBI Follow-up (n=47)
Age in years: median (range)	32 (19-53)	32 (21-53)	25 (19-58)	25 (19-58)
Education in years: median (range)	N/A	12.5 (11-17.5)	N/A	12 (8-17)
Race/ethnicity* - no (%)				
White	17 (80.9%)	15 (83.3%)	48 (76.2%)	34 (72.3%)
African American	3 (14.2%)	2 (11.1%)	7 (11.1%)	5 (10.6%)
Hispanic/Latino	1 (4.7%)	1 (5.5%)	9 (14.3%)	6 (12.7%)
Asian	0	0	2 (3.2%)	2 (4.3%)
Branch of Service - no (%)				
US Army	18 (85.7%)	15 (83.3%)	56 (88.9%)	42 (89.3%)
US Air Force	2 (9.5%)	2 (11.1%)	0	0
US Marine Corps	1 (4.8%)	1 (4.5%)	7 (11.1%)	5 (10.7%)
US Navy	0	0	0	0
Military Rank - no (%)				
Enlisted	19 (90.5%)	16 (88.9%)	60 (95.2)	44 (93.6)
Officer	2 (9.5%)	2 (11.1%)	3 (4.7)	3 (6.4)
Theatre of Operation - no (%)				
Iraq	15 (71.4%)	12 (66.7%)	25 (39.7%)	21 (44.7%)
Afghanistan	6 (28.6%)	6 (33.3%)	38 (60.3%)	26 (55.3%)

N/A: not assessed in subjects that did not follow-up.

* Self-reported. Subjects were not limited to one choice.

Table 2: Neuropsychological Test Performance

Test	Control (n=18)	TBI (n=47)	<i>P-value</i>	TBI GOS-E 7-8 (n=6)	TBI GOS-E <7 (n=41)	<i>P-value</i>	TBI No PTSD (n=18)	TBI+ PTSD (n=29)	<i>P-value</i>
25-Foot Walk (seconds) (<i>Motor Strength, Balance, Coordination</i>)	5.2±2.1	4.7±1.0	0.37 (U)	4.2±1.2	4.8±1.0	0.18 (U)	4.6±0.9	4.7±1.0	0.41 (t)
Conners' Continuous Performance Test II									
Omission Errors: (<i>Attention Lapses</i>)	-0.45±2.1	-0.14±1.3	0.47 (U)	0.36±0.4	-0.21±1.3	0.15 (t)	0.32±0.6	-0.42±1.5	0.04 (U)
Commission Errors: (<i>Impulsivity</i>)	-0.1±1.1	-0.17±1.0	0.38 (t)	-0.09±1.0	-0.19±1.0	0.41 (t)	0.11±0.9	-0.35±1.0	0.06 (t)
Hit Rate: (<i>Reaction Time</i>)	0.06±1.1	0.23±0.9	0.26 (t)	0.10±1.4	0.25±0.8	0.36 (t)	-0.06±0.9	0.41±0.9	0.04 (t)
Hit Rate Block Change: (<i>Sustained Vigilance</i>)	-0.26±1.0	-0.22±1.1	0.33 (U)	0.06±0.5	-0.26±1.1	0.34 (U)	-0.12±1.1	-0.28±1.1	0.20 (U)
Wisconsin Card Sorting Test: Total Errors (<i>Concept Formation, Mental Flexibility</i>)	0.58±0.8	0.66±0.9	0.38 (t)	0.62±0.6	0.66±1.0	0.46 (t)	0.63±0.7	0.67±1.1	0.43 (t)
Rey-Osterrieth Complex Figure Test: Delayed Recall (<i>Visual Memory</i>)	0.03±1.3	-0.55±1.7	0.10 (t)	-0.32±1.5	-0.58±1.7	0.36 (t)	-0.84±2.0	-0.37±1.5	0.18 (t)
Wechsler Test of Adult Reading (<i>Estimate of Pre-injury Verbal Intelligence</i>)	-0.24±1.3	-0.18±1.2	0.40 (U)	0.07±1.4	-0.22±1.1	0.27 (t)	-0.36±1.5	-0.07±0.9	0.26 (U)
California Verbal Learning Test II									
Long-Delay Free Recall (<i>Verbal Memory</i>)	0.0±0.9	-0.13±0.9	0.35 (U)	-0.7±1.0	-0.05±0.9	0.13 (U)	-0.11±0.9	-0.14±1.0	0.46 (t)
Total Intrusions (<i>Falsely Recalled Items</i>)	-0.44±1.5	-0.15±1.0	0.31 (U)	-0.42±0.5	-0.11±1.1	0.15 (U)	0.00±0.8	-0.24±1.1	0.32 (U)
List B vs. Trial 1 List A (<i>Proactive Memory Interference</i>)	0.11±1.1	-0.34±1.1	0.07 (t)	-0.08±0.9	-0.39±1.1	0.26 (t)	-0.36±1.0	-0.33±1.2	0.46 (t)
Grooved Pegboard									
(<i>Motor Speed & Coordination</i>)									
Dominant Hand Time	-1.4±0.6	-1.1±0.8	0.10 (t)	-1.35±0.5	-1.06±0.9	0.22 (t)	-1.27±0.7	-0.99±0.9	0.13 (U)
Non-Dominant Hand Time	-1.3±0.8	-1.0±0.8	0.16 (t)	-0.68±0.6	-1.07±0.8	0.15 (t)	-1.12±0.8	-0.96±0.8	0.26 (t)
Trail Making Test									
Trails A time (<i>Visual Scanning, Coordination</i>)	-0.09±0.9	-0.29±1.1	0.25 (t)	-0.02±1.3	-0.33±1.0	0.25 (t)	-0.01±1.1	-0.46±1.0	0.08 (t)
Trails B time (<i>Trails A + Mental Flexibility</i>)	0.02±0.9	-0.23±1.1	0.20 (t)	-0.02±0.9	-0.26±1.1	0.30 (t)	0.00±1.13	-0.38±1.0	0.12 (t)
Symbol Digit Modalities Test (<i>Working Memory</i>)	0.14±1.0	-0.22±0.8	0.04 (U)	0.08±0.5	-0.27±0.8	0.24 (U)	-0.17±0.7	-0.26±0.9	0.46 (U)
Controlled Oral Word Association Total Score: (<i>Verbal Fluency</i>)	-1.08±0.7	-0.80±0.9	0.12 (t)	-0.75±1.0	-0.81±0.9	0.44 (t)	-0.77±0.9	-0.82±1.0	0.42 (t)

Neuropsychological test results: Timed walk is reported in seconds. All other test results have been converted to Z-scores with higher scores representing better performance in all cases. The mean Z-scores for the US age and education-matched general male population are 0 and standard deviations are 1. All assessors were blinded to clinical and radiological information. GOS-E: Glasgow Outcome Scale-Extended. Scores of 7-8 represent good overall outcome and scores <7 represent moderate to severe overall disability.

PTSD: Post-traumatic stress disorder. PTSD was defined as meeting all criteria on the Clinician Administered PTSD Scale for DSM -IV. Note that many subjects in the "TBI no PTSD" group still have a substantial burden of PTSD symptoms, but did not meet all criteria for a categorical diagnosis of PTSD.

P-values represent results of 1-sided t-tests (t) or 1-sided Mann-Whitney U-tests (U); the prespecified hypotheses were that TBI patients would perform worse than controls, subjects with poor overall outcome would perform worse than those with good overall outcome, and subjects with TBI+PTSD would perform worse than those with TBI and no PTSD. Results have not been corrected for multiple comparisons. None were significant after Bonferroni correction for 17 variables.

Table 3: Neurobehavioral Rating Scale Results

Rating	Control (n=18)	TBI (n=47)	<i>P</i>	TBI	TBI	<i>P</i>	TBI	TBI+	<i>P</i>
				GOSE 7-8 (n=6)	GOSE <7 (n=41)		No PTSD (n=18)	PTSD (n=29)	
Total Score (Max 87, Higher Scores Worse)	7.9±6.8	11.6±7.3	0.03	8.7±5.5	12.0±7.5	0.18	7.8±4.3	13.9±7.8	0.10
Executive/Cognitive Dysfunction (Max. 24)	3.1±2.6	3.8±2.8	0.23	2.5±1.8	4.0±2.9	0.11	3.1±1.9	4.3±3.2	0.10
Positive Symptoms (Max 21)	1.1±1.8	1.4±1.6	0.11	0.8±0.4	1.5±1.7	0.31	0.6±0.7	2.0±1.8	0.005
Negative Symptoms (Max 12)	0.8±1.0	1.1±1.3	0.23	1.3±1.6	1.1±1.2	0.43	0.8±0.9	1.4±1.4	0.09
Mood/Affect Abnormalities (Max 15)	2.1±2.2	3.4±2.6	0.03	3.2±1.9	3.5±2.7	0.46	2.3±1.7	4.1±2.9	0.02
Oral/Motor Dysfunction (Max 12)	0.1±0.3	0.7±1.0	0.02	0.5±0.5	0.7±1.0	0.50	0.4±0.6	0.8±1.1	0.13
Worst Single Domain Score (Max 3)	1.4±0.8	1.8±0.6	0.04	1.7±0.5	1.9±0.6	0.25	1.7±0.5	1.9±0.7	0.18

Table 3: Neurobehavioral Rating Scale results. The Neurobehavioral Rating Scale score is based on a structured interview and

neurological exam followed by clinician ratings across 29 domains. Each domain is rated 0 (no abnormalities) through 3 (severe, disabling abnormalities). The total score is the sum of the ratings across all 29 domains. The 5 sub-scores are based on previously published principal component analyses from a large group of civilian TBI patients.[21] Each sub-score is the sum of scores from 4-8 domains. The “worst single domain score” was also assessed because the total scores are not necessarily ordinal, i.e. a single high score (2 or 3) in one domain can represent impairing or disabling symptoms and deficits, while several scores of 1 in multiple domains may not represent as much overall impairment. P-values represent results of 1-sided Mann-Whitney U tests, not corrected for multiple comparisons.

Characteristic	TBI No PTSD (n=18)	TBI + PTSD (n=29)	P-value
Age in years: median (range)	23.5 (21-58)	27 (19-45)	0.44 (U)
Education in years: median (range)	13 (10-17)	12 (8-17)	0.25 (U)
Race/ethnicity* - no (%)			0.49 (C)
White	12 (66.7%)	22 (75.9%)	
African American	3 (16.6%)	2 (6.9%)	
Hispanic/Latino	2 (11.1%)	4 (13.8%)	
Asian	1 (5.6%)	1 (3.4%)	
Branch of Service - no (%)			0.04 (C)
US Army	14 (77.8%)	28 (95.6%)	
US Air Force	0	0	
US Marine Corps	4 (22.2%)	1 (3.4%)	
US Navy	0	0	
Military Rank - no (%)			0.30 (C)
Enlisted	16 (88.9)	28 (95.6)	
Officer	2 (11.1)	1 (3.4)	
Theatre of Operation - no (%)			0.98 (C)
Iraq	8 (44.4%)	13 (44.9%)	
Afghanistan	10 (55.5%)	16 (55.1%)	

(U): Mann-Whitney U-test. (C) Chi square. For Race/ethnicity this comparison was for white vs. other.

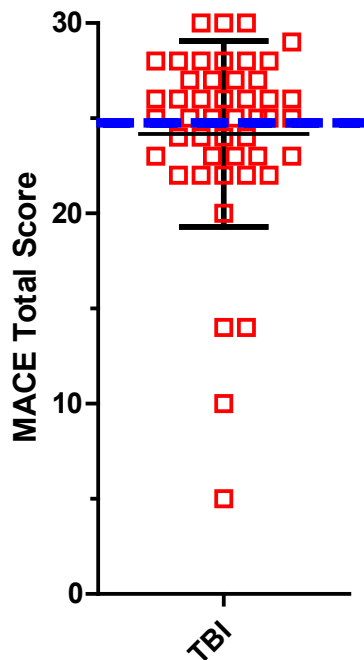


Figure 2: Military Acute Concussion Evaluation (MACE) scores in TBI subjects 1-90 days after injury at LRMC. Maximum score is 30. Higher scores indicate better performance. A cutoff of below 25 (blue dashed line) is considered to represent poor performance [17].

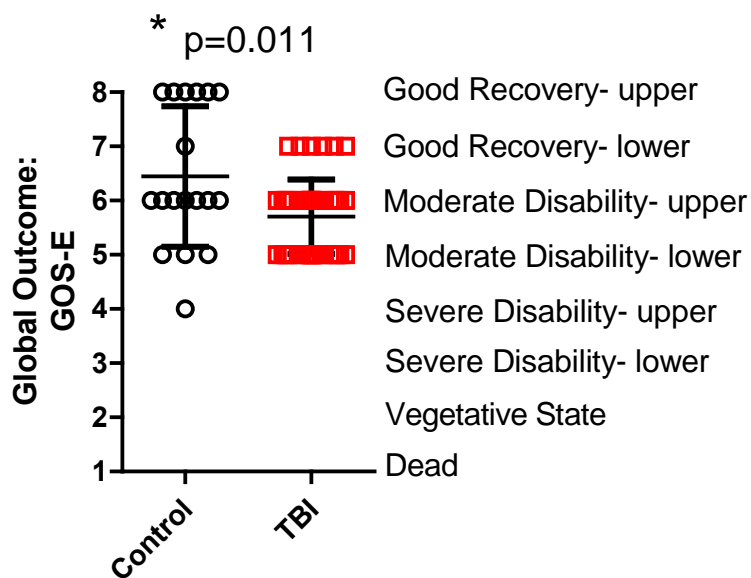


Figure 3: Global clinical outcomes assessed using the Glasgow Outcome Scale-Extended (GOS-E) scores 6-12 months after enrollment. * indicates 1-tailed Mann-Whitney U test.

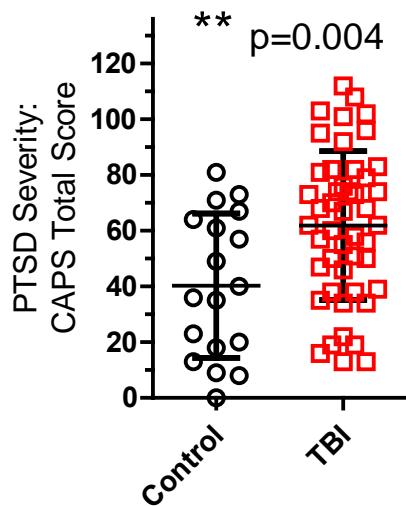


Figure 4: Post-traumatic stress disorder (PTSD) severity, based on the clinician administered PTSD scale (CAPS). Higher scores represent more severe PTSD, maximum score is 132. ** indicates 2-sided Student's t-test.

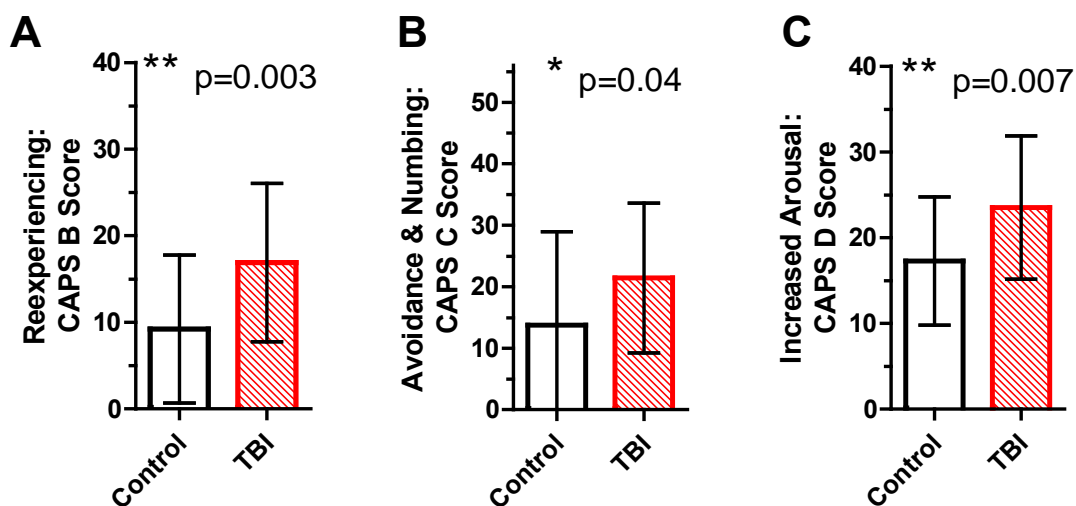


Figure 5: PTSD severity assessed using CAPS subscales. TBI subjects had significantly more severe PTSD symptoms in all 3 sub-domains. The sub-domains were based on the DSM-IV criteria for PTSD. The maximum scores are CAPS B: 40, CAPS C: 56, CAPS D: 40. Bars represent mean and standard deviation. * and ** indicate 1-sided Student's t-tests, not corrected for multiple comparisons.

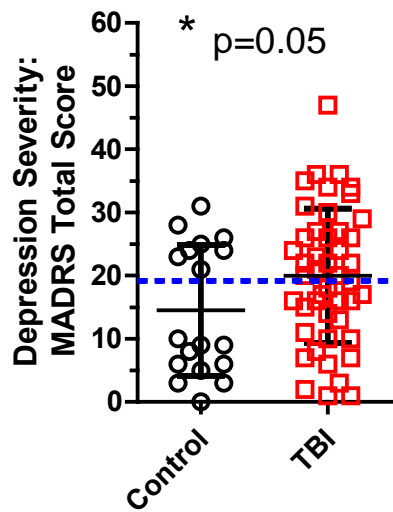


Figure 6: Depression severity assessed based on the Montgomery-Asberg Rating Scale structured interview. Dashed blue line indicated cutoff score of 19: >19 reflects moderate to severe depression. * indicates 1-sided Mann-Whitney U test.

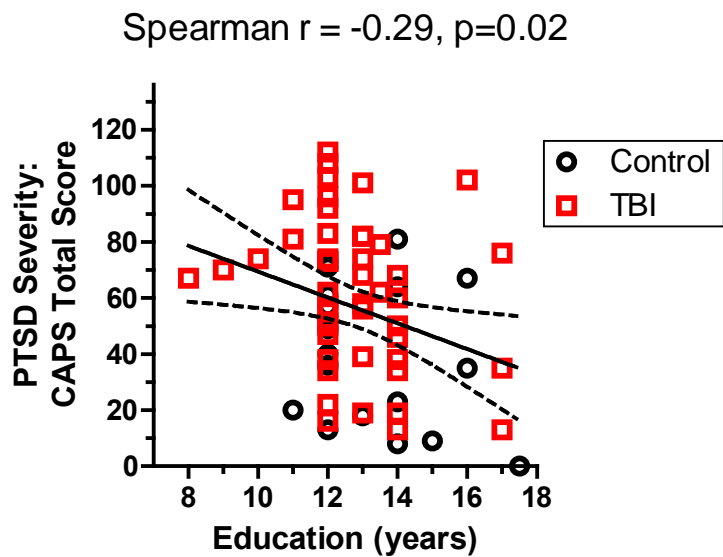


Figure 7: Inverse correlation between self-reported years of formal education and PTSD severity.

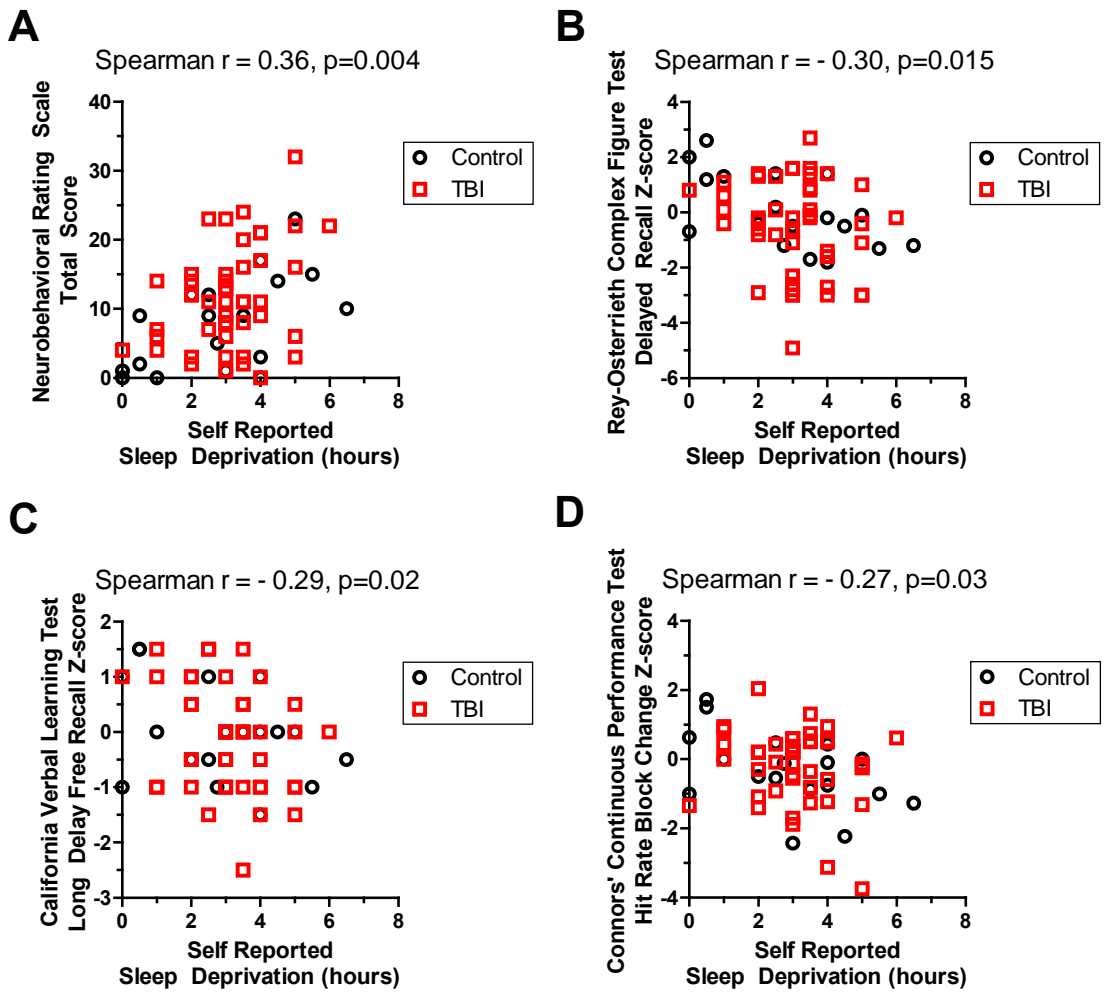


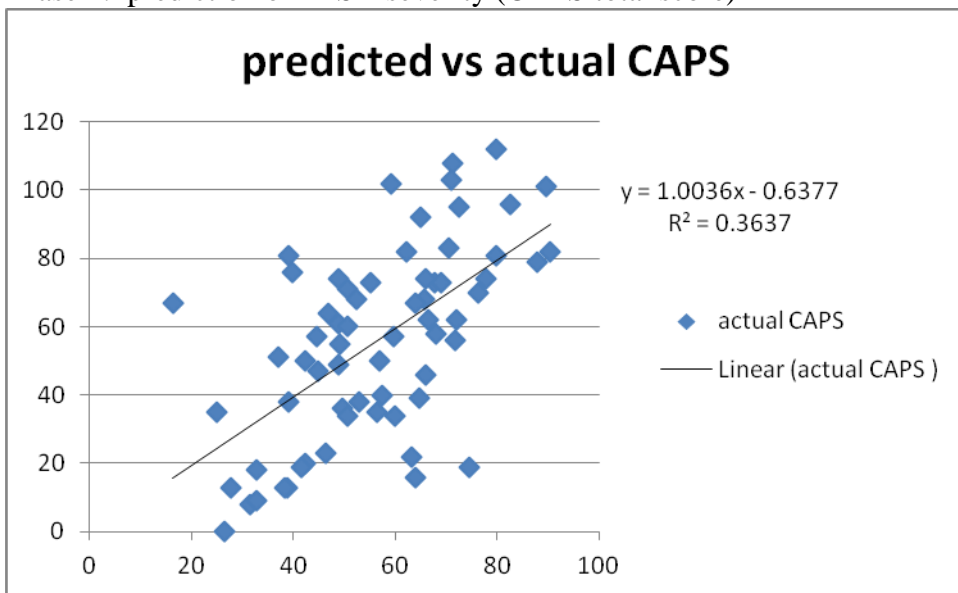
Figure 8: Correlations between self-reported sleep deprivation and test performance. **A.** Positive correlation with Neurobehavioral Rating Scale total score, where higher scores indicate worse performance. **B.** Negative correlation with visual memory performance on the delayed recall portion of the Rey-Osterrieth Complex Figure Test, where lower Z-scores indicate worse performance. **C.** Negative correlation with verbal memory performance on the long delay free recall portion of the California Verbal Learning Test, where again lower Z-scores indicate worse performance. **D.** Negative correlation with sustained vigilance, assessed using the hit rate block change measure from the Connors' Continuous Performance Test, where similarly lower Z-scores indicate worse performance.

Task 3) to extensively analyze the acute imaging predictors and correlates of 6-12 month clinical outcomes. Several prespecified hypotheses based on known brain anatomical-clinical correlations will be tested. Also, exploratory approaches will be used as the structural bases for many post-traumatic deficits and disorders are not well understood.

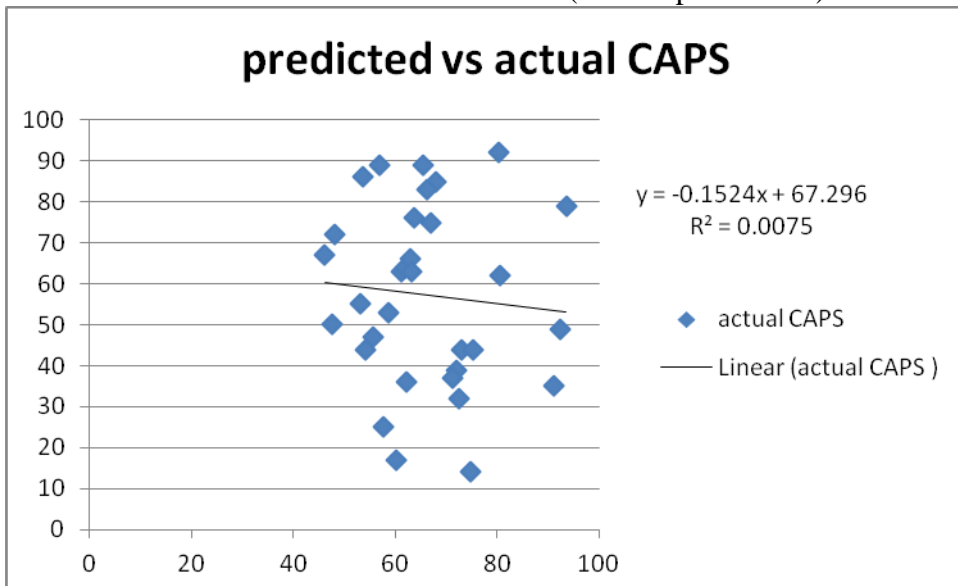
Result: We found initially promising scan-based early predictors of PTSD severity, as described fully in the attached poster presented at ATACCC in 2011. These early predictors unfortunately were not replicated in the second phase 31 blast-related TBI subjects.

It is not clear why this failure to replicate occurred. This may have been due to overfitting of the data, or to changes in the clinical features of the subjects from the first cohort (2008-2009) to the additional cohort (2010-2011).

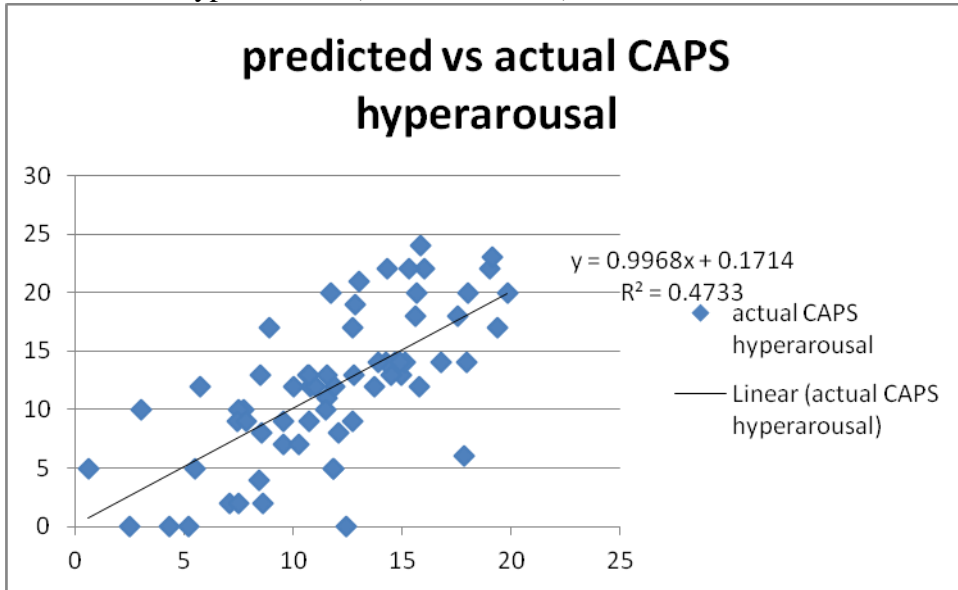
Phase 1: prediction of PTSD severity (CAPS total score)



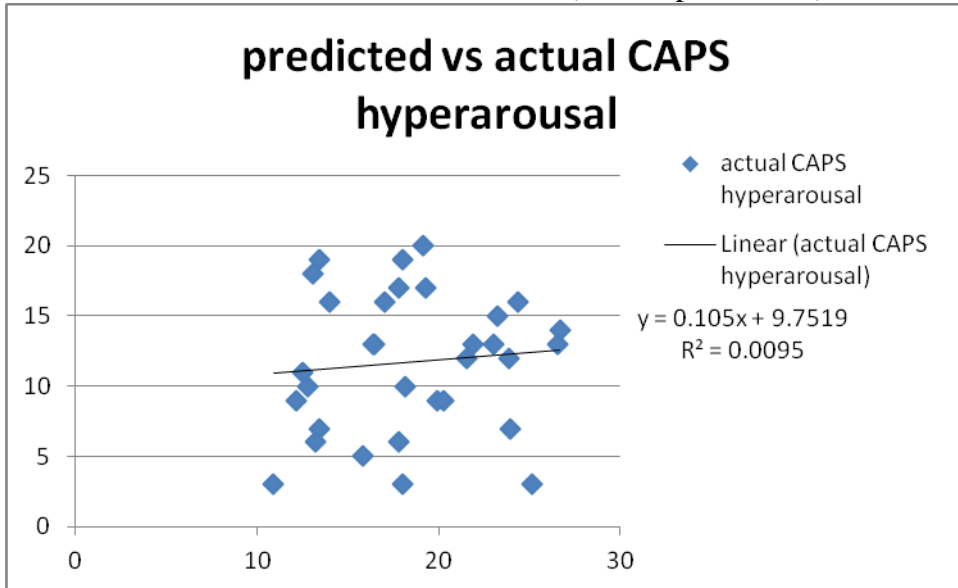
Phase 2: validation set with a locked model (no free parameters)



Prediction of hyperarousal (CAPS subscore)



Phase 2: validation set with a locked model (no free parameters)



Reportable Outcomes:

Papers:

C.L. Mac Donald, A.M. Johnson, D. Cooper, E. C. Nelson, N. J. Werner, J. S. Shimony, A. Z. Snyder, M. E. Raichle, J. R. Witherow, R. Fang, S. F. Flaherty, and D. L. Brody “Detection of Blast-Related Traumatic Brain Injury in US Military Personnel” New England Journal of Medicine 2011: 364: 2091-2100.

Abstracts and Presentations:

The PI and Dr. Mac Donald presented aspects of the results at several meetings and seminars:

1. 2012 Seminars at Baylor, Loma Linda, The University of Pennsylvania, Wayne State, and the University of Vancouver
2. 2012 National Neurotrauma Symposium
3. 2011 Society for Neuroscience Meeting
4. 2011 ATACCC
5. 2011 Research Seminar at The Ospedale Maggiore Policlinico, University of Milan, Italy
6. 2011 International Society for Magnetic Resonance in Medicine (ISMRM) meeting.
7. 2011 International Neurotrauma Society Meeting
8. 2011 Safar Symposium, University of Pittsburgh
9. 2011 MIT Blast-injury Modeling Symposium
10. 2011 Presentations during Gray Team III site visit to Afghanistan
11. 2010 Army Vice Chief of Staff Blue Ribbon Symposium on TBI and PTSD
12. 2010 Society for Neuroscience Meeting
13. 2010 ATACCC
14. 2009 Military Health Research Forum (MHRF),
15. 2009 LRMC Surgery Grand Rounds
16. 2009 National Neurotrauma Society meeting,

Personnel Supported:

David L Brody

Christine Mac Donald

Elliott Nelson

Ann M. Johnson

Nicole Schwarze Werner

Vera Bonsi

Justin Hampton,

Leslie Schart

Eric Shumaker

Elaine Tamez

Conclusions: Diffusion tensor imaging, an advanced MRI method, revealed abnormalities in some US military personnel with blast-related TBI that were not apparent using conventional MRI or CT. However, many subjects had normal DTI scans at 1.5T, and DTI using this approach cannot be recommended as a diagnostic tool at this time due to low sensitivity. Furthermore, DTI cannot yet predict the most important adverse clinical outcomes, and so cannot be recommended at this time for use in triage, return-to-duty, or guiding post-injury rehabilitation. It remains to be seen whether DTI will be a useful pharmacodynamic biomarker for therapeutics targeting traumatic axonal injury. Resting-state fMRI proved not to be sufficiently robust for individual subject use due to motion artifacts. Improvements in imaging acquisition and analysis, more focused clinical evaluations, and the addition of genetic resiliency factor assessments may improve clinical predictions.

The data generated during this New Investigator Award have seeded two additional research grants from CDMRP, both of which are ongoing.

Appendixes

- 1) Mac Donald et al NEJM 2011 published paper
- 2) Han et al 2013 *manuscript in preparation*
- 3) Mac Donald et al Military Health Research Forum 2009 poster
- 4) Mac Donald et al International Neurotrauma Society 2009 poster
- 5) Brody et al ATACCC 2010 abstract
- 6) Brody et al Society for Neuroscience 2010 poster
- 7) Brody et al ATACCC 2011 poster
- 8) Brody et al National Neurotrauma Society 2011 Abstract
- 9) Brody et al International Society for Magnetic Resonance in Medicine 2011 syllabus

The NEW ENGLAND JOURNAL of MEDICINE

ESTABLISHED IN 1812

JUNE 2, 2011

VOL. 364 NO. 22

Detection of Blast-Related Traumatic Brain Injury in U.S. Military Personnel

Christine L. Mac Donald, Ph.D., Ann M. Johnson, Dana Cooper, B.S., Elliot C. Nelson, M.D., Nicole J. Werner, Ph.D., Joshua S. Shimony, M.D., Ph.D., Abraham Z. Snyder, M.D., Ph.D., Marcus E. Raichle, M.D., John R. Witherow, M.D.,* Raymond Fang, M.D., Stephen F. Flaherty, M.D., and David L. Brody, M.D., Ph.D.

ABSTRACT

BACKGROUND

Blast-related traumatic brain injuries have been common in the Iraq and Afghanistan wars, but fundamental questions about the nature of these injuries remain unanswered.

METHODS

We tested the hypothesis that blast-related traumatic brain injury causes traumatic axonal injury, using diffusion tensor imaging (DTI), an advanced form of magnetic resonance imaging that is sensitive to axonal injury. The subjects were 63 U.S. military personnel who had a clinical diagnosis of mild, uncomplicated traumatic brain injury. They were evacuated from the field to the Landstuhl Regional Medical Center in Landstuhl, Germany, where they underwent DTI scanning within 90 days after the injury. All the subjects had primary blast exposure plus another, blast-related mechanism of injury (e.g., being struck by a blunt object or injured in a fall or motor vehicle crash). Controls consisted of 21 military personnel who had blast exposure and other injuries but no clinical diagnosis of traumatic brain injury.

RESULTS

Abnormalities revealed on DTI were consistent with traumatic axonal injury in many of the subjects with traumatic brain injury. None had detectible intracranial injury on computed tomography. As compared with DTI scans in controls, the scans in the subjects with traumatic brain injury showed marked abnormalities in the middle cerebellar peduncles ($P < 0.001$), in cingulum bundles ($P = 0.002$), and in the right orbitofrontal white matter ($P = 0.007$). In 18 of the 63 subjects with traumatic brain injury, a significantly greater number of abnormalities were found on DTI than would be expected by chance ($P < 0.001$). Follow-up DTI scans in 47 subjects with traumatic brain injury 6 to 12 months after enrollment showed persistent abnormalities that were consistent with evolving injuries.

CONCLUSIONS

DTI findings in U.S. military personnel support the hypothesis that blast-related mild traumatic brain injury can involve axonal injury. However, the contribution of primary blast exposure as compared with that of other types of injury could not be determined directly, since none of the subjects with traumatic brain injury had isolated primary blast injury. Furthermore, many of these subjects did not have abnormalities on DTI. Thus, traumatic brain injury remains a clinical diagnosis. (Funded by the Congressionally Directed Medical Research Program and the National Institutes of Health; ClinicalTrials.gov number, NCT00785304.)

From the Washington University School of Medicine, St. Louis (C.L.M.D., A.M.J., D.C., E.C.N., N.J.W., J.S.S., A.Z.S., M.E.R., D.L.B.); the Landstuhl Regional Medical Center, Landstuhl, Germany (J.R.W., R.F., S.F.F.); and the Walter Reed Army Medical Center, Washington, DC (S.F.F.). Address reprint requests to Dr. Brody at the Department of Neurology, Washington University School of Medicine, Biotech Bldg., Rm. 201, 660 S. Euclid Ave., Box 8111, St. Louis, MO 63110, or at brodyd@neuro.wustl.edu.

*Deceased.

N Engl J Med 2011;364:2091-100.
Copyright © 2011 Massachusetts Medical Society.

IN THE CURRENT WARS IN IRAQ AND Afghanistan, the number of blast-related traumatic brain injuries may be as high as 320,000.¹ Most of these injuries are categorized as uncomplicated “mild” or “concussive” traumatic brain injury on the basis of clinical criteria and the absence of intracranial abnormalities on computed tomography (CT) or conventional magnetic resonance imaging (MRI).² However, little is known about the nature of these “mild” injuries, and the relationship between traumatic brain injury and outcomes remains controversial.^{3,4} No human autopsy studies conducted with the use of current immunohistochemical methods^{5,6} have been published.^{7,8} Computer simulations of the effects of blast-induced pressure waves on the brain suggest that coup and contrecoup regions may be subject to high stresses.^{9,10} Simulations also suggest that the orbitofrontal regions and the posterior fossa (cerebellum and brain stem) may sustain intense stresses independently of the subject’s head orientation relative to the blast.¹⁰ Findings that are consistent with this view include a positron-emission tomographic study showing reduced cerebellar basal glucose metabolism¹¹ and a case report documenting a lesion in cerebellar white matter on MRI after blast injury.¹² In a swine model of experimental blast injury, traumatic axonal injury in several regions, including cerebellar tracts, was detected.¹³

We therefore hypothesized that traumatic axonal injury is a primary feature of human blast-related traumatic brain injury. To test this hypothesis noninvasively, we used an advanced MRI method called diffusion tensor imaging (DTI), which can be performed quickly on most clinical scanners.¹⁴ DTI involves the measurement of water diffusion in multiple directions. In the white matter of the brain, water diffuses faster along the predominant fiber direction and more slowly in perpendicular directions (see Fig. S1 and S2 in the Supplementary Appendix, available with the full text of this article at NEJM.org). The resulting anisotropy (directional asymmetry) of water diffusion is high in intact axons and reduced after axonal injury.¹⁵⁻¹⁷ The use of reduced anisotropy on DTI as a marker of traumatic axonal injury has been directly validated by means of comparison with immunohistochemical indicators of axonal injury in an animal model of traumatic brain injury, even when the findings on conventional MRI are normal.^{16,17} We explicitly assessed major orbitofrontal and posterior fossa white-matter tracts,

along with other regions commonly affected by traumatic brain injury.

METHODS

SUBJECTS

U.S. military personnel with positive results on screening for traumatic brain injury, performed at the Landstuhl Regional Medical Center (LRMC), were eligible for inclusion in the study. Screening was based on U.S. military clinical criteria for traumatic brain injury¹⁸: loss of consciousness, amnesia for the event, or another change in neurologic status, such as feeling “dazed” or “confused” or “seeing stars” immediately after the trauma. Additional criteria for inclusion in the study were injury from a blast, defined as primary injury from blast exposure with or without additional mechanisms of injury, within 90 days before study enrollment; membership in the U.S. military; the ability to provide informed consent in person; no contraindications to MRI, such as retained metallic fragments; no history of major traumatic brain injury or psychiatric disorder; and agreement to communicate by telephone or e-mail monthly for 6 to 12 months after enrollment and to travel to Washington University in St. Louis for follow-up. Inclusion criteria for controls were the same except that negative results of screening for traumatic brain injury were required. All subjects provided written informed consent before enrollment.

DTI AND CONVENTIONAL MRI ASSESSMENTS

The initial MRI scans obtained at the LRMC were acquired with the use of a 1.5-tesla MRI scanner (Magnetom Avanto, Siemens), without the administration of sedation or medication beyond that being administered as part of routine clinical care. The DTI protocol involved the acquisition of two scans at a resolution of 2.5 mm by 2.5 mm by 2.5 mm with 23 diffusion directions. The conventional MRI scans obtained included T₁-weighted and T₂-weighted sequences, fluid-attenuated inversion recovery (FLAIR) sequences, and T₂*-weighted sequences. Performance of the protocol required 21 minutes per subject (Table S1 in the Supplementary Appendix). (Further information on the image processing can be found in the Methods section in the Supplementary Appendix.) Subjects traveled to Washington University 6 to 12 months after enrollment for follow-up scans and in-person clinical assessments. The follow-up scans

were obtained on another 1.5-tesla MRI scanner (Magnetom Avanto) at Washington University in accordance with the same protocol.

REGION-OF-INTEREST ANALYSIS

Analysts who were unaware of the clinical assessments of the subjects manually traced 17 regions of interest on each scan. Each region of interest consisted of multiple brain slices fully covering three-dimensional anatomical structures (Fig. 1). The anatomical structures were defined in accordance with definitions provided in a standard DTI atlas.¹⁹ Analyze software, version 6.1 (Mayo Foundation), was used to extract quantitative DTI parameters, including relative anisotropy, axial diffusivity, radial diffusivity, and mean diffusivity for each region of interest. (The definitions of these parameters are provided in the Supplementary Appendix.) Intrarater reliability (two analyses were performed, 2 weeks apart) was 96% or higher, and interrater reliability was 90% or higher. Therefore, each region of interest was traced by a single analyst to optimize consistency.

STATISTICAL ANALYSES

All data were analyzed with the use of Statistica software, version 6.0 (StatSoft). The relationship between measures of relative anisotropy in the regions of interest was assessed by examining scatter plots and performing correlation analyses of relative anisotropy in the 21 controls. When significant positive correlations were detected between relative anisotropy values in pairs of regions, the correlated regions of interest were combined. The combined regions of interest included the genu and splenium of the corpus callosum, the right and left middle cerebellar peduncles, the right and left cerebral peduncles, the right and left uncinate fasciculi, and the right and left cingulum bundles. This approach reduced the number of DTI regions of interest from 17 to 12. There were no significant correlations between relative anisotropy values among these 12 regions. We grouped these regions into two prespecified categories: 4 posterior fossa and orbitofrontal regions predicted to be vulnerable to primary blast injury, and 8 other regions commonly affected by traumatic brain injury.

The normal distribution of each continuous variable was assessed with the use of the Shapiro–Wilk test. All DTI data sets were found to be normally distributed. Hotelling’s T^2 -tests were used to assess overall differences in groups across

the 12 regions of interest. Unpaired Student’s t -tests were then used to assess individual variables. For age, the only non-normally distributed continuous variable, the Mann–Whitney U test was used. Chi-square analyses were used to assess the relationships between categorical variables. One-sided tests were used when hypotheses were prespecified, and two-sided tests were used otherwise. Reported P values have not been corrected for multiple comparisons, but a P value of less than 0.05 was considered to be significant only after Bonferroni’s correction for multiple comparisons (e.g., $P < 0.0125$ [$0.05 \div 4$] for each of the four prespecified orbitofrontal and posterior fossa DTI regions of interest and $P < 0.00625$ [$0.05 \div 8$] for each of the eight other regions of interest).

For DTI assessments in individual subjects, the abnormalities consistent with traumatic axonal injury were defined as values for relative anisotropy that were more than 2 SD below the mean of the values for controls. To estimate the number of DTI abnormalities expected to occur by chance in each subject, a binomial distribution was used, with $p = 0.02275$ (the probability of each abnormality arising by chance) for 12 regions of interest in each subject. (In this instance, p denotes the parameter in the binomial distribution that indicates the probability of each event.) This estimate is based on the assumption that the regions of interest were statistically independent (see the Additional Statistical Methods section in the Supplementary Appendix).

RESULTS

CHARACTERISTICS OF THE SUBJECTS

We enrolled 63 subjects with traumatic brain injury and 21 controls over the course of 5 noncontiguous months between November 2008 and October 2009 (Table 1 and Fig. 2). The median time from injury to enrollment was 14 days (range, 1 to 90). All available clinical histories for the subjects with traumatic brain injury indicated primary blast exposure plus another mechanism of head injury, such as being injured in a fall or motor-vehicle crash or being struck by a blunt object. None of the subjects had isolated primary blast injury.

Inclusion in the group of subjects with traumatic brain injury was typically based on self-report of blast exposure, with immediate alteration of neurologic function meeting the standard criteria for traumatic brain injury used at the

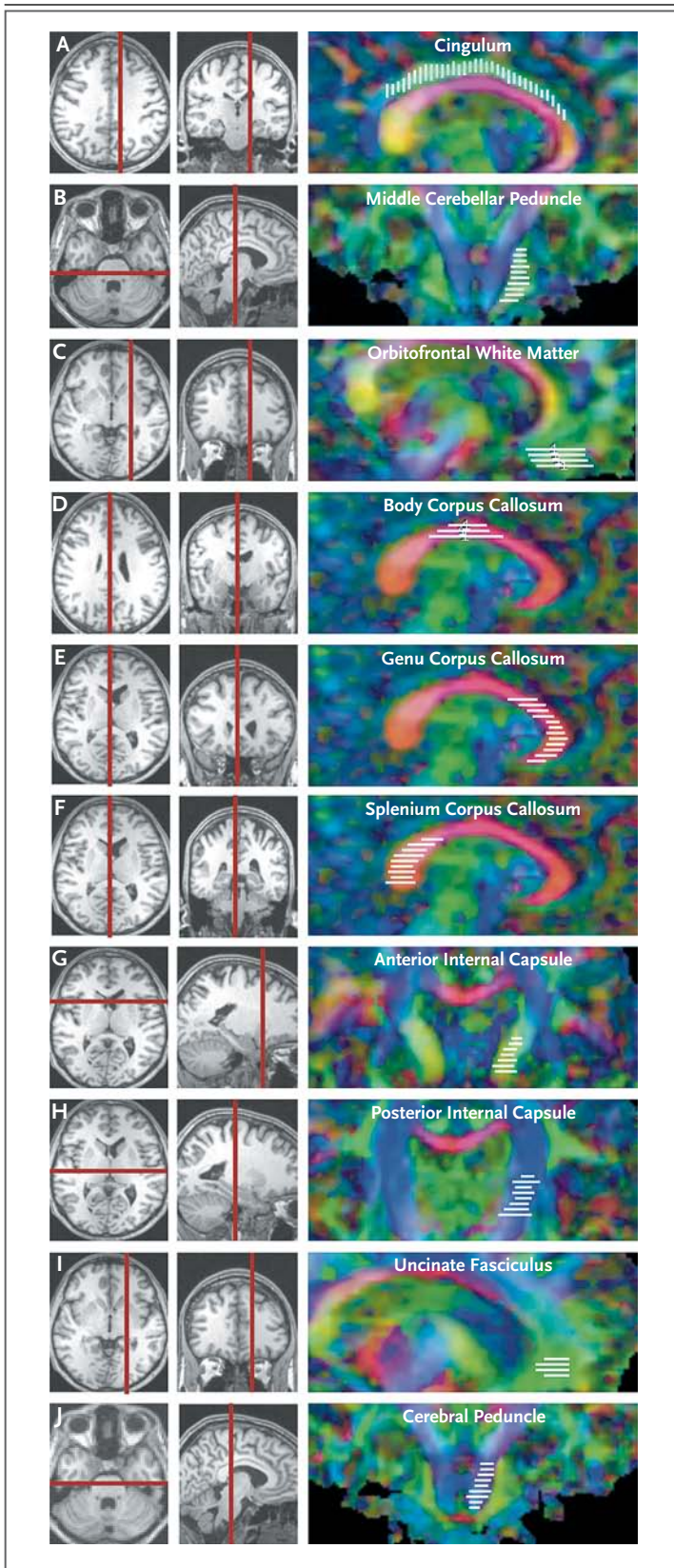


Figure 1. Brain Regions of Interest for Diffusion Tensor Imaging.

The scans in the left and center columns were obtained with conventional (T_1 -weighted) MRI and are shown for the purpose of anatomical localization. The scans in the right column are relative anisotropy maps obtained with diffusion tensor imaging (DTI). The vertical and horizontal red bars indicate the anatomical localization of the images in the right column. The white bars indicate the locations and orientation of the slices analyzed for multislice regions of interest. Red, green, and blue indicate the principal directions of diffusion, with red denoting right to left, green anterior to posterior, and blue dorsal to ventral. Panel A shows a sagittal section through the cingulum bundle, anterior–posterior, dorsal to the corpus callosum, and Panel B shows a coronal section through the middle cerebellar peduncle, anterior–posterior, in the dorsal brain stem and cerebellum. Panels C through F are sagittal sections, with Panel C showing orbitofrontal white matter, anterior–posterior, in the ventral frontal lobe, Panel D showing the body of the corpus callosum, right–left, between the lateral ventricles, Panel E showing the genu of the corpus callosum, right–left, anterior to the lateral ventricles, and Panel F showing the splenium of the corpus callosum, right–left, posterior to the lateral ventricles. Panels G and H are coronal sections, with Panel G showing the anterior limb of the internal capsule, anterior–posterior and right–left, between the caudate and putamen, and Panel H showing the posterior limb of the internal capsule, dorsal–ventral and right–left, between the putamen and thalamus. Panel I shows a sagittal section of the uncinate fasciculus, anterior–posterior, in the anterior frontal lobe, and dorsal and anterior to the orbitofrontal white-matter region of interest. Panel J shows a coronal section through the cerebral peduncle, dorsal–ventral in the midbrain and pons, medial to the middle cerebellar peduncle.

LRMC.¹⁸ All clinical histories were reviewed by study personnel, who also performed additional history taking and examined medical records. Medical documentation from the theater of operations regarding the duration of loss of consciousness and post-traumatic amnesia was often not available or not reliable. All available clinical histories indicated a change in level of consciousness or loss of consciousness for a few minutes and post-traumatic amnesia for less than 24 hours. Although the study had no restriction on the severity of injury, the requirement for in-person informed consent typically made patients with moderate-to-severe traumatic brain injury ineligible, and such patients were not enrolled. No intracranial abnormalities were detected on CT of the head without the administration of contrast material. Thus, all subjects with traumatic brain injury

met the criteria from the Department of Defense for mild, uncomplicated traumatic brain injury.² (These criteria are provided in the Methods section in the Supplementary Appendix.)

All controls had been exposed to blasts, but none had sustained traumatic brain injury according to the results of clinical screening.¹⁸ Specifically, most controls were evacuated to the LRMC for orthopedic or soft-tissue injuries to the arms or legs. Some controls also had gastrointestinal conditions. Many of these injuries occurred independently of blast exposure. None of the subjects in either group had other conditions that are known to or could reasonably be expected to affect DTI signal characteristics. Specifically, no subject in either group was known to have cerebrovascular disease, hypoxic or ischemic brain injury, central nervous system infection, sepsis, infection with the human immunodeficiency virus, severe electrolyte disturbance, liver failure, renal failure, heart failure, a history of alcohol abuse, or a long-standing psychiatric condition.

FINDINGS ON DTI AND CONVENTIONAL MRI

Initial DTI scanning performed at LRMC revealed abnormalities that were consistent with traumatic axonal injury. Reductions in relative anisotropy were apparent in several brain regions (Fig. 3). The results of conventional MRI were normal even when abnormalities were present on DTI (Fig. S3 in the Supplementary Appendix). An abnormality related to traumatic brain injury was detected with the use of conventional MRI in only one subject; the review was performed by a board-certified neuroradiologist, who found a small occipital contusion.

Quantitative analyses indicated significant reductions in relative anisotropy in the group of subjects with traumatic brain injury as compared with the control group ($P < 0.02$ according to Hotelling's T^2 -test). Among the brain regions commonly affected in civilian cases of mild traumatic brain injury,^{15,20-26} abnormalities were most frequently found in the cingulum bundle (Fig. 3A), uncinate fasciculus, and anterior limb of the internal capsule (Fig. S4 in the Supplementary Appendix). However, there were few abnormalities in the corpus callosum or the posterior limb of the internal capsule; notably, abnormalities were more frequent in the middle cerebellar peduncles and orbitofrontal white matter (Fig. 3A), both of which are among the regions predicted to sustain the

Table 1. Characteristics of the Study Participants.

Characteristic	Controls (N=21)	Subjects with TBI* (N=63)	P Value†‡
Age — yr			0.03‡
Median	31	24	
Range	19–49	19–58	
Male sex — no. (%)	21 (100)	63 (100)	1.0
Race — no. (%)§			0.87
White	17 (81)	48 (76)	
Other	4 (19)	18 (29)	
Branch of service — no. (%)			0.92
Army	18 (86)	56 (89)	
Air Force	2 (10)	0	
Marine Corps	1 (5)	7 (11)	
Navy	0	0	
Rank — no. (%)			0.46
Officer	2 (10)	3 (5)	
Enlisted	19 (90)	60 (95)	
Theater of operation — no. (%)			0.01
Iraq	15 (71)	25 (40)	
Afghanistan	6 (29)	38 (60)	

* TBI denotes traumatic brain injury.

† P values were calculated with the use of the chi-square test unless noted otherwise.

‡ The P value was calculated with the use of a two-tailed Mann–Whitney U test.

§ Race was self-reported, and subjects could select more than one category.

most intense stresses and therefore predicted to be vulnerable to primary blast injury.¹⁰

At an individual level, 18 of the 63 subjects with traumatic brain injury (29%) had abnormalities on DTI that were consistent with multifocal traumatic axonal injury. Specifically, relative anisotropy was reduced in two or more brain regions in each of these 18 subjects (Fig. 3B). Abnormalities detected on DTI were defined as relative anisotropy reductions of at least 2 SD below the mean for the 21 controls. On the basis of chance alone, no more than 2 of 63 healthy subjects would be expected to have two or more such abnormalities in 12 statistically independent regions of the brain ($P < 0.001$ by chi-square analysis). An additional 20 subjects (32%) with traumatic brain injury had one abnormality detected on DTI and 25 (40%) had no abnormalities according to the aforementioned definitions.

There were imbalances in age and theater of operation between the subjects with traumatic

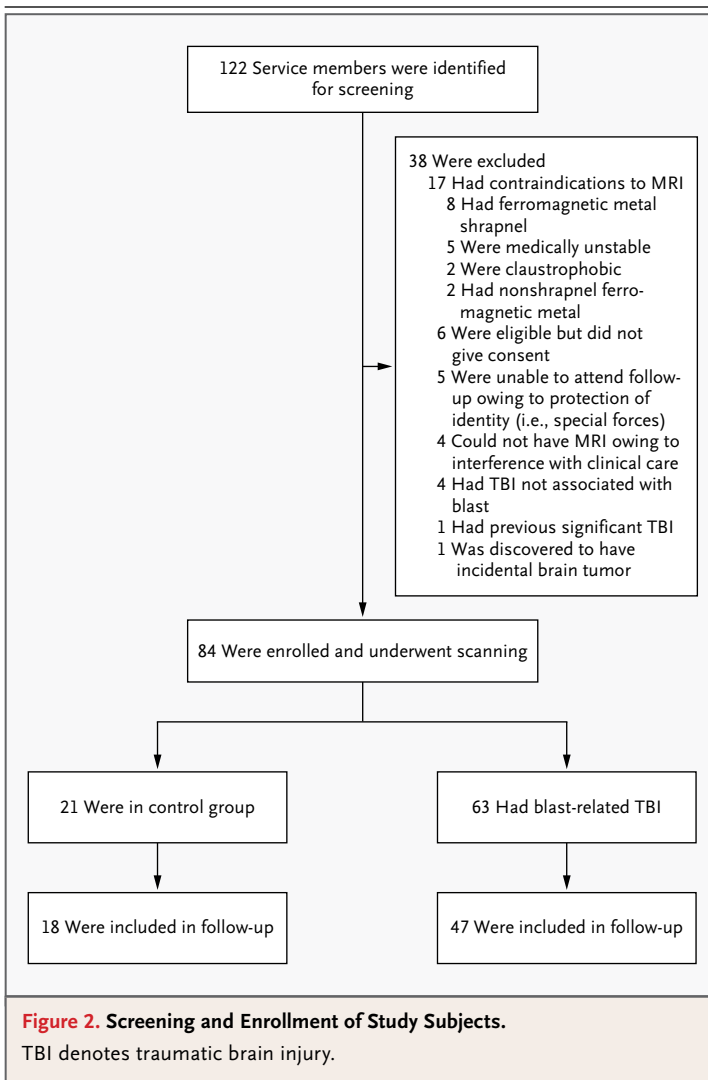
EVOLUTION OF DTI SIGNAL ABNORMALITIES

Relative anisotropy, the DTI parameter assessed in previous analyses, has been shown to be persistently reduced at several time points after traumatic brain injury in an animal model; however, other DTI parameters have been shown to change over time as the injuries evolve.¹⁶ We therefore analyzed these other DTI parameters and found clear evidence of changes in the DTI signal abnormalities over time in this cohort. Specifically, mean diffusivity and radial diffusivity were higher in subjects with traumatic brain injury than in controls on the initial scans (Fig. 4A) but normalized on follow-up scans (Fig. 4B). Axial diffusivity did not differ significantly between groups on the initial scans (Fig. 4A) but was lower in the subjects with traumatic brain injury than in controls on follow-up scans (Fig. 4B). These findings are consistent with an evolution of injury (Fig. 4C).

On the basis of the results of analyses in individual subjects, the sensitivity of DTI did not decline substantially over time. Of the 47 subjects with traumatic brain injury who underwent scanning twice, 12 (26%) had two or more abnormal regions of interest on the initial scans and 11 (23%) had two or more abnormal regions of interest on follow-up scans (Fig. 4D). These proportions were both greater than would be expected by chance ($P=0.004$ and $P=0.007$, respectively, by chi-square analysis). There were no significant differences in initial relative anisotropy between the 47 subjects with traumatic brain injury who underwent follow-up scanning and the 16 who did not (Fig. S7 in the Supplementary Appendix). This finding indicated that subjects available for follow-up DTI scanning were representative of the entire cohort.

DISCUSSION

With the use of DTI, we found abnormalities consistent with traumatic axonal injury in U.S. military personnel with blast-related mild traumatic brain injury. Substantial numbers of abnormalities were found in regions of the brain not known to be commonly injured in civilian cases of mild traumatic brain injury but predicted to be vulnerable to blast on the basis of computational simulations.¹⁰ Abnormalities were also found in some brain regions that are commonly affected in civilian cases of mild traumatic brain injury.^{15,20-26} Other regions, such as the corpus callosum,^{5,15,20,23,25-27} were generally spared. Overall, the distribution of

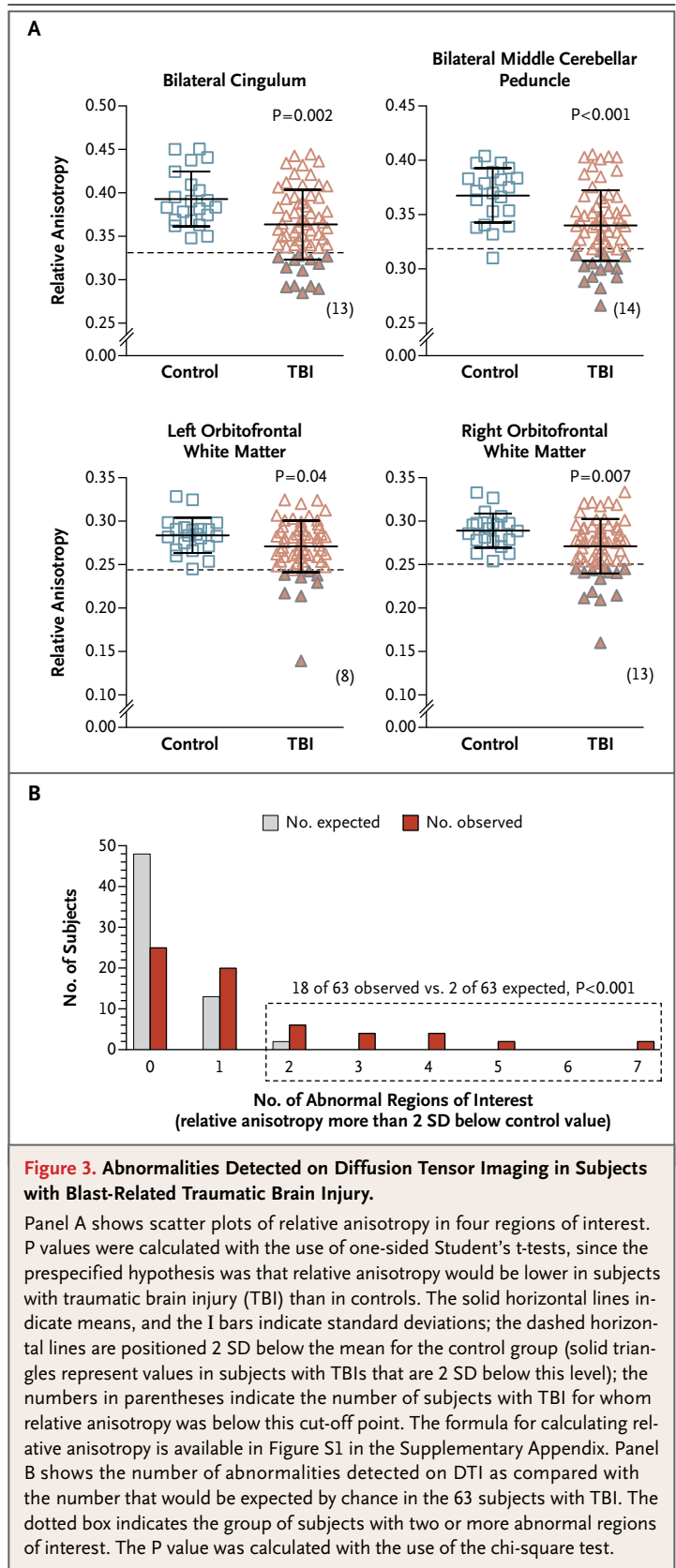


brain injury and the controls (Table 1), but these differences were unlikely to account for the primary results. Specifically, there were no correlations between age and relative anisotropy in this cohort (Fig. S5 in the Supplementary Appendix). Likewise, there were no significant differences between controls or subjects with traumatic brain injury who were injured in Iraq and those injured in Afghanistan (Fig. S6 in the Supplementary Appendix). The differences between subjects with traumatic brain injury and controls were robust after adjustments for propensity score (Tables S2 and S3 in the Supplementary Appendix). Post hoc subgroup analyses indicated that these differences were unlikely to have resulted from effects restricted to any specific subgroup of subjects (Table S4 in the Supplementary Appendix).

abnormalities can best be accounted for as a combination of traumatic axonal injuries in brain regions vulnerable to primary blast and in regions of the brain vulnerable to other mechanisms of injury. This explanation fits well with the clinical descriptions of the injuries, which in all cases included both primary blast exposure and another mechanism of injury, such as a fall, a motor-vehicle crash, or a blow to the head by a blunt object. However, it is also possible that injuries to the orbito-frontal white matter and cerebellar peduncles are more common in civilian cases of mild traumatic brain injury than currently recognized. Certainly, these and adjacent regions can be affected in more severe instances of civilian traumatic brain injury.²⁸⁻³¹ Likewise, primary blast injury could sensitize these regions to subsequent insults. Thus, the exact contributions of primary blast exposure and other types of injury cannot be determined with certainty.

The characteristics of the abnormal DTI signals changed between initial scanning and follow-up scanning in a fashion that was consistent with the evolution of relatively acute injuries. The pattern of abnormalities on the initial scans was most consistent with axonal injury plus a cellular inflammatory response and edema (Fig. 4C, and Fig. S8 in the Supplementary Appendix). Axial diffusivity has been shown to be decreased with axonal injury but concomitantly increased with edema and cellular inflammation. Thus, axial diffusivity can be pseudonormalized in complex injuries.¹⁶ On the follow-up scans, the pattern of abnormalities was most consistent with persistent axonal injury plus resolution of the edema and cellular inflammation (Fig. 4C, and Fig. S8 in the Supplementary Appendix). This evolution over time also confirms that the DTI abnormalities were unlikely to have been preexisting.

The limitations of this study include a moderate sample size, an all-male study population, a finite number of prespecified regions of interest for DTI analysis, and the lack of a direct comparison with identically assessed subjects who had traumatic brain injury that was not blast-related. Another limitation, despite our best efforts at circumvention, is the possibility that some uncharacterized differences between the subjects and the controls, in addition to that of brain injury, affected the DTI signals in such a way as to produce the observed results. Additional research with independent cohorts will be required to validate these findings.



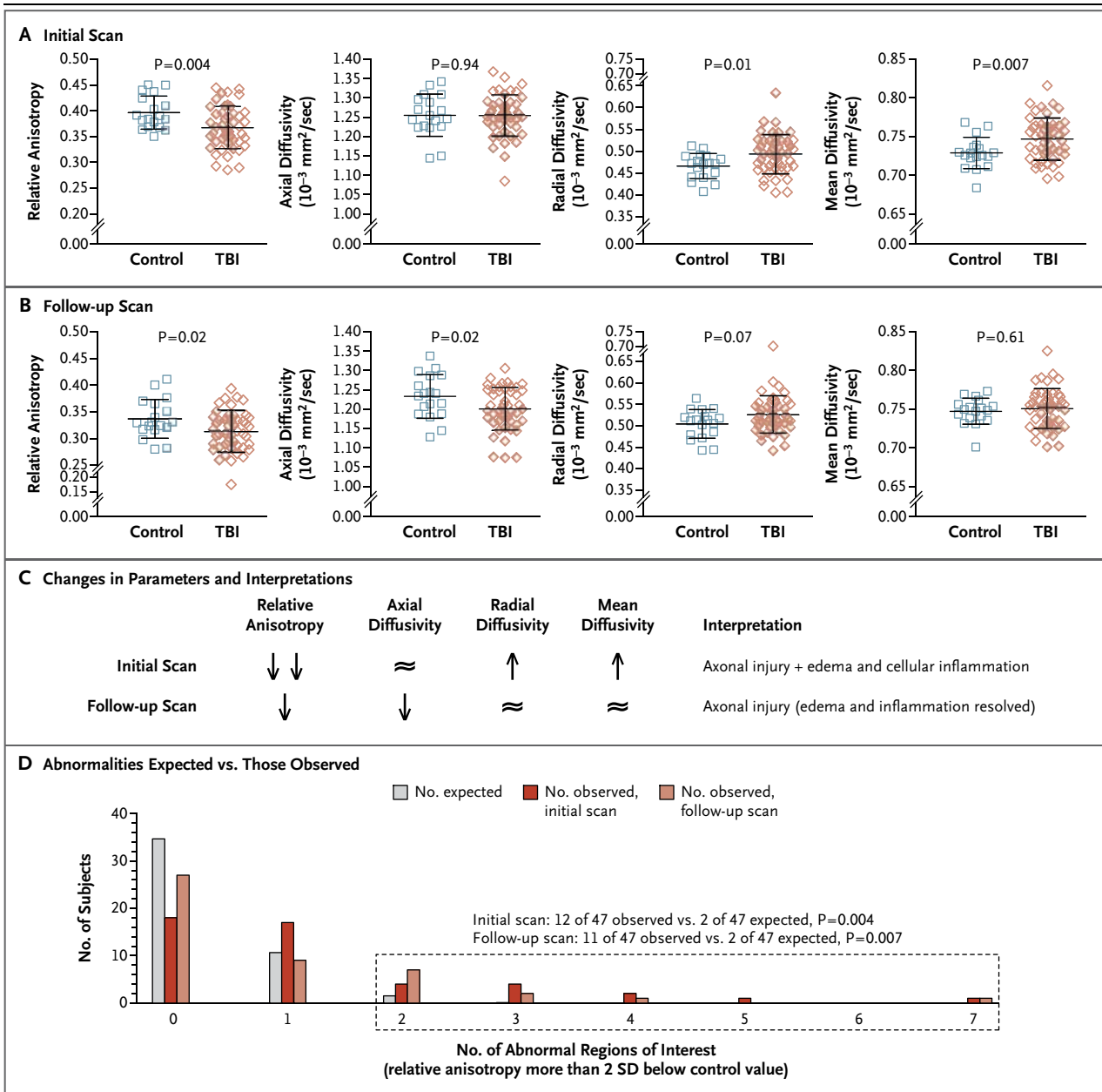


Figure 4. Evolution of Abnormalities over Time as Assessed with Diffusion Tensor Imaging.

All data in Panels A through D are from the 18 controls and 47 subjects with traumatic brain injury (TBI) who underwent both initial and follow-up diffusion tensor imaging (DTI). The formulas for calculating relative anisotropy, axial diffusivity, radial diffusivity, and mean diffusivity are available in Figure S1 and S8 in the Supplementary Appendix. In Panels A and B, the longer horizontal lines indicate the means and the I bars indicate standard deviations. Panel A shows the results of the initial scans (obtained within 90 days after injury) in the cingulum bundles, with reduced relative anisotropy, increased radial diffusivity, and increased mean diffusivity in the subjects with TBI as compared with the controls. Panel B shows the follow-up scans (obtained 6 to 12 months after study enrollment) in the cingulum bundles, with reduced relative anisotropy and reduced axial diffusivity. Panel C shows the changes in DTI parameters between initial and follow-up scanning in subjects with TBI as compared with controls and the interpretation of these changes (see also Fig. S4 in the Supplementary Appendix). The double arrows indicate more extensive reduction in relative anisotropy; the ≈ symbol indicates that there was no significant difference between subjects with TBI and controls. Panel D shows differences in observed versus expected DTI abnormalities on initial and follow-up scans in the 47 subjects with TBI. The dotted box indicates the group of subjects with two or more abnormal regions of interest.

We have not been able to address questions regarding isolated primary blast-related traumatic brain injury. All our subjects had primary blast exposure plus another blast-related mechanism of injury, indicating that the incidence of isolated primary blast-related traumatic brain injury may be low (see the Discussion section in the Supplementary Appendix).

Our cohort consisted of active-duty U.S. military personnel with injuries or medical conditions severe enough to prompt commanding officers and medical personnel to at least temporarily remove them from duty. It is not known whether these subjects are representative of all U.S. military personnel with mild traumatic brain injury sustained in Iraq or Afghanistan. Military personnel were brought to the LPMC for a variety of reasons, the most common of which was to obtain specific types of medical care that were not available in Iraq or Afghanistan. Examples include consultations with specialists, certain surgical procedures, and radiologic studies such as MRI. It is possible that many of the subjects with the most mild injuries were returned to duty without being sent to the LPMC.³² Thus, there is a possibility of selection bias toward more seriously injured patients in our cohort. The LPMC serves as a central triage point for the wars in Iraq and Afghanistan; it is not yet possible to perform MRI-based studies in Iraq and Afghanistan because functioning scanners are not currently available to the U.S. military medical system in those countries.

Because DTI can be performed relatively quickly on the MRI scanners at U.S. military facilities and civilian hospitals, DTI-based assessments may be useful in diagnosis, triage, and treatment planning in clinical practice. The analytic methods used here allowed assessment of individual patients with traumatic brain injury, just as it would in a clinical setting. However, it must be emphasized that only 18 of the 63 subjects with traumatic brain injury had definitively abnormal scans

when the scans were analyzed individually. For now, mild traumatic brain injury remains primarily a clinical diagnosis. Normal findings on a DTI scan do not rule out traumatic brain injury, nor are DTI findings in isolation sufficient to make this diagnosis with certainty (see the Discussion section in the Supplementary Appendix).

The relationship between DTI abnormalities and clinical outcomes in U.S. military personnel has yet to be determined. A great deal of research along these lines has been conducted in civilians with traumatic brain injury.^{20,21,31,33-38} However, unique aspects of traumatic brain injury sustained by military personnel include blast injuries and the high rate of post-traumatic stress disorder.^{3,39-43} The relationships among blast-related traumatic brain injury, axonal injury, and outcomes that include post-traumatic stress disorder are topics of active research. DTI and other advanced MRI techniques are tools that may be useful in probing these relationships.

The views expressed in this article are those of the authors and do not reflect the official policy of the Department of the Army, Department of the Air Force, Department of Defense, or federal government.

Supported by a grant from the Congressionally Directed Medical Research Program (W81XWH-08-2-0061, to Dr. Brody) and the National Institutes of Health (F32NS062529, to Dr. Mac Donald; 5K23HD053212, to Dr. Shimony; P30NS048056, to Dr. Snyder; P50NS06833, to Drs. Raichle and Snyder; and 5K08NS49237, to Dr. Brody.)

Disclosure forms provided by the authors are available with the full text of this article at NEJM.org.

We thank the participants, their families, the commanding officers, and the clinical care providers for making this study possible; the staff at the LPMC MRI clinic, including Don Albrant, Kenny Caywood, Kelly McKay, Tim McKay, Tim Roberts, Kris Robertson, Carl Russell, Stephen Sauter, M.D., Antoinette Sherman, and Ludwig Williams; the TBI Screening Team at the LPMC, including Marcel Flores, Shawn Nelson, Pamela Nyman, Shawna Scully, M.D., Karen Williams, and Janna Welch; the staff at the LPMC Trauma Program, including Daniel Lovasz, Kathleen Martin, Caroline Tuman, and Linda Wierzechowski; the Washington University assessment team, including Vera Bonsi, Justin Hampton, Leslie Schart, Ph.D., Eric Shumaker, and Elaine Tamez; and Gina D'Angelo, Ph.D., Washington University Statistical Consulting Service.

Dedicated to the memory of John Witherow, who died in July 2010.

REFERENCES

1. Tanielian TL, Jaycox LH, eds. Invisible wounds of war: psychological and cognitive injuries, their consequences, and services to assist recovery. Santa Monica, CA: RAND, 2008.
2. Casscells SW. Traumatic brain injury: definition and reporting. Washington, DC: Department of Defense, October 2007 (memorandum). (<http://mhs.osd.mil/Content/docs/pdfs/policies/2007/07-030.pdf>).
3. Hoge CW, McGurk D, Thomas JL, Cox AL, Engel CC, Castro CA. Mild traumatic brain injury in U.S. soldiers returning from Iraq. *N Engl J Med* 2008;358:453-63.
4. Jones E, Fear NT, Wessely S. Shell shock and mild traumatic brain injury: a historical review. *Am J Psychiatry* 2007; 164:1641-5.
5. Blumberg PC, Scott G, Manavis J, Wainwright H, Simpson DA, McLean AJ. Staining of amyloid precursor protein to study axonal damage in mild head injury. *Lancet* 1994;344:1055-6.

6. Blumbergs PC, Scott G, Manavis J, Wainwright H, Simpson DA, McLean AJ. Topography of axonal injury as defined by amyloid precursor protein and the sector scoring method in mild and severe closed head injury. *J Neurotrauma* 1995;12:565-72.
7. Mott FW. The microscopic examination of the brains of two men dead of commotio cerebri (shell shock) without visible external injury. *J R Army Med Corps* 1917;29:662-77.
8. Benzinger TL, Brody D, Cardin S, et al. Blast-related brain injury: imaging for clinical and research applications: report of the 2008 St. Louis workshop. *J Neurotrauma* 2009;26:2127-44.
9. Chafi MS, Karami G, Ziejewski M. Biomechanical assessment of brain dynamic responses due to blast pressure waves. *Ann Biomed Eng* 2010;38:490-504.
10. Taylor PA, Ford CC. Simulation of blast-induced early-time intracranial wave physics leading to traumatic brain injury. *J Biomech Eng* 2009;131:061007.
11. Peskind ER, Petrie EC, Cross DJ, et al. Cerebrocerebellar hypometabolism associated with repetitive blast exposure mild traumatic brain injury in 12 Iraq War veterans with persistent post-concussive symptoms. *Neuroimage* 2011;54:Suppl 1:S76-S82.
12. Warden DL, French LM, Shupenko L, et al. Case report of a soldier with primary blast brain injury. *Neuroimage* 2009;47:Suppl 2:T152-T153.
13. Bauman RA, Ling G, Tong L, et al. An introductory characterization of a combat-casualty-care relevant swine model of closed head injury resulting from exposure to explosive blast. *J Neurotrauma* 2009;26:841-60.
14. Pierpaoli C, Jezzard P, Basser PJ, Barnett A, Di Chiro G. Diffusion tensor MR imaging of the human brain. *Radiology* 1996;201:637-48.
15. Arfanakis K, Houghton VM, Carew JD, Rogers BP, Dempsey RJ, Meyerand ME. Diffusion tensor MR imaging in diffuse axonal injury. *AJNR Am J Neuroradiol* 2002;23:794-802.
16. Mac Donald CL, Dikranian K, Bayly P, Holtzman D, Brody D. Diffusion tensor imaging reliably detects experimental traumatic axonal injury and indicates approximate time of injury. *J Neurosci* 2007;27:11869-76.
17. Mac Donald CL, Dikranian K, Song SK, Bayly PV, Holtzman DM, Brody DL. Detection of traumatic axonal injury with diffusion tensor imaging in a mouse model of traumatic brain injury. *Exp Neurol* 2007;205:116-31.
18. Dempsey KE, Dorlac WC, Martin K, et al. Landstuhl Regional Medical Center: traumatic brain injury screening program. *J Trauma Nurs* 2009;16:6-12.
19. Mori S, Wakana S, Nagae-Poetscher LM, van Zijl PCM. MRI atlas of human white matter. London: Elsevier, 2005.
20. Niogi SN, Mukherjee P, Ghajar J, et al. Extent of microstructural white matter injury in postconcussive syndrome correlates with impaired cognitive reaction time: a 3T diffusion tensor imaging study of mild traumatic brain injury. *AJNR Am J Neuroradiol* 2008;29:967-73.
21. Wu TC, Wilde EA, Bigler ED, et al. Evaluating the relationship between memory functioning and cingulum bundles in acute mild traumatic brain injury using diffusion tensor imaging. *J Neurotrauma* 2010;27:303-7.
22. Wilde EA, Ramos MA, Yallampalli R, et al. Diffusion tensor imaging of the cingulum bundle in children after traumatic brain injury. *Dev Neuropsychol* 2010;35:333-51.
23. Singh M, Jeong J, Hwang D, Sungkarat W, Gruen P. Novel diffusion tensor imaging methodology to detect and quantify injured regions and affected brain pathways in traumatic brain injury. *Magn Reson Imaging* 2010;28:22-40.
24. Geary EK, Kraus MF, Pliskin NH, Little DM. Verbal learning differences in chronic mild traumatic brain injury. *J Int Neuropsychol Soc* 2010;16:506-16.
25. Lipton ML, Gellella E, Lo C, et al. Multifocal white matter ultrastructural abnormalities in mild traumatic brain injury with cognitive disability: a voxel-wise analysis of diffusion tensor imaging. *J Neurotrauma* 2008;25:1335-42.
26. Inglese M, Makani S, Johnson G, et al. Diffuse axonal injury in mild traumatic brain injury: a diffusion tensor imaging study. *J Neurosurg* 2005;103:298-303.
27. Blumbergs PC, Jones NR, North JB. Diffuse axonal injury in head trauma. *J Neurol Neurosurg Psychiatry* 1989;52:838-41.
28. Strich SJ. Diffuse degeneration of the cerebral white matter in severe dementia following head injury. *J Neurol Neurosurg Psychiatry* 1956;19:163-85.
29. Adams JH, Doyle D, Ford I, Gennarelli TA, Graham DI, McLellan DR. Diffuse axonal injury in head injury: definition, diagnosis and grading. *Histopathology* 1989;15:49-59.
30. Gurdjian ES, Gurdjian ES. Cerebral contusions: re-evaluation of the mechanism of their development. *J Trauma* 1976;16:35-51.
31. Sidaros A, Engberg AW, Sidaros K, et al. Diffusion tensor imaging during recovery from severe traumatic brain injury and relation to clinical outcome: a longitudinal study. *Brain* 2008;131:559-72.
32. Luethcke CA, Bryan CJ, Morrow CE, Isler WC. Comparison of concussive symptoms, cognitive performance, and psychological symptoms between acute blast-versus nonblast-induced mild traumatic brain injury. *J Int Neuropsychol Soc* 2011;17:36-45.
33. Huisman TA, Schwamm LH, Schaefer PW, et al. Diffusion tensor imaging as potential biomarker of white matter injury in diffuse axonal injury. *AJNR Am J Neuroradiol* 2004;25:370-6.
34. Kraus MF, Susmaras T, Caughlin BP, Walker CJ, Sweeney JA, Little DM. White matter integrity and cognition in chronic traumatic brain injury: a diffusion tensor imaging study. *Brain* 2007;130:2508-19.
35. Niogi SN, Mukherjee P, Ghajar J, et al. Structural dissociation of attentional control and memory in adults with and without mild traumatic brain injury. *Brain* 2008;131:3209-21.
36. Perlberg V, Puybasset L, Tollard E, Lhéricy S, Benali H, Galanaud D. Relation between brain lesion location and clinical outcome in patients with severe traumatic brain injury: a diffusion tensor imaging study using voxel-based approaches. *Hum Brain Mapp* 2009;30:3924-33.
37. Wang JY, Bakhadirov K, Devous MD, et al. Diffusion tensor tractography of traumatic diffuse axonal injury. *Arch Neurol* 2008;65:619-26.
38. Lipton ML, Gulko E, Zimmerman ME, et al. Diffusion-tensor imaging implicates prefrontal axonal injury in executive function impairment following very mild traumatic brain injury. *Radiology* 2009;252:816-24.
39. Carlson KF, Kehle SM, Meis LA, et al. Prevalence, assessment, and treatment of mild traumatic brain injury and posttraumatic stress disorder: a systematic review of the evidence. *J Head Trauma Rehabil* 2011;26:103-15.
40. Carlson KF, Nelson D, Orazem RJ, Nugent S, Cifu DX, Sayer NA. Psychiatric diagnoses among Iraq and Afghanistan war veterans screened for deployment-related traumatic brain injury. *J Trauma Stress* 2010;23:17-24.
41. Chemtob CM, Muraoka MY, Wu-Holt P, Fairbank JA, Hamada RS, Keane TM. Head injury and combat-related posttraumatic stress disorder. *J Nerv Ment Dis* 1998;186:701-8.
42. Vasterling JJ, Constans JI, Hannapladly B. Head injury as a predictor of psychological outcome in combat veterans. *J Trauma Stress* 2000;13:441-51.
43. Levin HS, Wilde E, Troyanskaya M, et al. Diffusion tensor imaging of mild to moderate blast-related traumatic brain injury and its sequelae. *J Neurotrauma* 2010;27:683-94.

Supplementary Appendix

This appendix has been provided by the authors to give readers additional information about their work.

Supplement to: Mac Donald CL, Johnson AM, Cooper D, et al. Detection of blast-related traumatic brain injury in U.S. military personnel. *N Engl J Med* 2011;364:2091-100.

SUPPLEMENTAL APPENDIX

Advanced MRI Detection of Blast-Related Traumatic Brain Injury in US Military

Personnel

Christine L. Mac Donald PhD, Ann M. Johnson, Dana Cooper, Elliot C. Nelson MD, Nicole J. Werner PhD, Joshua S. Shimony MD PhD, Abraham Z. Snyder MD PhD, Marcus E. Raichle MD, LTC John R. Witherow MD, LTC Raymond Fang MD, COL Stephen F. Flaherty MD and David L. Brody MD PhD.

Contents:

Supplemental Figures S1-S8 and Tables S1-S5

Supplemental Methods

Supplemental Results

Supplemental Discussion

Supplemental References

SUPPLEMENTAL FIGURES AND TABLES

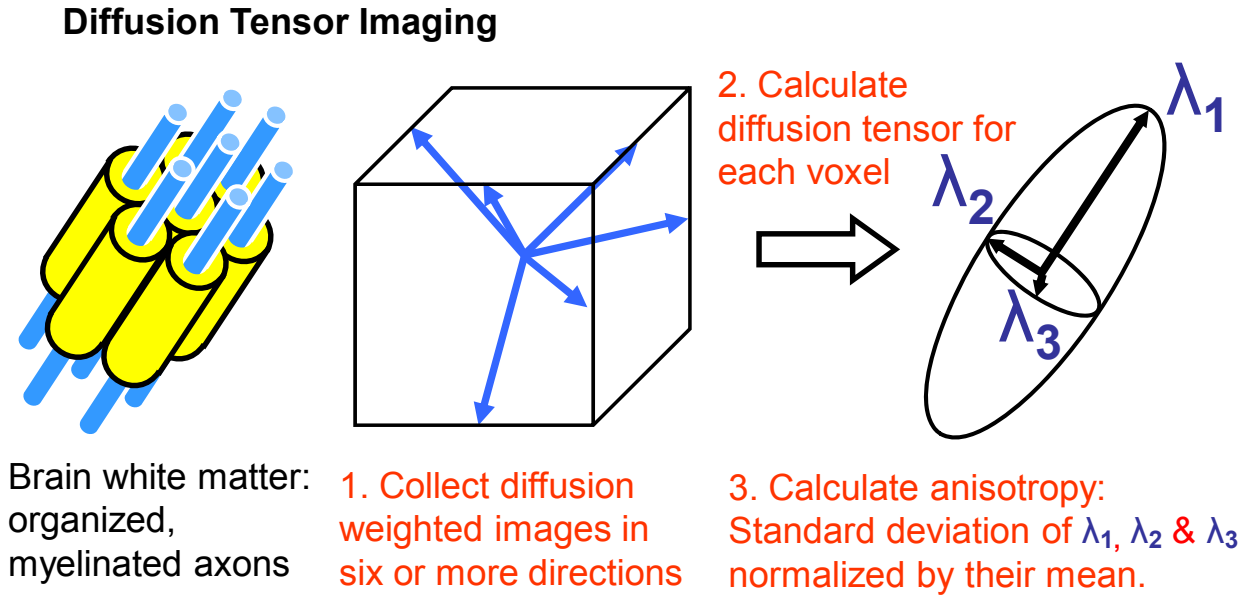


Figure S1: Diffusion Tensor Imaging (DTI) involves measurement of water diffusion in multiple directions and assessment of anisotropy (directional asymmetry) of water diffusion. Anisotropy is high in intact white matter and reduced when axons are injured.¹⁻⁴ A common parameter used for DTI analysis is relative anisotropy, defined as the standard deviation of the 3 principal eigenvalues (λ_1, λ_2 and λ_3) of the diffusion tensor normalized by their mean.

$$\text{Relative Anisotropy} = \frac{\sqrt{(\lambda_1 - \langle D \rangle)^2 + (\lambda_2 - \langle D \rangle)^2 + (\lambda_3 - \langle D \rangle)^2}}{\sqrt{3}\langle D \rangle}, \quad \langle D \rangle = (\lambda_1 + \lambda_2 + \lambda_3)/3$$

(Figure design by M. Budde)

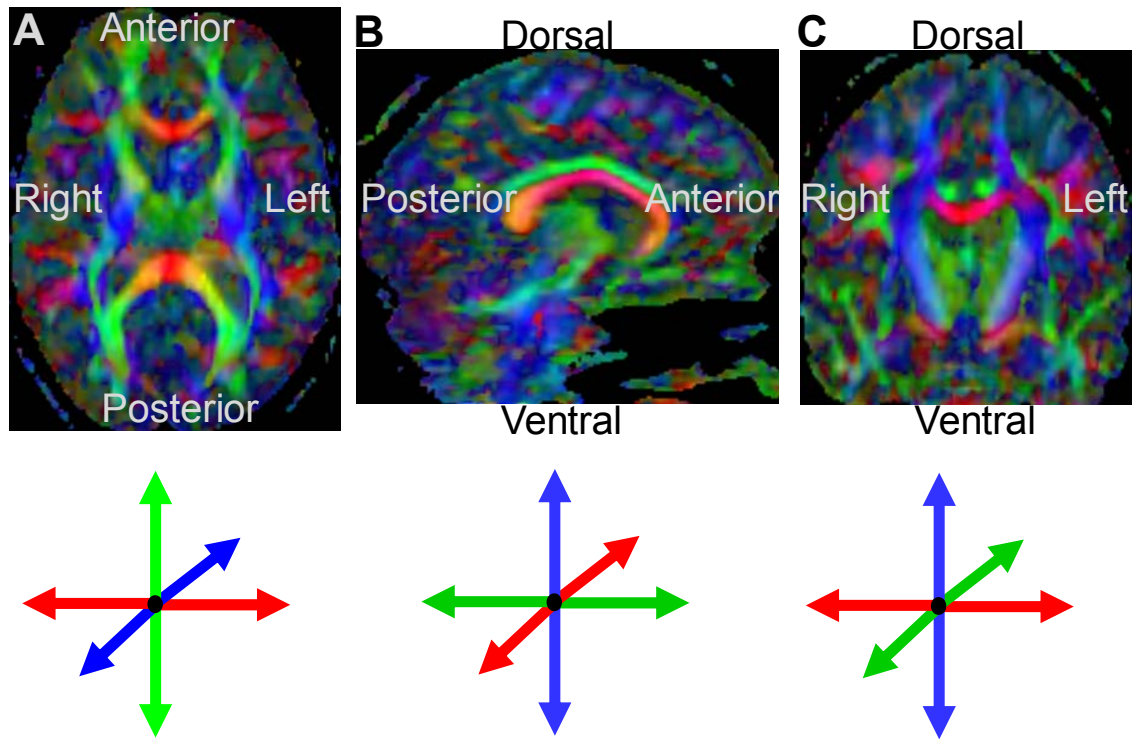


Figure S2: DTI relative anisotropy maps from a control subject. Colors indicate principal diffusion directions: red = right-left, green = anterior-posterior, blue = dorsal-ventral. Brighter colors indicate higher relative anisotropy. **A.** Axial. **B.** Sagittal. **C.** Coronal.

All images displayed in radiological convention, with the subject's right side on the left and left side on the right.

Table S1: MRI Scan Acquisition Protocol						
Scan	In-Plane Resolution (mm)	Slice Thickness (mm)	TE (ms)	TR (ms)	Time (min)	
Scout Image	1 x 1	7	4	8.6	0:13	
T1-Weighted (MP-RAGE)	1 x 1	1	2.92	2000	4:40	
T2-Weighted (BLADE)	0.7 x 0.7	2.5	99	4000	2:32	
Diffusion Tensor Imaging	2.5 x 2.5	2.5	102	10200	4:25	
Diffusion Tensor Imaging	2.5 x 2.5	2.5	102	10200	4:25	
FLAIR	0.8 x 0.8	5	77	9000	4:32	
T2*	1.7 x 1.7	5	63	2780	0:03	
Total Time (min)					20:50	

Table S1: MRI acquisition protocols performed on Siemens Avanto 1.5T MRI scanners at LRMC and Washington University.

MP-RAGE: Magnetization Prepared RApid Gradient Echo

BLADE is not an acronym, but refers to a Siemens radial k-space filling scheme that is less sensitive to motion artifacts.

FLAIR: FLuid Attenuated Inversion Recovery

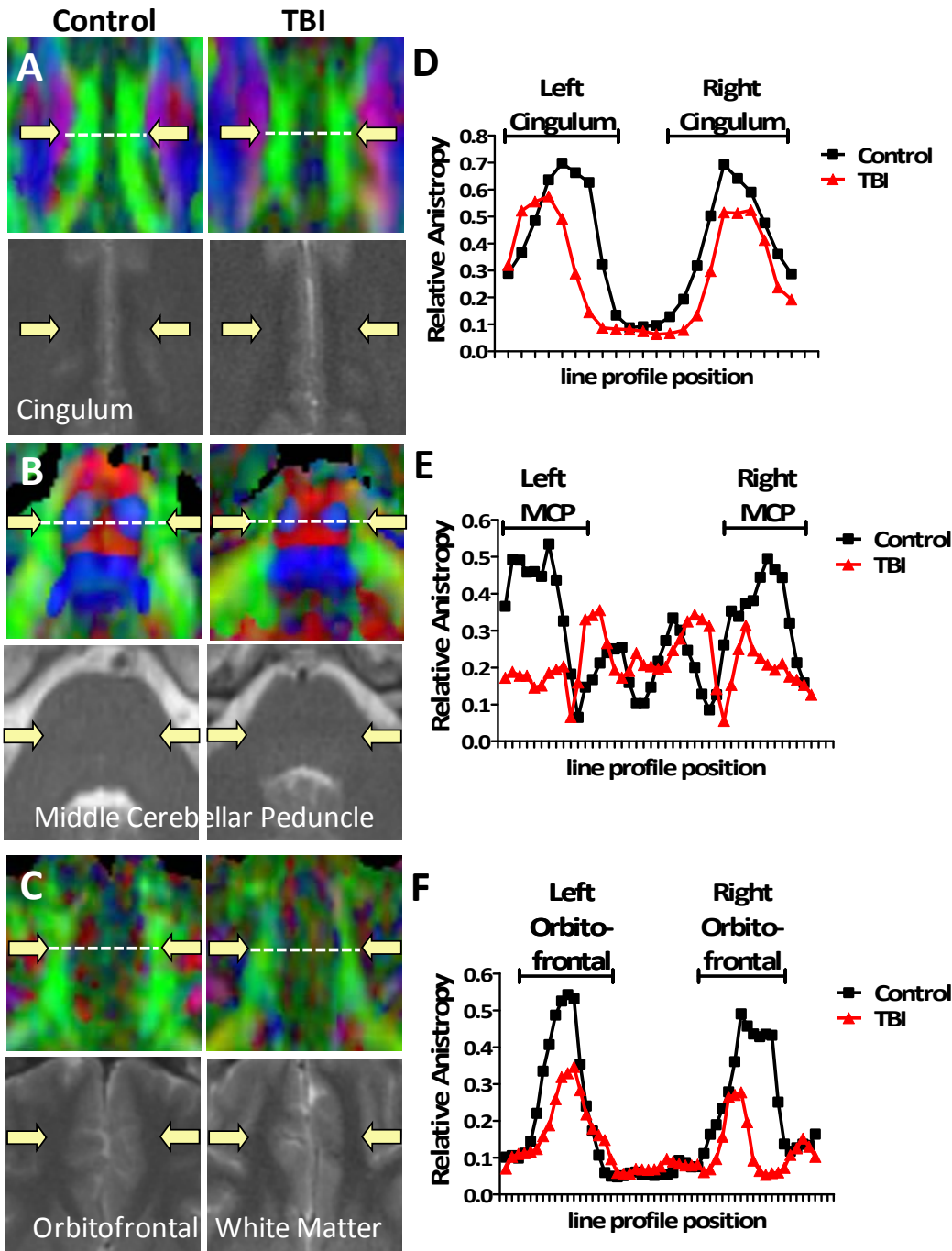


Figure S3: DTI

reveals abnormalities after blast-related TBI that are not apparent on conventional MRI. Top panels: DTI relative anisotropy maps. Arrows indicate regions with abnormally low relative anisotropy (less bright green) on DTI in the TBI subjects compared with controls. Bottom panels: conventional T2-

weighted MRI showing no detectible abnormalities at the same locations in the same subjects. (Small differences in the appearance of the T2 weighted images are due to normal subject-to-subject variability.) **A.** Cingulum bundles. **B.** Middle cerebellar peduncles. **C.** Orbitofrontal white matter. The color intensity scales in the anisotropy maps are all identical; the panels have not been manipulated

individually in any way. Images from 3 individual TBI subjects and 3 individual controls. **D-F.** Line profiles of relative anisotropy as a function of distance along the white lines displayed in panels A-C.

MCP: middle cerebellar peduncle.

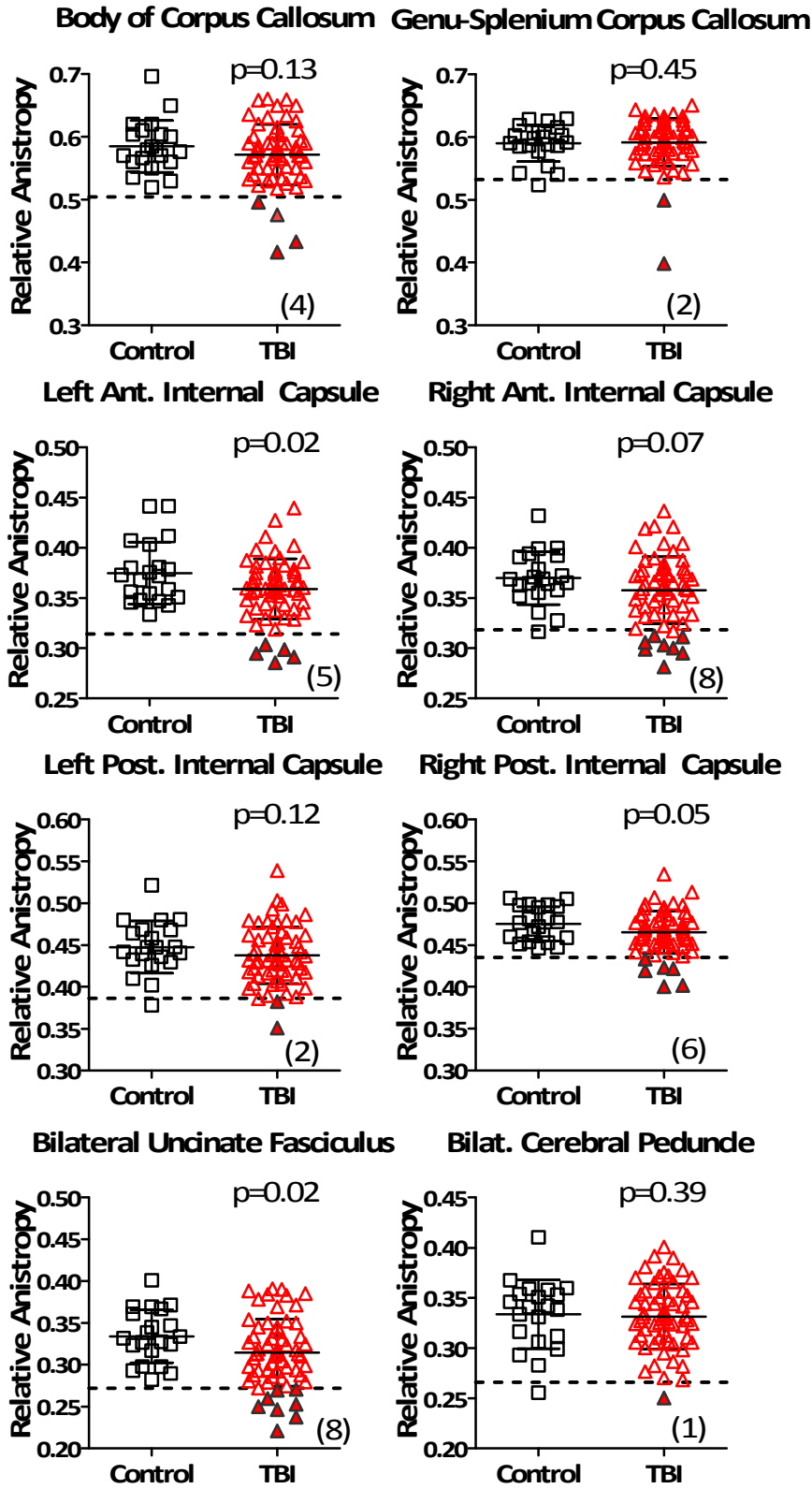


Figure S4: Additional DTI abnormalities in blast-related TBI subjects. Column scatter plots of relative anisotropy in 8 additional regions of interest. P-values indicate 1-sided Student t-tests, as the prespecified hypothesis was that relative anisotropy would be lower in TBI subjects than controls. Bars indicated means and standard deviations. Dashed lines indicate 2 standard deviations below the mean of the control group. Numbers in parentheses indicate the number TBI subjects with relative anisotropy below this cutoff.

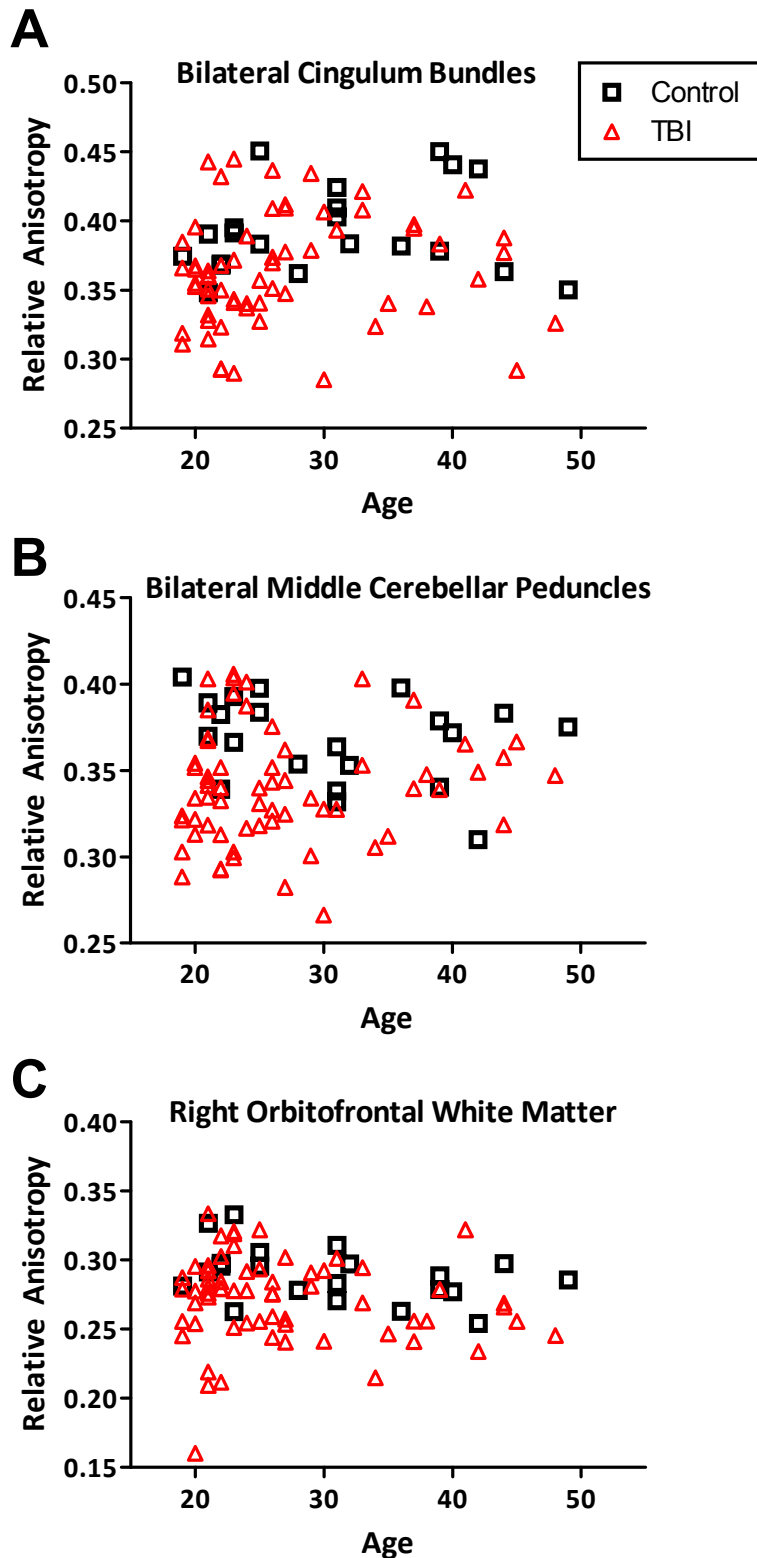


Figure S5: No correlation between age and relative anisotropy in either control or TBI subjects. **A.** Bilateral cingulum bundles. Spearman $r=0.17$, $p=0.22$ for control subjects, $r=0.10$, $p=0.21$ for TBI subjects. **B.** Bilateral middle cerebellar peduncles. Spearman $r=-0.28$, $p=0.11$ for control subjects, $r=0.09$, $p=0.23$ for TBI subjects. **C.** Right orbitofrontal white matter. Spearman $r=-0.38$, $p=0.04$ for control subjects (considered not significant after Bonferroni correction for multiple comparisons), $r=-0.12$, $p=0.17$ for TBI subjects.

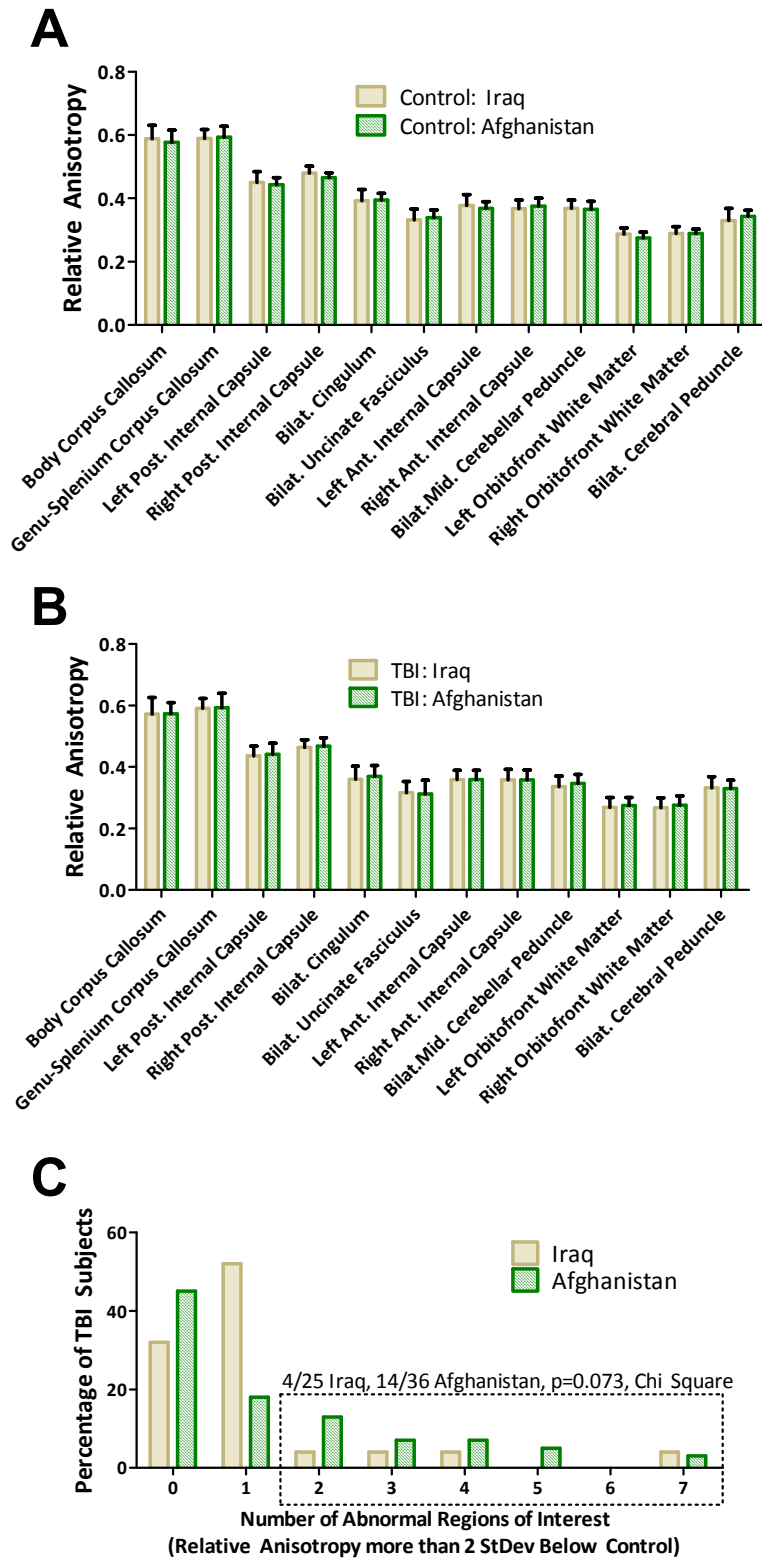


Figure S6: No significant differences in DTI between subjects enrolled following injury in Iraq vs. Afghanistan. **A-B.** No statistically significant differences in relative anisotropy in either the controls or TBI groups. ($p < 0.67$ Hotelling's T^2 -test) **C.** No significant difference in the number of abnormal regions of interest on DTI ($p=0.07$, Chi Square).

Table S2. Propensity Adjusted Analyses						
Relative Anisotropy	Age, Theater, Time to Enrollment			Age, Theater, Time to Enrollment, Army vs. Other Branch		
	CTL (n=21)	TBI (n=63)	p	CTL (n=21)	TBI (n=63)	p
Bilat. Cingulum	0.39 (0.01)	0.36 (0.01)	0.001	0.39 (0.02)	0.37 (0.01)	0.001
Bilat. Middle Cerebellar Peduncle	0.37 (0.01)	0.34 (0.008)	0.0003	0.36 (0.01)	0.34 (0.008)	0.0003
Left Orbitofrontal White Matter	0.28 (0.01)	0.27 (0.007)	0.038	0.28 (0.01)	0.27 (0.007)	0.038
Right Orbitofrontal White Matter	0.29 (0.01)	0.27 (0.007)	0.008	0.29 (0.01)	0.27 (0.007)	0.008
Body Corpus Callosum	0.59 (0.02)	0.57 (0.01)	0.133	0.59 (0.01)	0.57 (0.01)	0.133
Genu-Splenium Corpus Callosum	0.59 (0.02)	0.59 (0.009)	0.445	0.59 (0.01)	0.59 (0.009)	0.445
Left Anterior Internal Capsule	0.37 (0.01)	0.36 (0.008)	0.021	0.37 (0.01)	0.36 (0.008)	0.020
Right Anterior Internal Capsule	0.37 (0.01)	0.36 (0.008)	0.069	0.37 (0.01)	0.36 (0.008)	0.068
Left Posterior Internal Capsule	0.45 (0.01)	0.44 (0.008)	0.126	0.45 (0.01)	0.44 (0.008)	0.126
Right Posterior Internal Capsule	0.47 (0.01)	0.47 (0.006)	0.051	0.47 (0.01)	0.47 (0.006)	0.050
Bilat. Uncinate Fasciculus	0.34 (0.02)	0.31 (0.01)	0.022	0.34 (0.02)	0.31 (0.01)	0.023
Bilat. Cerebral Peduncle	0.34 (0.02)	0.33 (0.01)	0.38	0.33 (0.01)	0.33 (0.008)	0.384

Table S2: Relative Anisotropy values: Means and 95% confidence intervals computed for covariate propensity score at its mean.

P-values: 1-sided Bonferroni post-hoc tests.

Table S3. Propensity Analysis Matching Subset			
Relative Anisotropy	CTL (n=19)	TBI (n=19)	p
Bilat. Cingulum	0.40 (0.03)	0.37 (0.04)	0.01
Bilat. Middle Cerebellar Peduncle	0.37 (0.03)	0.35 (0.04)	0.02
Left Orbitofrontal White Matter	0.28 (0.02)	0.28 (0.03)	0.26
Right Orbitofrontal White Matter	0.29 (0.02)	0.28 (0.03)	0.13
Body Corpus Callosum	0.59 (0.04)	0.58 (0.04)	0.24
Genu & Splenium Corpus Callosum	0.59 (0.03)	0.59 (0.05)	0.28
Left Anterior Internal Capsule	0.38 (0.03)	0.37 (0.03)	0.30
Right Anterior Internal Capsule	0.37 (0.03)	0.37 (0.03)	0.48
Left Posterior Internal Capsule	0.45 (0.03)	0.44 (0.04)	0.30
Right Posterior Internal Capsule	0.48 (0.02)	0.47 (0.03)	0.25
Bilat. Uncinate Fasciculus	0.34 (0.03)	0.31 (0.05)	0.05
Bilat. Cerebral Peduncle	0.34 (0.03)	0.32 (0.02)	0.07
Age (years)	30.6 (9.4)	31.2 (9.5)	0.86
Time to Scan 1 (days)	24.5 (26.7)	31.6 (31.3)	0.46
Iraq / Afghanistan	13 / 6	13 / 6	0.97
Propensity Score	0.68 (0.16)	0.68 (0.15)	0.99

Table S3: Relative Anisotropy values:

Mean and Standard Deviations.

P-values for relative anisotropy and propensity score: 1-sided Student t-tests.

P-values for age and time to scan 1:

Mann-Whitney U test.

P-value for Iraq vs. Afghanistan: Chi Square.

Table S4. Post-Hoc Subgroup Analyses									
Relative Anisotropy	Army Only			Enlisted Only			White/Caucasian Only		
	CTL (n=18)	TBI (n=56)	P	CTL (n=19)	TBI (n=60)	P	CTL (n=17)	TBI (n=45)	P
Bilat. Cingulum	0.39 (0.03)	0.36 (0.04)	*0.0025	0.39 (0.03)	0.36 (0.04)	*0.0024	0.39 (0.03)	0.36 (0.04)	*0.0009
Bilat. Middle Cerebellar Peduncle	0.36 (0.02)	0.34 (0.03)	*0.002	0.37 (0.03)	0.34 (0.03)	*0.0009	0.37 (0.02)	0.34 (0.03)	*0.0002
Left Orbitofrontal White Matter	0.28 (0.02)	0.27 (0.03)	*0.025	0.28 (0.02)	0.27 (0.03)	*0.025	0.28 (0.02)	0.27 (0.03)	0.08
Right Orbitofrontal White Matter	0.29 (0.02)	0.27 (0.03)	*0.007	0.29 (0.02)	0.27 (0.03)	*0.01	0.29 (0.02)	0.27 (0.03)	*0.02
Body Corpus Callosum	0.56 (0.04)	0.57 (0.05)	0.14	0.59 (0.04)	0.57 (0.05)	0.08	0.59 (0.04)	0.57 (0.05)	0.10
Genu-Splenium Corpus Callosum	0.59 (0.03)	0.59 (0.04)	0.43	0.59 (0.03)	0.59 (0.04)	0.47	0.59 (0.03)	0.60 (0.03)	0.21
Left Anterior Internal Capsule	0.37 (0.03)	0.36 (0.03)	0.05	0.37 (0.03)	0.36 (0.03)	0.04	0.38 (0.03)	0.36 (0.03)	*0.001
Right Anterior Internal Capsule	0.36 (0.03)	0.36 (0.03)	0.12	0.37 (0.03)	0.36 (0.03)	0.08	0.37 (0.03)	0.36 (0.03)	*0.03
Left Posterior Internal Capsule	0.45 (0.03)	0.43 (0.03)	*0.03	0.45 (0.03)	0.43 (0.03)	0.08	0.45 (0.03)	0.43 (0.03)	0.08
Right Posterior Internal Capsule	0.48 (0.02)	0.46 (0.03)	0.04	0.47 (0.02)	0.47 (0.03)	0.14	0.47 (0.02)	0.46 (0.02)	0.06
Bilat. Uncinate Fasciculus	0.33 (0.03)	0.31 (0.04)	0.04	0.33 (0.03)	0.31 (0.04)	0.02	0.34 (0.03)	0.32 (0.04)	*0.03
Bilat. Cerebral Peduncle	0.33 (0.03)	0.33 (0.03)	0.45	0.33 (0.03)	0.33 (0.03)	0.44	0.34 (0.03)	0.33 (0.03)	0.17
# of Abnormal Regions of Interest		20	0.0001		20	0.0001		17	0.0001

Table S4: Relative Anisotropy values: Mean and Standard Deviations.

P-values for relative anisotropy: 1-sided Student t-tests,

* significant after Bonferroni correction for multiple comparisons.

P-values for # of Abnormal Regions of Interest: Chi square vs. # expected by chance.

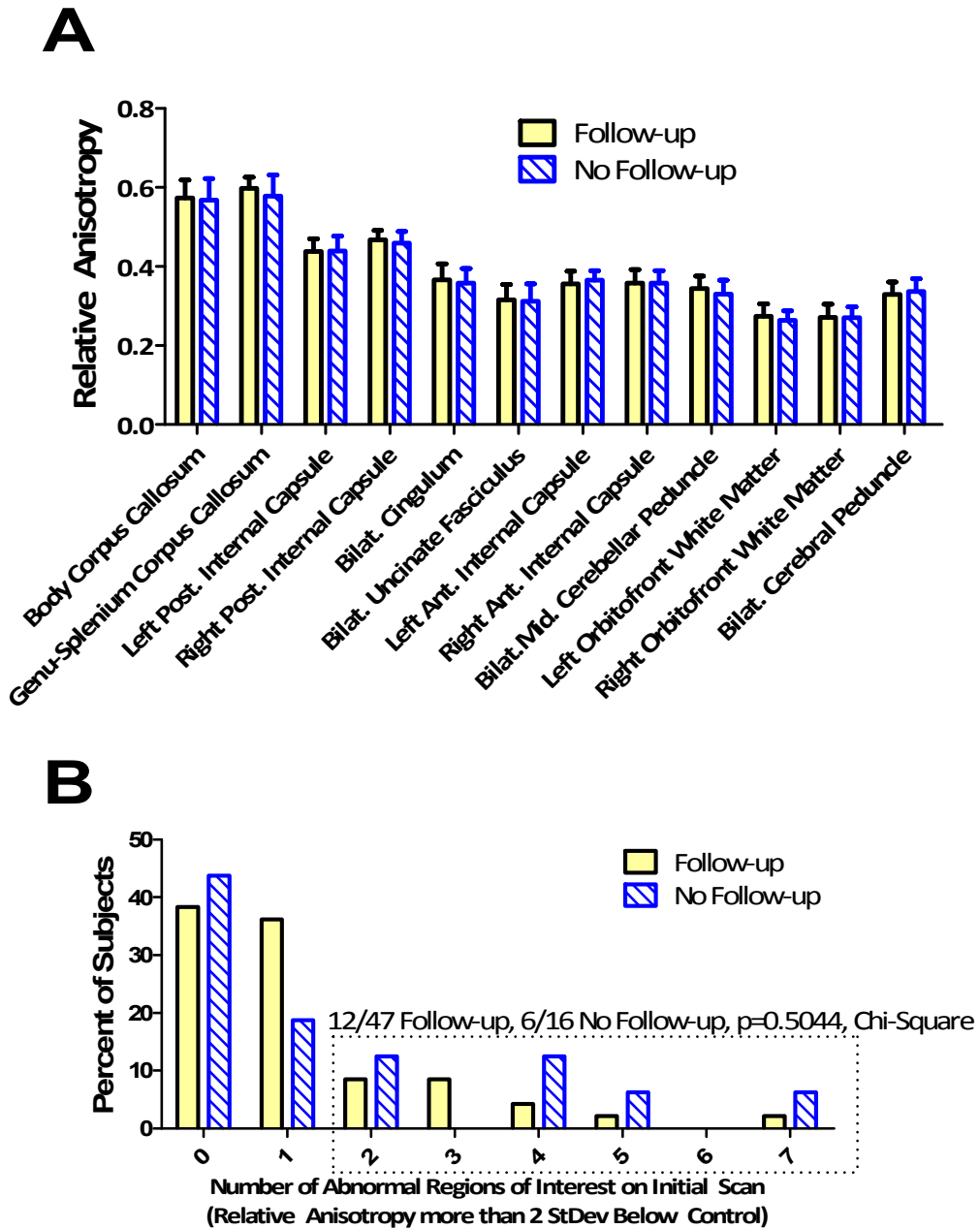


Figure S7: No differences in the initial DTI scans of TBI subjects that completed follow up compared to those that did not. **A.** No significant differences in relative anisotropy across the regions of interest. ($p < 0.24$, Hotelling T^2 -test) **B.** No significant differences in the number of subjects with 2 or more abnormal regions of interest ($p = 0.50$, Chi-square).

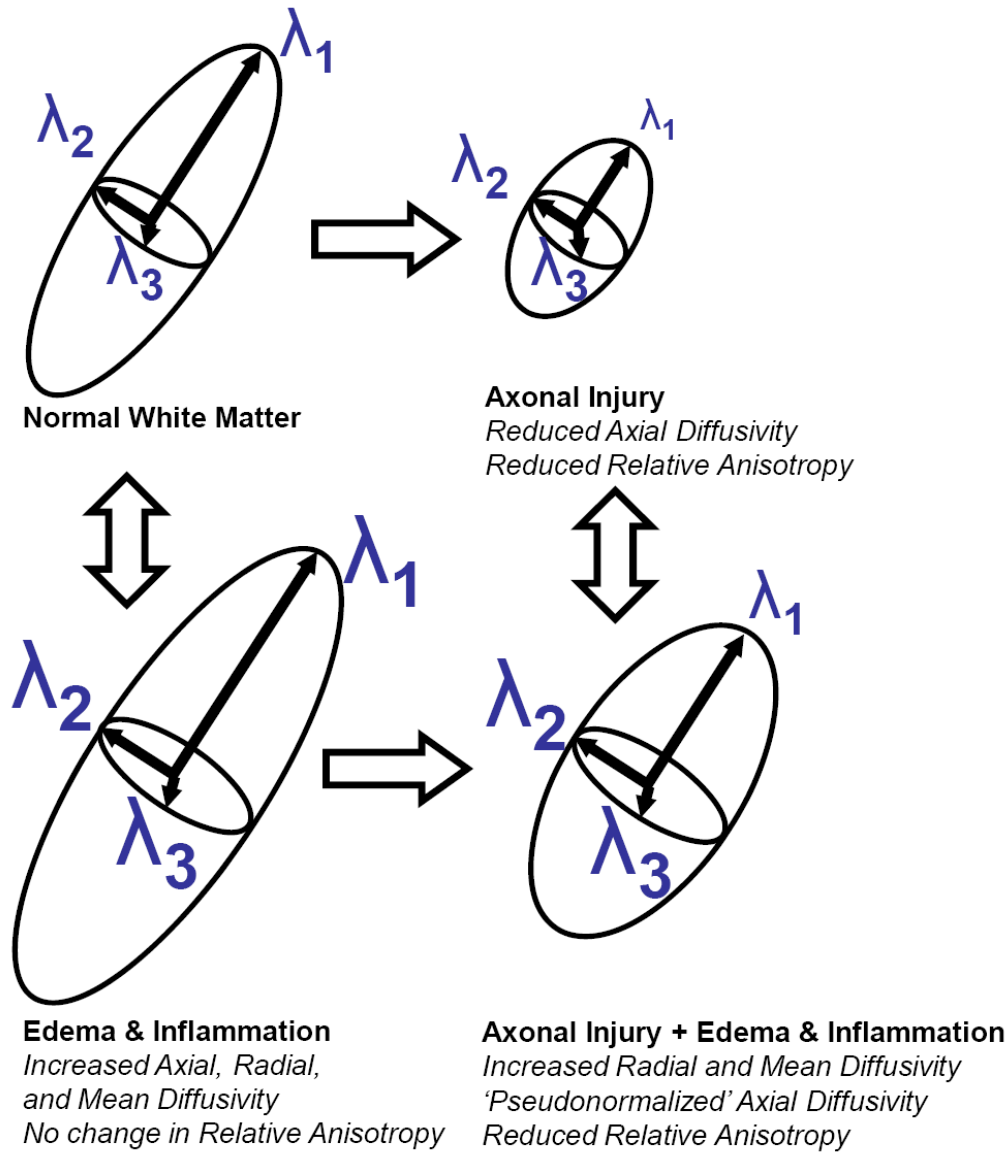


Figure S8: Interpretation of the evolution of DTI parameter abnormalities.

Axial Diffusivity = λ_1 , Radial Diffusivity = $(\lambda_1 + \lambda_2)/2$, Mean Diffusivity =

$\langle D \rangle = (\lambda_1 + \lambda_2 + \lambda_3)/3$. Experimental TBI studies have shown that reduced axial diffusivity correlates histologically with relatively pure axonal injury whereas increased radial and mean diffusivity plus near-normal axial diffusivity correlates histologically with axonal injury plus edema and cellular inflammatory response (i.e. microgliosis).¹

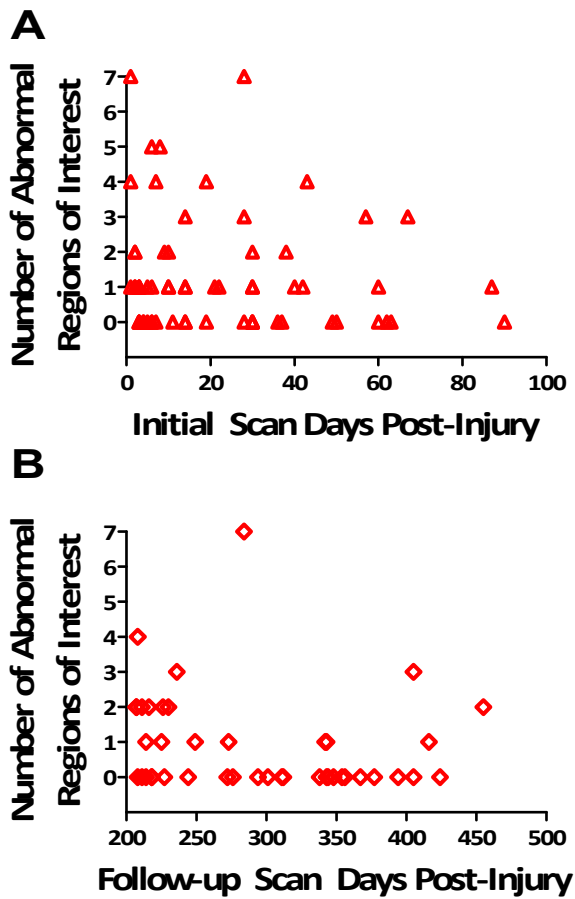


Figure S9: No correlation between the numbers of abnormal brain regions of interest on DTI and time after injury. **A.** Number of abnormalities vs. number of days from injury to initial scan. (Spearman $r=0.14$, $p=0.28$) **B.** Number of abnormalities vs. number of days from injury to follow up scan. (Spearman $r= -0.27$, $p=0.07$)

Table S5. DTI Anisotropy Results

Region of Interest	Relative Anisotropy (RA)			Fractional Anisotropy (FA)		
	CTL (n=21)	TBI (n=63)	p	CTL (n=21)	TBI (n=63)	p
Bilat. Cingulum	0.39 (0.03)	0.36 (0.04)	*0.0015	0.55 (0.04)	0.53 (0.05)	0.01
Bilat. Middle Cerebellar Peduncle	0.37 (0.03)	0.34 (0.03)	*0.0003	0.57 (0.03)	0.53 (0.04)	*0.0007
Left Orbitofrontal White Matter	0.28 (0.02)	0.27 (0.03)	0.04	0.47 (0.03)	0.45 (0.04)	0.09
Right Orbitofrontal White Matter	0.29 (0.02)	0.27 (0.03)	*0.007	0.44 (0.03)	0.42 (0.04)	0.02
Body Corpus Callosum	0.59 (0.04)	0.57 (0.05)	0.13	0.76 (0.02)	0.74 (0.06)	0.09
Genu-Splenium Corpus Callosum	0.59 (0.03)	0.59 (0.04)	0.45	0.76 (0.01)	0.74 (0.08)	0.11
Left Anterior Internal Capsule	0.37 (0.03)	0.36 (0.03)	0.02	0.54 (0.04)	0.53 (0.05)	0.19
Right Anterior Internal Capsule	0.37 (0.03)	0.36 (0.03)	0.07	0.59 (0.03)	0.57 (0.06)	0.04
Left Posterior Internal Capsule	0.45 (0.03)	0.44 (0.03)	0.12	0.65 (0.02)	0.64 (0.05)	0.26
Right Posterior Internal Capsule	0.48 (0.02)	0.47 (0.03)	0.05	0.65 (0.02)	0.64 (0.05)	0.39
Bilat. Uncinate Fasciculus	0.33 (0.03)	0.31 (0.04)	0.02	0.51 (0.04)	0.48 (0.06)	0.04
Bilat. Cerebral Peduncle	0.33 (0.03)	0.33 (0.03)	0.39	0.52 (0.04)	0.52 (0.05)	0.37

Table S5: DTI Anisotropy values: Mean and Standard Deviations.

P-values: 1-sided Student t-tests,

* significant after Bonferroni correction for multiple comparisons

SUPPLEMENTAL METHODS

Regulatory Review: The research protocol was approved by the Human Research Protection Office at Washington University, the Institutional Review Board for LRMC at Brooke Army Medical Center, and the Clinical Investigation Regulatory and Human Research Protection Offices of the U.S. Army Medical Research and Materiel Command. The study was registered at clinicaltrials.gov (NCT00785304).

Written informed consent was obtained in person from all subjects in person at LRMC; no surrogate consent was allowed by the funding agency. Competence to provide informed consent was assessed in a standardized fashion based on responses to questions regarding the purpose of the study, expected requirements for participation, and potential risks. Additional written consent was obtained from the subjects who came for follow-up at Washington University in St Louis. Subjects were assigned a random 4 digit code number to protect confidentiality and all research data were identified by code number only. Active duty military subjects were not paid for participation, though travel expenses to St Louis were covered. Subjects not on active duty subjects at the time of follow-up in St Louis were paid \$240 plus travel expenses for participation.

Definition of Uncomplicated “Mild” TBI: The Department of Defense has defined TBI as follows⁵:

A traumatically induced structural injury and/or physiological disruption of brain function as a result of an external force that is indicated by new onset or worsening of at least one of the following clinical signs immediately following the event:

- 1) Any period of loss of or a decreased level of consciousness*
- 2) Any loss of memory for events immediately before or after the injury*
- 3) An alteration of mental state at the time of the injury (confusion, disorientation, slowed thinking, etc.)*

4) Neurological deficits (weakness, loss of balance, change in vision, praxis, paresis/plegia, sensory loss, aphasia, etc.) that may or may not be transient.

5) Intracranial lesion.

For a TBI to be categorized as “mild” all of the following must be true:

1) Normal structural imaging (CT or conventional MRI)

2) Loss of consciousness for 0-30 minutes

3) Alteration of consciousness or mental state for a moment up to 24 hours

4) Post-traumatic amnesia for 0-1 day.

If any one of these criteria is exceeded, the TBI is categorized as more than “mild”.

Safety and Data Monitoring: Subjects were screened using a hand-held metal detector for objects such as shrapnel that would contraindicate MRI scanning. All x-rays and CT scans acquired for clinical purposes were also reviewed for metallic objects. A standard clinical checklist for MRI contraindications was filled out by each subject prior to each scan. The subjects tolerated MRI scans well with no safety concerns arising.

For MRI scans, quality control for movement artifacts or other technical issues was performed immediately and scans were repeated if technically indicated. All conventional scans were read within 24 hours by a board-certified neuroradiologist at Landstuhl Regional Medical Center for initial scans (J. Witherow) and at Washington University for follow-up scans (J. Shimony). Abnormalities detected in Landstuhl requiring clinical action included a Chiari 1 malformation and an unsuspected intraparenchymal contusion. These two subjects were referred to their treating physicians at LRMC for clinical evaluation. Their imaging data were included in the analyses as the abnormalities were not located near any of the regions of interest.

Differences in absolute DTI parameter values (**Fig. 4**) may be due to subtle differences in hardware between nominally identical Siemens Avanto 1.5T scanners.

Analysis of Imaging Data: DTI data were preprocessed and transformed into standardized Talairach atlas space.^{6,7} Briefly, co-registration of each image set was performed using vector gradient measure (VGM) maximization.⁸ The first acquired, unsensitized ($b = \sim 0 \text{ s/mm}^2$; I0) DTI volume was registered to the T2 image; stretch and shear were enabled (9-parameter affine transform) to partially compensate for subject motion and eddy current distortion. T2 was then co-registered similarly to T1. Finally, atlas transformation was computed via the T1 weighted image, which itself was registered to an atlas representative target. The target atlas was produced by mutual coregistration of T1 images from a separate group of 12 normal young adults and conformed to the Talairach system.⁹

Additional Statistical Methods: To estimate the number of DTI abnormalities expected to occur by chance in each subject, the binomial distribution was used with $p=0.02275$ and $n=12$ regions of interest assumed to be statistically independent. This p-value corresponds to the fractional area under the normal distribution 2 or more standard deviations below the mean.

Specifically, the expected probability of m abnormalities was calculated as follows:

$$Pr(\text{Number of abnormalities} = m) = \binom{n}{m} p^m (1 - p)^{n-m}$$

Where $\binom{n}{m}$ (“ n choose m ”) is the number of possible ways a set of m items can be chosen from a group of n items:

$$\binom{n}{m} = \frac{n!}{m!(n-m)!} = \frac{n(n-1)(n-2) \dots}{m(m-1)(m-2) \dots (n-m)(n-m-1)(n-m-2) \dots}$$

The expected numbers of abnormalities are based on the assumption that the regions of interest are statistically independent. We found no evidence for correlation between the regions of interest, but acknowledge there could be changes in the expected number of abnormalities if there were undetected correlations.

We generated propensity scores¹⁰ for membership in the TBI vs. control groups using logistic regression. The following variables were initially entered into the full model: age, theater (Iraq vs. Afghanistan), race (white/caucasian vs. other), branch (army vs. other), rank (enlisted vs. officer), time to enrollment (days). The full model and several sub-models failed to converge because of sparse cell counts. Two sub-models did converge and were used to generate propensity scores. The first sub-model included age, theater, and time to enrollment. The second sub-model included age, theater, time to enrollment and branch. The propensity scores were then used as covariates in generalized linear models analyses, addressing the question of whether relative anisotropy on the initial scans (the primary DTI variable of interest) in TBI subjects differed from controls. In addition, we analyzed the relative anisotropy data from subgroups of subjects with closely matched propensity scores using the first sub-model. To create the matched subgroups, the nearest neighbor approach was used: For each control subject, the subject from the TBI cohort with the closest matched propensity score was selected. Two control subjects did not have close matches, so a subgroup of 19 controls and their 19 best matched TBI subjects was selected. These subgroups did not differ in propensity score, age, theater, or time to initial scan (Supplementary Table S3).

Author Contributions: The study was conceived by D. Brody and S. Flaherty. The protocol was designed by D. Brody, C. Mac Donald, E. Nelson and N. Werner. The data were gathered by C. Mac Donald, A. Johnson, J. Shimony, J. Witherow, and D. Brody. The data were analyzed by C. Mac Donald, D. Cooper, and D. Brody using methods developed with the assistance of J. Shimony, A. Snyder, and M. Raichle. D. Brody vouches for the integrity of the data and analysis. The figures were prepared by D. Brody and C. Mac Donald. D. Brody wrote the first draft on the manuscript. D. Brody, S. Flaherty and C Mac Donald decided to publish the paper. There were no agreements concerning confidentiality between the sponsor and the authors or institutions other than the requirement that all data be approved by the Operational Security offices at LRMC and Walter Reed Army Hospital.

SUPPLEMENTAL RESULTS

We used relative anisotropy (RA) as the primary outcome measure for DTI analyses. For comparison with other studies using fractional anisotropy (FA), we have also calculated fractional anisotropy for each of the regions of interest (**Supplementary Appendix, Table S5**). This indicated that the choice of relative anisotropy (RA) vs. fractional anisotropy (FA) analysis did not affect any of the central results of the study, though for some regions of interest, the difference between groups was more statistically significant for RA (e.g. cingulum bundles, right orbitofrontal white matter)

We tested the possibility that some TBI patients would have elevated RA rather than reduced RA.^{11 12} Of the 63 TBI subjects enrolled, 4 subjects had one region of abnormally high RA on the initial MRI scan and one subject had 2 regions of abnormally high RA. Abnormally high RA was defined as RA greater than two standard deviations above the mean RA in the control group for each region. These subjects were scanned 3 days, 3 days, 30 days, 43 days, and 50 days after injury. The number of subjects with abnormally high RA is not more than would be expected by chance (20 subjects with one abnormally high RA region and 2 subjects with 2 abnormally high RA regions.) Furthermore, there was no indication that increased RA was specifically associated with initial scans at early times after TBI.

Follow-up scans at Washington University were obtained 6-12 months after enrollment in 47/63 TBI subjects and 18/21 controls (**Fig. 2**). Reasons for inability of 19 subjects (3 controls and 16 with TBI) to follow-up included inability or unwillingness to travel to St. Louis (10 subjects), withdrawal of consent (4 subjects), inability to maintain telephone or email contact (2

subjects), severe psychiatric illness (1 subject), redeployment overseas (1 subject), and other severe illness (1 subject).

There was no detectible correlation between the time interval from injury to initial scan and the number of abnormalities detected (**Supplementary Appendix, Fig. S9A**). Likewise, the interval between injury and follow-up scan had a modest, non-significant correlation with the number of abnormalities detected ($r = -0.27$, $p = 0.07$, **Supplementary Appendix, Fig. S9B**).

SUPPLEMENTAL DISCUSSION

There are several possible explanations for the pattern of white matter abnormalities seen in our cohort of subjects. Based on animal studies, computer simulations, PET scan data, and a case report with MRI data, we formulated the hypothesis that cerebellar and other posterior fossa tracts would be especially vulnerable to primary blast injuries. Based on this hypothesis, the distribution of abnormalities can best be accounted for as an admixture of traumatic axonal injury in brain regions vulnerable to primary blast and regions vulnerable to other mechanism of brain injury. However, we cannot rule out the possibility that primary blast injuries sensitized the posterior fossa white matter to the effects of additional injuries. Pure primary blast-related TBI seems to be quite rare, so it will be challenging to address this directly from clinical data. However, this ‘sensitization’ hypothesis could be tested experimentally in animal models.

A limitation of this study is that primary blast injury was not studied in isolation. However, the consequent limitation of generalizability is likely to be minor. We have re-reviewed the relevant literature on the topic of blast-related TBI. Warden et al described a patient with concussive symptoms and cerebellar abnormalities on MRI following exposure to several

explosions, but without any secondary, tertiary or additional mechanisms of injury.¹³ They stated, “This is the first case known to us of CNS intraparenchymal injury following primary blast concussion.” Murray et al. reported 41 head injuries due to IED/mortar attacks, but did not state whether these caused TBI, nor whether they were isolated primary blast vs. additional mechanisms.¹⁴ The two case reports by Okie did not indicate whether there was isolated blast injury vs. additional mechanisms.¹⁵ Warden, in her 2006 review¹⁶, stated that, “because of the nature of blasts in a war environment, most casualties have experienced some mechanical injury (secondary or tertiary blast) as well as any contribution from the primary blast wave.” Xydakis et al. did not describe whether blast exposures causing loss of consciousness were associated with other mechanisms of injury.¹⁷ The RAND Report survey did not collect information on mechanism of injury.¹⁸ Hoge et al. did not report whether their blast-injured subjects had isolated primary blast injury vs. additional mechanisms.¹⁹ Likewise, Peskind et al. did not specify whether their blast injury exposed subjects had isolated primary blast injury vs. additional mechanisms.²⁰ Similarly neither Levin et al nor Belanger et al. specified whether their blast-injured subjects had isolated primary blast injury vs. additional mechanisms.^{21,22} Belanger et al stated that “TBI that is exclusively due to blast may be unusual. The force of the blast may propel the individual or nearby objects, thereby increasing the likelihood of secondary injuries (that are due to blunt force trauma rather than the pressure wave).” The recently released report by Luethcke et al. describes an attempt to assess injury mechanism by detailed clinical interview.²³ They state, “In cases in which participants were exposed to primary and other mechanisms of blast injury, participants were categorized based on whether primary blast injury was the most proximal cause of injury. For example, if a blast overturned a service member’s vehicle, two potential head injury mechanisms could exist (i.e., blast and MVA). If no evidence

for a nonblast mechanism was reported or could be identified, the injury was coded as a blast injury. If, however, a nonblast mechanism was clearly related to the injury (e.g., the service member remained conscious up until the point of striking his head against the door frame), the mechanism of injury was coded as a nonblast injury.” They do not specifically report whether there were any cases of isolated primary blast injury in their cohort, vs. cases where the primary blast injury was the most proximal cause of injury but other injury mechanisms occurred as well. Thus, at present we are aware of only 1 well-documented case of isolated primary blast TBI in the literature.

Our study found statistically significant DTI abnormalities, whereas a previous study of chronic mild blast-related TBI subjects did not.²² Our study involved earlier DTI scans, a larger and potentially more representative cohort of participants, and a different and potentially more sensitive analytical approach. The differences in the timing of the scans relative to the injury did not seem to be the main factor accounting for our results; initial and follow-up scans in our study had comparable overall sensitivity to abnormalities at the individual subject level (**Fig. 4C**). However, group differences in DTI parameters appeared to be greater at initial scans than at follow-up 6-12 months later (**Fig. 4A-B**).

As a clinical diagnostic, our criterion for a definitively abnormal scan (2 or more DTI abnormalities in 12 brain regions) would have a sensitivity of 29% and an expected specificity of 97%. While modest, this is a substantial improvement over CT and conventional MRI which had 1.5% sensitivity in this cohort. This sensitivity estimate is based on the assumption that all of the subjects with a clinical diagnosis of TBI had structural injury to the brain. This assumption may not be correct: some may have structural injury, some may have injury-related physiological derangements^{20,24}, and some may have had other responses to injury that could not be

distinguished clinically from TBI.²⁵ Likewise, it is possible that some of the control subjects had unreported TBI related to blast or other events. This would also have reduced the sensitivity of our approach.

The sensitivity of DTI could potentially be improved in several ways. Pre-deployment imaging in military personnel or others at high risk of sustaining blast-related TBI could be especially helpful. There was moderate variability between subjects' DTI values in the control group. This may have obscured some abnormalities when a threshold at 2 standard deviations below the mean of the control group was applied. Differences between post-injury scans and pre-injury scans in individual patients would be expected to be more sensitive than comparisons of single scans with a normal control group. Improved DTI signal-to-noise, more advanced analytical methods, and possibly the assessment of additional brain regions could improve the sensitivity as well.

An alternative explanation for the specific pattern of DTI abnormalities observed on the initial scans is that demyelination primarily underlies the increase in radial and mean diffusivity.^{26,27} This would suggest that is that these changes on the follow-up scans were due to resolution of earlier demyelination plus markedly delayed axonal injury. This alternative is less biologically plausible. Furthermore, we cannot definitively distinguish between vasogenic and cytotoxic edema without direct histological validation. Previous reports have considered a reduction in mean diffusivity an indication of cytotoxic edema^{12,28} while increases in ADC have been reported in experimental animal models of TBI to be attributed to vasogenic edema.²⁹ We observed an increase in mean diffusivity in our study which is more likely due to vasogenic edema. The exact interpretation of DTI signal abnormalities is still an area of active

investigation, and direct radiological-pathological correlations in the human brain will be required to definitively address this issue.

There has been debate in the literature about the relative merits of RA vs. FA. Both are valid measures of diffusion anisotropy, and both are likely to be sensitive to disruption of normal white matter integrity. They differ in the way that the variability between the 3 eigenvalues is quantified:

$$\text{Relative Anisotropy} = \frac{\sqrt{(\lambda_1 - \langle D \rangle)^2 + (\lambda_2 - \langle D \rangle)^2 + (\lambda_3 - \langle D \rangle)^2}}{\sqrt{3}\langle D \rangle}, \quad \langle D \rangle = (\lambda_1 + \lambda_2 + \lambda_3)/3$$

$$\text{Fractional Anisotropy} = \sqrt{\frac{1}{2} \frac{\sqrt{(\lambda_1 - \lambda_2)^2 + (\lambda_2 - \lambda_3)^2 + (\lambda_1 - \lambda_3)^2}}{\sqrt{\lambda_1^2 + \lambda_2^2 + \lambda_3^2}}}$$

It is agreed that RA varies linearly with the eigenvalues and that FA does not³⁰ thus providing more desirable characteristics when performing signal to noise (SNR) analysis. Some have reported that FA has higher SNR³¹, others claim they are essentially equivalent³², while a more recent report suggests benefits of RA.³³ Our own internal data demonstrate no SNR differences. We have published RA values for many years^{1,2,6,7} so our preference is to continue doing so, although ours may be a minority opinion.

We have used the term ‘traumatic axonal injury’ to refer to damage to brain white matter tracts. We prefer the term ‘traumatic axonal injury’ over the term ‘diffuse axonal injury’ because it is clear that axonal injury is not diffusely distributed throughout the brain in our mild TBI patients nor in many more severely injured patients.³⁴⁻⁴¹ In fact, ‘focal traumatic axonal injury’ or

‘multifocal traumatic axonal injury’ are more accurate descriptors, though the term ‘diffuse axonal injury’ is still used to describe patients with >3 regions of signal abnormality.^{42,43}

SUPPLEMENTAL REFERENCES

1. Mac Donald CL, Dikranian K, Bayly P, Holtzman D, Brody D. Diffusion tensor imaging reliably detects experimental traumatic axonal injury and indicates approximate time of injury. *J Neurosci* 2007;27:11869-76.
2. Mac Donald CL, Dikranian K, Song SK, Bayly PV, Holtzman DM, Brody DL. Detection of traumatic axonal injury with diffusion tensor imaging in a mouse model of traumatic brain injury. *Exp Neurol* 2007;205:116-31.
3. Arfanakis K, Haughton VM, Carew JD, Rogers BP, Dempsey RJ, Meyerand ME. Diffusion tensor MR imaging in diffuse axonal injury. *AJNR Am J Neuroradiol* 2002;23:794-802.
4. Van Boven RW, Harrington GS, Hackney DB, et al. Advances in neuroimaging of traumatic brain injury and posttraumatic stress disorder. *J Rehabil Res Dev* 2009;46:717-57.
5. Casscells S. Traumatic Brain Injury: Definition and Reporting. In: Defense ASo, ed.: Department of Defense; 2007.
6. Shimony JS, Burton H, Epstein AA, McLaren DG, Sun SW, Snyder AZ. Diffusion tensor imaging reveals white matter reorganization in early blind humans. *Cereb Cortex* 2006;16:1653-61.
7. Mac Donald CL, Schwarze N, Vaishnavi SN, et al. Verbal memory deficit following traumatic brain injury: assessment using advanced MRI methods. *Neurology* 2008;71:1199-201.
8. Rowland DJ, Garbow JR, Laforest R, Snyder AZ. Registration of [18F]FDG microPET and small-animal MRI. *Nucl Med Biol* 2005;32:567-72.
9. Talairach J, Tournoux P. Co-Planar Stereotaxic Atlas of the Human Brain. New York: Thieme Medical Publishers; 1988.
10. Rosenbaum PR, Rubin DB. The Central Role of the Propensity Score in Observational Studies for Causal Effects. *Author. Biometrika*, 1983;70:41-55.
11. Bazarian JJ, Zhong J, Blyth B, Zhu T, Kavcic V, Peterson D. Diffusion tensor imaging detects clinically important axonal damage after mild traumatic brain injury: a pilot study. *J Neurotrauma* 2007;24:1447-59.
12. Wilde EA, McCauley SR, Hunter JV, et al. Diffusion tensor imaging of acute mild traumatic brain injury in adolescents. *Neurology* 2008;70:948-55.
13. Warden DL, French LM, Shupenko L, et al. Case report of a soldier with primary blast brain injury. *Neuroimage* 2009;47 Suppl 2:T152-3.
14. Murray CK, Reynolds JC, Schroeder JM, Harrison MB, Evans OM, Hospenthal DR. Spectrum of care provided at an echelon II Medical Unit during Operation Iraqi Freedom. *Mil Med* 2005;170:516-20.
15. Okie S. Traumatic brain injury in the war zone. *N Engl J Med* 2005;352:2043-7.

16. Warden D. Military TBI during the Iraq and Afghanistan wars. *J Head Trauma Rehabil* 2006;21:398-402.
17. Xydakis MS, Bebarta VS, Harrison CD, Conner JC, Grant GA, Robbins AS. Tympanic-membrane perforation as a marker of concussive brain injury in Iraq. *N Engl J Med* 2007;357:830-1.
18. Tanielian TL, Jaycox LH. *Invisible Wounds of War: Psychological and Cognitive Injuries, Their Consequences, and Services to Assist Recovery*: RAND Corporation 2008.
19. Hoge CW, McGurk D, Thomas JL, Cox AL, Engel CC, Castro CA. Mild traumatic brain injury in U.S. Soldiers returning from Iraq. *N Engl J Med* 2008;358:453-63.
20. Peskind ER, Petrie EC, Cross DJ, et al. Cerebrocerebellar hypometabolism associated with repetitive blast exposure mild traumatic brain injury in 12 Iraq war Veterans with persistent post-concussive symptoms. *Neuroimage* 2010; *Advance Online Publication*.
21. Belanger HG, Kretzmer T, Yoash-Gantz R, Pickett T, Tupler LA. Cognitive sequelae of blast-related versus other mechanisms of brain trauma. *J Int Neuropsychol Soc* 2009;15:1-8.
22. Levin HS, Wilde E, Troyanskaya M, et al. Diffusion tensor imaging of mild to moderate blast-related traumatic brain injury and its sequelae. *J Neurotrauma* 2010;27:683-94.
23. Luethcke CA, Bryan CJ, Morrow CE, Isler WC. Comparison of Concussive Symptoms, Cognitive Performance, and Psychological Symptoms Between Acute Blast-Versus Nonblast-Induced Mild Traumatic Brain Injury. *J Int Neuropsychol Soc* 2011:1-10.
24. Bergsneider M, Hovda DA, Lee SM, et al. Dissociation of cerebral glucose metabolism and level of consciousness during the period of metabolic depression following human traumatic brain injury. *J Neurotrauma* 2000;17:389-401.
25. Hoge CW, Goldberg HM, Castro CA. Care of war veterans with mild traumatic brain injury--flawed perspectives. *N Engl J Med* 2009;360:1588-91.
26. Song SK, Sun SW, Ju WK, Lin SJ, Cross AH, Neufeld AH. Diffusion tensor imaging detects and differentiates axon and myelin degeneration in mouse optic nerve after retinal ischemia. *Neuroimage* 2003;20:1714-22.
27. Song SK, Yoshino J, Le TQ, et al. Demyelination increases radial diffusivity in corpus callosum of mouse brain. *Neuroimage* 2005;26:132-40.
28. Gallucci M, Limbucci N, Paonessa A, Caranci F. Reversible focal splenic lesions. *Neuroradiology* 2007;49:541-4.
29. Barzo P, Marmarou A, Fatouros P, Hayasaki K, Corwin F. Contribution of vasogenic and cellular edema to traumatic brain swelling measured by diffusion-weighted imaging. *J Neurosurg* 1997;87:900-7.
30. Ulug AM, van Zijl PC. Orientation-independent diffusion imaging without tensor diagonalization: anisotropy definitions based on physical attributes of the diffusion ellipsoid. *J Magn Reson Imaging* 1999;9:804-13.
31. Hasan KM, Alexander AL, Narayana PA. Does fractional anisotropy have better noise immunity characteristics than relative anisotropy in diffusion tensor MRI? An analytical approach. *Magn Reson Med* 2004;51:413-7.
32. Kingsley PB, Monahan WG. Contrast-to-noise ratios of diffusion anisotropy indices. *Magn Reson Med* 2005;53:911-8.
33. Lobel U, Sedlacik J, Gullmar D, Kaiser WA, Reichenbach JR, Mentzel HJ. Diffusion tensor imaging: the normal evolution of ADC, RA, FA, and eigenvalues studied in multiple anatomical regions of the brain. *Neuroradiology* 2009;51:253-63.

34. Strich SJ. Diffuse Degeneration of the Cerebral White Matter in Severe Dementia Following Head Injury. *Journal of Neurology, Neurosurgery and Psychiatry* 1956;19:163-85.
35. Strich SJ. Shearing of nerve fibres as as cause of brain damage due to head injury. *Lancet* 1961;2:443-8.
36. Adams JH, Doyle D, Ford I, Gennarelli TA, Graham DI, McLellan DR. Diffuse axonal injury in head injury: definition, diagnosis and grading. *Histopathology* 1989;15:49-59.
37. Adams JH, Doyle D, Graham DI, Lawrence AE, McLellan DR. Gliding contusions in nonmissile head injury in humans. *Arch Pathol Lab Med* 1986;110:485-8.
38. Adams JH, Graham DI, Murray LS, Scott G. Diffuse axonal injury due to nonmissile head injury in humans: an analysis of 45 cases. *Ann Neurol* 1982;12:557-63.
39. Blumbergs PC, Jones NR, North JB. Diffuse axonal injury in head trauma. *J Neurol Neurosurg Psychiatry* 1989;52:838-41.
40. Blumbergs PC, Scott G, Manavis J, Wainwright H, Simpson DA, McLean AJ. Staining of amyloid precursor protein to study axonal damage in mild head injury. *Lancet* 1994;344:1055-6.
41. Blumbergs PC, Scott G, Manavis J, Wainwright H, Simpson DA, McLean AJ. Topography of axonal injury as defined by amyloid precursor protein and the sector scoring method in mild and severe closed head injury. *J Neurotrauma* 1995;12:565-72.
42. Duhaime AC, Gean AD, Haacke EM, et al. Common data elements in radiologic imaging of traumatic brain injury. *Arch Phys Med Rehabil* 2010;91:1661-6.
43. Haacke EM, Duhaime AC, Gean AD, et al. Common data elements in radiologic imaging of traumatic brain injury. *J Magn Reson Imaging* 2010;32:516-43.

Title: Disrupted modular organization of resting-state cortical functional connectivity in U.S. military personnel following concussive ‘mild’ blast-related traumatic brain injury[†]

Authors: Kihwan Han, PhD^a, Christine L. Mac Donald, PhD^a, Ann M. Johnson^b, Yolanda Barnes, RN^c, Linda Wierzechowski, RN^c, David Zonies, MD MPH^c, John Oh, MD^c, Stephen Flaherty, MD^c, Raymond Fang, MD^c, Joshua S. Shimony, MD PhD^d, Abraham Z. Snyder, MD PhD^{a,d}, Marcus E. Raichle, MD^{a,d,e,f,g}, David L. Brody, MD PhD^{a,*}

Affiliations:

^aDepartment of Neurology, Washington University School of Medicine, St. Louis, MO, USA

^bCenter for Clinical Studies, Washington University School of Medicine, St. Louis, MO, USA

^cDepartment of Trauma and Critical Care, Landstuhl Regional Medical Center, Landstuhl, Germany

^dDepartment of Radiology, Washington University School of Medicine, St. Louis, MO, USA

^eDepartment of Neurobiology, Washington University School of Medicine, St. Louis, MO, USA

^fDepartment of Biomedical Engineering, Washington University School of Medicine, St. Louis, MO, USA

^gDepartment of Psychology, Washington University School of Medicine, St. Louis, MO, USA

Corresponding author: David L. Brody, MD PhD

Department of Neurology

Washington University in St. Louis

660 South Euclid Avenue, Box 8111

St. Louis, MO, 63110

USA

Email: brodyd@neuro.wustl.edu

Tel: 1-314-362-1381

Fax: 1-314-362-3279

[†]The views and opinions expressed in this article are those of the authors and do not reflect the official policy or position of the Department of the Army, Department of the Air Force, Department of Defense or United States Government.

ABSTRACT

Blast-related traumatic brain injury (TBI) has been one of the “signature injuries” of the wars in Iraq and Afghanistan. However, neuroimaging studies in concussive ‘mild’ blast-related TBI have been challenging due to the absence of abnormalities in computed tomography or conventional magnetic resonance imaging (MRI) and the heterogeneity of the blast-related injury mechanisms. The goal of this study was to address these challenges utilizing single-subject, module-based graph theoretic analysis of resting-state functional MRI (fMRI) data. We acquired 20 minutes of resting-state fMRI in 63 U.S. military personnel clinically diagnosed with concussive blast-related TBI and 21 U.S. military controls who had blast exposures but no diagnosis of TBI. All subjects underwent an initial scan within 90 days post-injury and 65 subjects underwent a follow-up scan 6 to 12 months later. A second independent cohort of 40 U.S. military personnel with concussive blast-related TBI patients served as a validation dataset. The second independent cohort underwent an initial scan within 30 days post-injury. 75% of scans were of good quality, with exclusions primarily due to excessive subject motion. Network analysis of the subset of these subjects in the first cohort with good quality scans revealed spatially localized reductions in participation coefficient, a measure of between-module connectivity in the TBI patients relative to the controls at the time of the initial scan. These reductions were less prominent on the follow-up scans. The 15 brain areas with the most prominent reductions in participation coefficient were next used as regions of interest (ROIs) for single-subject analyses. In the first TBI cohort, more subjects than would be expected by chance (27/47 versus 2/47 expected, $p < 0.0001$) had 3 or more brain regions with abnormally low between-module connectivity relative to the controls on the initial scans. On the follow-up scans, more subjects than expected by chance (5/37, $p = 0.044$) but fewer subjects than on the initial

scans had 3 or more brain regions with abnormally low between-module connectivity. Analysis of the second TBI cohort validation dataset with no free parameters provided a partial replication; again more subjects than expected by chance (8/31, $p = 0.006$) had 3 or more brain regions with abnormally low between-module connectivity on the initial scans, but the numbers were not significant (2/27, $p = 0.276$) on the follow-up scans. A single-subject, multivariate analysis on the identified ROIs, showed that both TBI cohorts had TBI patients with relatively 'abnormal' between-module connectivity in a fairly consistent manner. Taken together, these results indicate that single-subject, module-based graph theoretic analysis of resting-state fMRI provides potentially useful information for concussive blast-related TBI if high quality scans can be obtained. The underlying biological mechanisms and consequences of disrupted between-module connectivity are unknown, thus further studies are required.

Key words: functional connectivity; traumatic brain injury; graph theory; modularity; functional magnetic resonance imaging (fMRI); blast injury

INTRODUCTION

Traumatic brain injury (TBI) has been called a “signature injury” in the wars of Iraq and Afghanistan (Okie, 2006). As of the first quarter of 2012, the total incidence of TBI in U.S. military personnel since 2000 is 244,217 with 76.8% of these incidents are concussive or ‘mild’ TBI (Defense Medical Surveillance System and Theater Medical Data Store, <http://www.health.mil/Libraries/TBI-Numbers-Current-Reports/dod-tbi-worldwide-2000-2012Q1-as-of-120516.pdf>). Concussive or ‘mild’ TBI is characterized by loss of consciousness up to 30 minutes, altered consciousness and mental state up to 24 hours, post-traumatic amnesia up to 24 hours and the absence of abnormalities in computed tomography or conventional magnetic resonance imaging (MRI) (Casscells, 2007). However, utilizing advanced neuroimaging techniques such as functional magnetic resonance imaging (fMRI), diffusion tensor imaging (DTI), magnetoencephalography and electroencephalography, reports have described abnormalities in concussive TBI subjects (e.g., fMRI: Scheibel et al. (2012), Slobounov et al. (2011), Tang et al. (2011); DTI: Levin et al. (2010), Mac Donald et al. (2011), Niogi et al. (2008, 2010), Shenton et al. (2012); fMRI and DTI: Mayer et al. (2011); magnetoencephalography: Castellanos et al. (2010, 2011); electroencephalography and DTI: Sponheim et al. (2011)).

Most of these previous functional neuroimaging studies in TBI have focused on group comparisons and have adopted hypothesis-driven approaches with predefined regions of interest, seed, or networks of interests. However, high individual variability of functional topology (van Essen and Dierker, 2007) is major source of variability in group analysis in healthy normal

subjects. In TBI populations, the heterogeneity of injury types and locations (Doppenberg and Bullock, 1997; Saatman et al., 2008) further increases between-subject variability. In blast-related TBI (bTBI), the heterogeneity is further increased by the variety of blast-related injury mechanisms. Blast-related injuries may occur by (1) blast overpressure inducing mechanical damage to the brain, (2) having the head struck by debris or other objects set in motion by the blast (3) being thrown to the ground or against another stationary object or (4) inhaling toxic fumes, smoke or dust (Finkel, 2006; Warden, 2006). Different combinations of these injury types and other variables such as direction, distance and open field versus enclosed space associated with the blast exposures may make group analysis insufficient for the assessment of bTBI. The aforementioned heterogeneity of concussive bTBI also increases the chance for hypothesis-driven approaches with predefined regions or networks of interest to miss regions or networks with alterations of functional connectivity in concussive bTBI patients. Thus, single-subject based, data-driven approaches would be more meaningful in these heterogeneous concussive bTBI populations.

Recently, graph theory has become increasingly popular in neuroimaging research (see Rubinov and Sporns (2010) and Bullmore and Sporns (2009) for review), offering new insights into the understanding of the brain as a complex network. Several studies (Achard et al., 2006; He et al., 2007; Salvador et al., 2005; van den Heuvel et al., 2008) have found that the brain network has economical ‘small world’ properties having high levels of clustering and short path length for efficient global and local communications (Latora and Marchiori, 2001; Watts and Strogatz, 1998). Early studies of graph theoretic analysis in clinical populations have demonstrated disrupted ‘small world’ properties in patients with dementia of the Alzheimer’s type (Stam et al.,

2006), schizophrenia (Micheloyannis et al., 2006) and epilepsy (Ponten et al., 2007). Taking advantage of the ‘small world’ properties of the brain network, subsequent studies (Chen et al., 2008; Hagmann et al., 2008; He et al., 2009; Power et al., 2011; Valencia et al., 2009; Yeo et al., 2011) have identified modular or community structure of the normal, healthy human brain. With regard to clinical populations, Valencia et al. (2009) raised the possibility that characterizing the modular structure of the brain may be important to understand the brain organization during different pathological or cognitive states. Indeed, graph theoretic analysis of magnetoencephalography data has revealed disrupted modular structure in patients with dementia of the Alzheimer’s type (de Haan et al., 2012).

Another advantage of graph theoretic analyses over simple network approaches is that they do not require assumptions regarding hypothesized (thus predefined) seed regions or networks of interest. Thus, in this regard, graph theoretic analyses are useful in heterogeneous populations. With this advantage in heterogeneous populations over simple network approaches, recent studies (Caeyenberghs et al., 2012; Castellanos et al., 2011; Nakamura et al., 2009) have utilized graph theoretic analyses to provide more comprehensive understanding of abnormal functional connectivity in TBI patients. In particular, Nakamura et al. (2009) demonstrated disrupted ‘small worldness’, defined as the level of clustering relative to path length, of functional networks in patients with moderate to severe TBI. To our knowledge, there are no previous studies that have investigated modular structure in resting-state functional connectivity MRI in patients with bTBI or any other concussive ‘mild’ TBI populations.

In this study, we posited that module-based connectivity in patients with concussive bTBI may be disrupted. In our previous report (Mac Donald et al., 2011), we demonstrated DTI ‘abnormalities’ in white matter integrity of active duty U.S. military personnel with concussive bTBI relative to controls who had blast exposure but no diagnosis of TBI. At the time of the DTI and structural MRI collections in each of these subjects, resting-state blood oxygenation level dependent (BOLD) fMRI scans were also acquired. Here, we assessed modular organization of these active duty U.S. military personnel with concussive bTBI, utilizing whole brain, module-based graph theoretic analysis of these resting-state BOLD fMRI scans. Because of the heterogeneity of the concussive bTBI patients, we investigated module-based resting-state network properties at both the group and single-subject levels.

MATERIALS AND METHODS

2.1 Subjects

Three groups (controls and two TBI cohorts) of active duty U.S. military personnel deployed to the wars in Iraq and Afghanistan participated in this study. All of them had been exposed to blasts in a combat environment. The two TBI cohorts had sustained clinically diagnosed bTBI. The 21 controls (20 males; 19-49 years old with median = 29; 11-17.5 years of education with median = 12.5) had other injuries but screened negative for TBI (Dempsey et al., 2009). The first TBI cohort (TBI I cohort) consisted of a subset of the subjects about which we have reported previously (Mac Donald et al., 2011). Screening, enrollment, and initial scans were performed at the Landstuhl Regional Medical Center (LRMC), a U.S. Military hospital in Landstuhl, Germany. 63 TBI patients (all males; 19-57 years old with median = 25; 8-17 years of education with median = 12) were diagnosed with mild, uncomplicated traumatic brain injury based on the criteria from the Department of Defense (Casscells, 2007), marked by less than 30 minutes of loss of consciousness and the absence of abnormalities in conventional MRI and CT. Post blast exposure time on the initial scans at LRMC were within 90 days (median = 14). After 6-12 months from their initial scans, 65 out of these subjects traveled to Washington University in St. Louis for follow-up scans. More details and demographics of this cohort are in Mac Donald et al. (2011).

The same screening criteria as on the TBI I cohort and controls allowed the second TBI cohort (TBI II cohort) to comprise 40 additional concussive bTBI patients (37 males; 19-44 years old with median = 23; 9-16 years of education with median = 12). The TBI II cohort underwent the initial scans within 30 days (median = 7) after the blast exposure. After 6-12 months from

their initial scans, 32 out of these subjects underwent follow-up scans at Washington University in St. Louis. The first cohort underwent initial scans in 2008-2009 whereas the second cohort was scanned in 2010-2011.

All subjects participated in this study after obtaining written informed consent and this study was approved by the Human Research Protection Office at Washington University, the Institutional Review Board for LRMC at Brooke Army Medical Center, and the Clinical Investigation Regulatory and Human Research Protection Offices of the U.S. Army Medical Research and Materiel Command. This study was also registered at clinicaltrials.gov (NCT00785304).

2.2 MRI data acquisition

Both initial scans at LRMC and follow-up scans in St. Louis were acquired using Siemens Magnetom Avanto 1.5 Tesla MRI scanners (Siemens, Germany) with identical imaging protocols. In each imaging session, three 412.5-second runs (total 1237.5 seconds) of resting-state BOLD fMRI were acquired using a 12-channel phase-arrayed head coil supplied by the manufacturer with T_2^* -weighted blipped EPI sequence (TR/TE = 2500/50 msec; flip angle (FA) = 90°; field of view (FOV) = 25.6 × 25.6 cm; matrix = 64 × 64) to obtain 165 images of each of 30 axial slices (4.0 mm thick) of the whole cerebrum. During resting-state fMRI acquisition, the subjects were asked to remain still during the scan, but no specific requests were made regarding eyes open versus eyes closed and no specific attempts were made to keep subjects awake. In the setting of acute injury, this was not feasible as some subjects had orbital injuries and extracranial injuries and analgesic medications after enrollment. See the discussion for the relevant limitations of the study findings due to these constraints.

For surface reconstruction and alignment to resting-state BOLD fMRI of each subject, the same head coil was used with one high resolution T_1 -weighted sagittal magnetization prepared rapid acquisition gradient echo (MPRAGE) image of the whole brain (TR/TE = 2000/2.92 msec; FA = 8°; FOV = 25.6 × 25.6 cm; matrix = 256 × 256; 176 slices, 1.0 mm thick).

2.3 MRI preprocessing

Briefly, our analyses consisted of cortical surface reconstruction of structural MRI, preprocessing of resting-state BOLD fMRI, projection of BOLD fMRI onto the reconstructed cortical surface, network construction and finally graph theoretic analysis (see Fig. 1). We used Freesurfer (Dale et al., 1999; Fischl et al., 1999a, 2002) for cortical surface reconstruction of structural MRI, AFNI (Cox, 1996) for fMRI preprocessing and SUMA (Saad et al., 2004) for surface mapping and surface-based analysis of fMRI time series. fMRI data were preprocessed in the three dimensional subject-native space of each participant.

[Fig. 1 goes here]

2.3.1 Surface reconstruction of structural imaging

Cortical surface reconstruction (Fig. 1 (a) to (b)) was performed with the Freesurfer image analysis suite (version 5.1.0), online documented and freely available for download (<http://surfer.nmr.mgh.harvard.edu/>). The technical details of these procedures are described in previous publications (Dale et al., 1999; Dale and Sereno, 1993; Fischl et al., 1999a, 1999b, 2001, 2002, 2004a, 2004b; Jovicich et al., 2006; Segonne et al., 2004). Cortical surface reconstruction

results for each image of the subjects were visually inspected to ensure the accuracy of skull stripping, Talairach transformation, gray/white matter boundary (white surface), gray matter/cerebrospinal fluid boundary (pial surface) and cerebral cortex label. When necessary, manual intervention was performed in order for Freesurfer to correctly reconstruct the cortical surface. The surface reconstruction was performed unblinded to group membership. See the discussion for the limitation of this study related to manual intervention and unblindness to group membership.

2.3.2 fMRI preprocessing

Volumetric BOLD fMRI data were preprocessed (Fig. 1(c) to (d)) with standard methods using a modified version of a shell script generated by *afni_proc.py*

(http://afni.nimh.nih.gov/pub/dist/doc/program_help/afni_proc.py.html) from AFNI (Cox, 1996).

Each subject's whole-brain structural images were first skull-stripped and coregistered (affine transform with 12 parameters) to the fifth time point of the first fMRI run. For each fMRI run, the initial four time points were discarded to allow T_1 magnetization saturation. Standard preprocessing methods were then used, including despiking, slice timing correction, motion correction, normalization to whole brain mode of 1000, linear regression and band-pass filtering ($0.009 < f < 0.08$ Hz). At the motion correction stage, the 6 rigid body motion profiles were obtained for the linear regression. After the motion correction, subject masks indicating voxels that have fMRI signal were obtained for each of the subjects. In the linear regression, several sources of signal fluctuation unlikely to be of neuronal origin were regressed out as the nuisance variables: (1) six parameters for the rigid body head motion acquired from the motion correction (Johnstone et al., 2006), (2) the signal averaged over the lateral ventricles, (3) the signal

averaged over a region centered in the deep cerebral white matter, (4) the signal averaged over the whole brain (Fox et al., 2005; see the control analyses and their results for the effects of global signal regression on graph theoretic analysis) and (5) the first temporal derivatives of aforementioned parameters. After the band-pass filtering, motion ‘scrubbing’ (Power et al., 2012) was performed with frame-to-frame head movement rate of 0.12 mm/s and standardized DVARS (<http://www2.warwick.ac.uk/fac/sci/statistics/staff/academic-research/nichols/scripts/fsl/DVARS.sh>) of 1.49 to prevent potential motion artifacts (Power et al., 2012; Satterthwaite et al., 2012; van Dijk et al., 2012). To prevent the introduction of artificial correlations in the fMRI signal between voxels (1) adjacent to each other in space distant in terms of cortical surface topology (e.g., voxels on opposite sides of the midline) or (2) that were located near the boundary of functional subdivisions unrelated to each other in functional connectivity (e.g., primary motor versus primary somatosensory cortex), spatial smoothing was not applied at this preprocessing step (van den Heuvel et al., 2008).

2.3.3 Inter-subject alignment and surface mapping of volumetric fMRI

The total number of mesh nodes in the reconstructed cortical surface by Freesurfer varies across subjects. To allow for cross-subject analysis while preserving geometry of sulcal and gyral patterns in the original surface of each individual and minimizing unnecessary interpolation artifacts (Argall et al., 2006), we used SUMA (Saad et al., 2004) to standardize surface meshes (i.e., coordinates) of each individual (i.e., the total number of mesh nodes is same across subjects and each mesh node corresponds to same anatomical location in each surface of the subjects). When calculating new coordinates, SUMA allowed us to set the total number of mesh nodes in the standard mesh surface of each subject (Fig. 1(e)) to be 11,524 so that the average distance

between two nodes (3.7 mm) is close to the spatial resolution of original volumetric fMRI data (4 mm isotropic) while maintaining topology shown in the original high resolution (1 mm isotropic) structural MRI.

Volumetric functional time series were then projected onto these standard mesh surfaces of each subject by interpolating the time series located along the line between two matching nodes of the white and pial surfaces. For each mesh node, five equally-spaced coordinates were sampled between corresponding white and pial surfaces. At each time point, functional data were projected by averaging across the unique 3D voxels belonging to these coordinates.

Consequently, surface-based functional time series (Fig. 1(f)) contained signal only from voxels within the cortical gray matter. In the same way, the voxel-based subject masks were converted to surface-based subject masks. For more technical details of the surface mapping procedure, readers are referred to Saad et al. (2004). Due to susceptibility artifacts (Ojemann et al., 1997) and inclusion of only cortical areas of surface (i.e., exclusion of the surface areas of the amygdala, putamen, hippocampus, caudate, ventricles and corpus callosum), not all nodes had fMRI signal, and surface-based subject masks indicating existence of fMRI signal on mesh nodes were different across the subjects. Thus, to make a comparison across subjects, further analyses on network measures considered only the mesh nodes (8,977 nodes) having fMRI signal across all subjects. This was performed by obtaining a subject-intersection mask and subsequently applying the intersection mask to surface-based functional time series of each of the subjects.

2.3.4 Quality assurance

We restricted our analysis to the subjects whose data quality was reliable within tolerable range. In the cortical surface reconstruction step, the quality of T₁ images was visually inspected to determine if surface reconstruction was feasible. In fMRI preprocessing, the quality of preprocessed data was visually inspected at each step. After visual inspection, a subset of subjects' data were excluded for following reasons: (1) a superior part of the functional images did not fall within the prescribed FOV due to substantial run-to-run change of head position, (2) intensity variation artifacts of low spatial frequency presumably due to constant oscillating head movement in a certain direction, (3) substantial susceptibility artifacts (Ojemann et al., 1997) in inferior frontal and inferior temporal regions, (4) motion correction failure due to large amount of abrupt motion and (5) lack of fMRI frames due to subject's refusal to stay in the scanner. After motion 'scrubbing', additional subjects' data were excluded if total length of remaining volumes after the 'scrubbing' was less than 4 minutes, the length minimum length required to reliably estimate functional connectivity (van Dijk et al., 2010). See Table I for the details of the number of datasets excluded by this quality assurance procedure.

Visual inspection on each module of the subjects identified by the Louvain algorithm allowed us to verify that, in 1 control, 4 TBI I and 2 TBI II subjects on the initial scans and 1 control and 1 TBI II subjects on the follow-up scans, a substantial portions of nodes were trivial modules or module assignments were severely scattered yielding failure to identify major modules shown in group module assignment maps (Fig. 2). Thus, we conservatively excluded datasets with fragmented modules in subsequent analyses as we were not sure whether these module assignments were results of subjects' condition or merely failures of the module identification algorithm (Table I).

After quality assurance exclusion, we analyzed functional images of 12/21 control subjects on the initial scans, 12/18 controls subjects on the follow-up scans, 47/63 TBI I subjects on the initial scans, 37/47 TBI I subjects on the follow-up scans, 31/40 TBI II subjects on the initial scans and 27/32 TBI II subjects on the follow-up scans for the subsequent network analyses. Thus, 75% of all subjects' data acquired as described above were of sufficient quality for further analyses.

2.4 Network analysis

2.4.1 Network construction

Weighted and undirected networks were constructed (Fig. 1(g)–(i)) for module-based graph theoretic analysis. For the network analysis, a node, a basic element of graph theoretic analysis, was defined as a mesh node in the cortical surface. An edge of the graph was defined from correlation matrix (Fig. 1(g)) whose components are Pearson correlation coefficients of time series at each pair of the mesh nodes in the brain. In other words, the weights of the edges were the correlation coefficients. Correlation coefficients between time series at short-distance nodes (20 mm in Euclidean distance), presumably associated with non-biological origins such as increased correlation by preprocessing and subject motion, were excluded in selecting edges of the graph (Power et al., 2011). The remaining correlation coefficients were thresholded at 3% tie density, i.e., density of the retained strongest correlations, to define edges of the graph (a colored dot and a yellow line in Fig. 1(h) and (i), respectively). Here, only positive correlation coefficients were considered for the network connections, as there is ongoing debate about the

meaning of negative correlations assessed after global signal regression (Anderson et al., 2011; Chai et al., 2012; Chang and Glover, 2009; Fox et al., 2009; Murphy et al., 2009; Saad et al., 2012).

2.4.2 Module identification and module-based network properties

With the constructed binary and undirected brain networks, module-based graph theoretic analysis was performed using brain connectivity toolbox in MATLAB (Rubinov and Sporns, 2010) freely available online (<http://www.brain-connectivity-toolbox.net>) after applying the previously described subject-intersection mask for the nodes having functional times series across all subjects. First, the modules were identified (Fig. 1(j)). After module identification, global and node-specific module-based network properties were obtained.

Identification of modules is a complex and computationally demanding problem. For the module identification, modularity of a weighted and undirected network, Q_M^w , was defined:

$$Q_M^w = \sum_{s=1}^M [l_s / L - (d_s / 2L)^2],$$

where M is the number of modules, l_s is the sum of the weights of all within-module connections in module s , L is the total sum of all weights in the network d_s is the sum of the strength at each node in the module s and strength of a node is sum of the weights of all edges associated with the given node (Newman, 2004; Guimera and Amaral, 2005). In theory, Q_M^w is bounded between 0 and 1 (Newman, 2004; Guimera and Amaral, 2005). $Q_M^w = 0$ when nodes are randomly partitioned or all nodes belong to the same module. Thus, higher modularity means deviations from random networks with no community structure. In practice, modularity of typical networks

with strong modular structure ranges from 0.3 to 0.7, and higher values are rare (Newman and Girvan, 2004). Assuming the brain network has modular structure (i.e., many within-module connections whereas few between-module connections), a module identification algorithm optimizes the total number of modules and the associated module membership of nodes for maximum modularity. For the implementation of our analysis, we used the Louvain algorithm (Blondel et al., 2008), a fast and relatively accurate algorithm, suitable for large networks. Due to “heuristic” nature of this algorithm (i.e., a ‘good enough’ approximation of the exact solution is implemented, resulting in faster execution time), the module identification algorithm was executed ten times. Then, we selected single module identification result from among the 10 executions that yielded the highest modularity to report modularity and assess subsequent module-based network measures. Overall, the variation of modularity over the executions was negligible, as in Blondel et al. (2008). For comparison, we additionally identified modules using the Infomap algorithm (Rosvall and Bergstrom, 2008), another module identification algorithm (See Supplemental Figs S2, S3).

Given the identified modules, weighted within-module degree z -score (Fig. 1(k); Guimera and Amaral, 2005) and weighted participation coefficient (Fig. 1(l); Guimera and Amaral, 2005) were measured at each node of the individual brain network. In calculating within-module degree z -scores and participation coefficients, we excluded trivial and severely fragmented modules whose size is less than 1% of the total number of nodes.

Briefly, weighted within-module degree z -score of node i , z_i^w , measures normalized strength of connections from a node within the corresponding module s . z_i can be written as:

$$z_i^w = (k_i^w(s_i) - \overline{k^w(s_i)}) / \sigma_{k^w(s_i)},$$

where s_i is the module containing node i , $k_i^w(s_i)$, within-module strength, is the total sum of weights of edges connecting node i and all other nodes within s_i , $\overline{k^w(s_i)}$ and $\sigma_{k^w(s_i)}$ are the respective mean and standard deviation of the $k_j^w(s_i)$ for all nodes $j \in s_i$. So, high weighted within-module degree z -score of a node means the node has a larger than expected strength within its own module.

Weighted participation coefficient of node i , PC_i^w , is defined as:

$$PC_i^w = 1 - \sum_{s=1}^M (k_i^w(s) / k_i^w)^2,$$

where $k_i^w(s)$ is the total sum of weights of edges connecting node i and all other nodes in module s and k_i^w , strength of node i , is the total sum of weights of edges connecting between node i and all other nodes in the entire network. Weighted participation coefficient shows how well a node communicates with other modules. Weighted participation coefficient is close to 1 if the distribution of connections at a node across modules is uniform. Weighted participation coefficient becomes 0 if there is no inter-module connection. A high value of weighted participation coefficient means nodes' inter-module connections are 'well-distributed' over multiple modules, thus are likely to span more modules.

Each node-specific measure was then spatially smoothed (10 mm full-width-at-half-maximum (FWHM)) on the cortical surface of each individual. To identify 'abnormal' regions in the TBI patients, we counted the number of patients whose network measures were outside two standard deviations from the mean of the controls.

2.5 Region of interest analysis

In the region of interest (ROI) analysis, the TBI I cohort served as an exploratory dataset to identify functional ROIs exhibiting noticeable difference in node-specific network measures between the controls and TBI patients from the TBI I cohort. The TBI II cohort served as a validation dataset with no free parameters with regard to ROI selection. Surface-based ROIs were selected on the standard mesh template in reference to Destrieux surface atlas (Destrieux et al., 2010) using SUMA (Saad et al., 2004) to define the center of each ROI. Similar to the method described in Hagler et al. (2006), we slid a threshold level between $p_{\text{uncorr}} = 0.05$ and 0.01 from the group comparison map for participation coefficients to identify functional ROIs. We first identified ROI candidates with cluster area (white matter surface) greater than 150 mm^2 at $p_{\text{uncorr}} = 0.05$. Then we subdivided large clusters in reference to the Destrieux atlas (Destrieux et al., 2010) and slid the threshold level up to $p_{\text{uncorr}} = 0.01$. With peaks that survived at $p_{\text{uncorr}} = 0.01$, we selected ROIs comprising nodes within 15 mm geodesic distance (along the white matter surface) from the peaks and whose $p_{\text{uncorr}} < 0.05$. If nodes within 15 mm geodesic distance from the peaks of these preliminary ROIs were part of 2 neighboring ROIs such that there was overlap, the boundaries of these ROIs were determined by sliding the threshold down from $p_{\text{uncorr}} = 0.01$ towards 0.05 allowing the clusters to grow until the ROIs reached the edge of the neighboring clusters. With these identified ROIs from the first dataset (i.e., the controls versus TBI I cohort), we performed ROI analysis on the second dataset (i.e., the controls versus TBI II cohort). For each ROI, we defined that a TBI patient had an ‘abnormal’ network measure relative to the controls in the ROI if the average network measure of the patient in the ROI was outside the mean plus or minus two-standard deviation band of the controls group. This

procedure to identify TBI patients with ‘abnormal’ network measure in ROIs was carried out after the normality test of the controls’ ROI-specific network measures.

2.6 Multivariate Region of interest analysis

A multivariate approach was then used to decide which TBI patients had ‘abnormal’ measures relative to the controls over all ROIs by aggregating average node-specific measures within each of the ROIs. After confirming that controls’ network measure at each ROI passed the normality test, multivariate Gaussian distribution of the network measures for the controls was estimated. Since the sample size of the controls after the module identification was small compared to the number of ROIs, estimating covariance structure was challenging. In order to circumvent this ‘curse of dimensionality’ issue (Duda et al., 2001), the vector dimension was reduced using probabilistic principal component analysis (PPCA; Minka, 2000). PPCA automatically estimates the number of reduced components preserving the variability of the original high dimensional vector while eliminating spurious and noisy components. Based on reduced components of ROI-based network measures via PPCA, we defined relatively ‘abnormal’ TBI patients whose components were located within the lower and upper tails (less than the 2.5th percentile and greater than the 97.5th percentile) of the estimated multivariate normal distribution from the controls.

2.7 Statistical analyses

All statistical analyses were assessed in MATLAB. First, we performed the Shapiro-Wilk test at $\alpha = 0.05$ to assess the normality of distributions of each group’s demographics (age, years of education and post-injury time at the initial scan) and each network measure. The

aforementioned demographics did not pass the Shapiro-Wilk normality test. Thus, the Mann-Whitney U test was used to compare the demographics between each pair of groups: (1) the controls versus TBI I cohort, (2) control versus TBI II cohort and (3) TBI I cohort versus TBI II cohort. Chi-square tests were used to compare the gender distributions between each pair of groups.

All network measures for the control group passed the Shapiro-Wilk normality test, but some measures for the TBI groups did not. Thus, for group comparison of the network measures, two sided hypothesis tests were taken using permutation tests (10,000 permutations; Nichols and Holmes, 2001) on group means of each measure by permuting group membership. For global and region-specific network properties, permutation tests were performed on the *t*-statistics.

We performed the one-sided *z*-test (TBI > control) to compare the distributions of the number of TBI patients with more than two relatively ‘abnormal’ regions versus those expected, respectively. To calculate the expected number of TBI patients with relatively ‘abnormal’ regions, the binomial distribution was used with the probability that a region is relatively ‘abnormal.’ This probability was calculated from both upper and lower tails (i.e., two-standard deviations \pm mean) of the normal distribution.

2.8 Control analyses

To assess effects of motions on module-based graph theoretic measures obtained from our cohorts, each subject’s average frame-to-frame head movement after censoring was calculated and compared between cohorts. We also assessed the effect of thresholds on our findings by

applying two different threshold levels at 2% and 1.5% tie densities to the correlation matrices and subsequently performing group and ROI analyses of participation coefficients. To assess the effect of global signal regression on our results, we additionally preprocessed our data without global signal regression and constructed a correlation and connectivity matrix. ROI analyses after group comparisons were then performed for participation coefficients. Lastly, we selected a different version of ROIs comprising nodes within 20 mm geodesic distance from the peaks, and we repeated the ROI analyses to verify effects of different size of ROIs on our results.

RESULTS

3.1 Demographics comparisons between the groups

There were no statistically significant differences in age, education, gender, or post-injury time between the subjects whose scans were included in graph theoretical analyses and their respective whole cohorts (Table II). The whole cohorts did not show statistically significant differences in age, education and post-injury time comparing the control vs. TBI I, control vs. TBI II, and TBI I vs. TBI II cohorts. There were differences in gender that were significant only between the two TBI cohorts ($p = 0.03$; chi-square test) as only the TBI II cohort had females (Table II). For the subjects whose scans (initial or follow-up scans) were included in graph theoretical analyses, there were no statistically significant differences in the demographics between each cohort except gender between the two TBI cohorts ($p = 0.04$; chi-square test).

3.2. Seed-based approach results for the default mode network

To ensure that the preprocessed resting-state BOLD fMRI had acceptable data quality for the further network analyses, we obtained the seed-based correlation maps from the left posterior cingulate cortex (-7, -55, 27) per each subject dataset that passed the quality assurance procedure prior to checking module assignment results. Group statistic maps (Fig. S1) for the seed-based correlation maps of each control and TBI I group on both scans showed the default mode network (See Fig. S1 legend for the detailed methods for the seed-based approach we used).

3.3. Module identification results

Color maps for identified modules from group averaged correlation matrix (Fig. 2) allowed us to compare major modules (comprising more than 1% of the total number of nodes) between groups at each tie density. In the control group, there were typically 4 major modules identified (except at 1.5% tie density on the follow-up scans, where there were 5). The identified 4 major modules in the control group corresponded to the default mode (Greicius et al., 2002; Raichle et al., 2001), executive control (Seeley et al., 2007; Vincent et al., 2008), visual (Lowe et al., 1998) and somatosensory-motor (Biswal et al., 1995) networks. In contrast, the TBI I cohort generally had more than 4 modules (except at 3% tie density on the follow-up scans). These module identification results were consistent with modular organization maps from young healthy subjects reported elsewhere (Liang et al., 2013) using the same module identification algorithm. At 3% tie density, subdivided modules (light green and yellow modules) in the TBI I cohort on the initial scans reorganized (merged to other modules) on the follow-up scans and their module assignments became similar to modular structures of the control groups. At 2% and 1.5% tie densities, modules of the TBI I cohort on the initial scans were fragmented in lateral prefrontal cortex and anterior cingulate cortex (white circles) and less fragmented on the follow-up scans.

An alternative module identification algorithm (Infomap) also demonstrated fragmented modules and increased total number of modules in the TBI I cohort on the initial scans (Fig. S2). Note that we did not further compare Louvain algorithm results with those obtained by the Infomap algorithm as the Infomap algorithm did not reliably identify modules in some of our cohorts at the single-subject level (e.g., see Fig. S3).

3.4 Global network properties

Group differences in modularity (Fig. 3a) and averaged participation coefficient (Fig. 3b), a measure of between-module connectivity, were statistically significant at $\alpha = 0.05$ on the initial scans, but not on the follow-up scans. The TBI I cohort had higher modularity and lower participation coefficient on the initial scans than the controls. All these global measures in both groups passed the Shapiro-Wilk normality test. Modularity of the controls ranged from 0.3 to 0.55 (Fig. 3b). This range is slightly low, especially on the initial scans, but the range is comparable to the modularity range (0.4 to 0.6) previously described in healthy normal subjects (Meunier et al., 2009a, 2009b; Valencia et al., 2009). At the single subject level, 14 TBI patients on the initial scans had ‘abnormally’ high modularity and 2 had ‘abnormally’ low modularity (Fig. 3a). 7 TBI patients on the initial scans had ‘abnormally’ low participation coefficient (Fig. 3b). Note that by chance only 2 subjects out of 47 (4.8%) would be expected to be outside of the 2-standard deviation range; 1 above and 1 below.

When the global network properties were compared across the initial and follow-up scans at each group, the global network properties were apparently changed in the controls whereas they appeared to remain stable on average in the TBI I cohort. Therefore, we performed additional, direct comparisons between the initial and follow-up scans with subjects who underwent both scans at the single-subject level (See Fig. S4 and supplemental results for further details). Single subject analyses demonstrated a wide variety of changes (both increases and decreases) in modularity and participation coefficient over time in both controls and the TBI I cohort.

3.5 Node-specific network properties

Node-specific analysis allowed us to identify localized patterns of module-based network measures that differed between TBI and control subjects (Figs. 4, 5). Overall, the spatial pattern of group comparisons (Fig. 4) and the number of TBI patients with ‘abnormal’ network measures relative to the controls (Fig. 5) were clear on the initial scans but less prominent on the follow-up scans. On the initial scans, the TBI I cohort had small areas of increased and decreased within-module connectivity relative to the controls (Fig. 4a). On the contrary, the TBI subjects had extensive and more markedly decreased participation coefficient (Fig. 4b) compared with the controls. Maps for count of the TBI patients with ‘abnormal’ node-specific measures relative to the controls were similar to the corresponding group comparison maps (Fig. 5).

3.5.1 Group comparisons

The spatial pattern of group differences in within-module connectivity changed over time. At the time of the initial scan, within-module connectivity in the TBI I cohort was slightly elevated, on average, compared with the controls in the right precentral gyrus, right medial superior frontal gyrus, and right dorsomedial superior frontal gyrus (R G_precentral, R G_front_sup-medial and R G_front_sup-dorsomedial in Fig. 4a left panel). Subtle decreases in within-module connectivity of the TBI patients compared with the controls were also observed in the right supramarginal gyrus and right opercular part of the inferior frontal gyrus (R G_pariet_inf-Supramar and R G_front_inf-Opercular in Fig. 4a left panel). Though there were trends in group differences on the initial scans, none of the group differences were statistically significant at $q_{\text{FDR}} < 0.05$ (FDR: false discovery rate (Genovese et al., 2002)). At the time of the follow-up scan, such disturbances in within-module connectivity resolved (Figure 4a, right panel).

In contrast to the scattered subtle increases and decreases in the within-module connectivity, the group comparison maps for participation coefficient (Fig. 4b *left panel*) exhibited more widespread decreases in the TBI I cohort compared with the controls. At the time of the initial scan, such patterns were localized over the central sulcus, left anterior transverse temporal gyrus, right long insular gyrus and central sulcus of the insula, superior frontal gyrus and sulcus, anterior part of the cingulate gyrus and sulcus, right superior part of the precentral sulcus, right superior temporal sulcus, right orbital gyri, posterior-ventral part of the cingulate gyrus near the calcarine sulcus, lingual gyrus, right parieto-occipital sulcus and left cuneus. These differences on the initial scans were significant based on uncorrected p -values. However, such group differences on the initial scans did not survive after correction for multiple comparisons at $q_{\text{FDR}} < 0.05$. At the time of the second scan, the widespread decrease in participation coefficient mostly resolved. (Fig 4b, *right panel*)

3.5.2 Counts of the numbers of TBI patients with relatively ‘abnormal’ node-specific network measures

Color maps for the number of TBI patients with ‘abnormal’ network measures relative to the controls in each of the nodes (Fig. 5) allowed us to identify regions where functional connectivity appeared most vulnerable to bTBI. Here, ‘abnormal’ was defined if a network measure of a patient was outside two standard deviations from the mean of the controls. Though abnormalities revealed on group comparison maps did not survive at $q_{\text{FDR}} < 0.05$, the ‘abnormality’ maps demonstrated that substantial portions of the TBI patients (up to 25%) had ‘abnormally’ low participation coefficient relative to the controls (Fig. 5c). None had ‘abnormally’ high participation coefficient. These findings are notable in that by chance 2.4% of

the TBI I cohort would be expected to be lower than the mean of the controls minus the 2-standard deviations.

3.6 ROI analysis results

Since participation coefficient was the most prominent among the module-based network measures in the group-wide node-specific analysis, we focused on participation coefficient in further analyses. From the group comparison map in participation coefficient (Fig. 4b), we identified 15 regions (Fig. 6) for ROI analysis using the Destrieux atlas (Destrieux et al., 2010). These identified ROIs were (1) central sulcus (S_central), (2) left anterior transverse temporal gyrus (L G_temp_sup-G_T_transv), (3) right long insular gyrus and central sulcus of the insula (R G_Ins_lg_and_S_cent_ins), (4) superior frontal sulcus (S_front_sup), (5) the medial portion of the superior frontal gyrus (G_front_sup-medial), (6) the anterior portion of the superior frontal gyrus (G_front_sup-anterior), (7) deep anterior part of the cingulate gyrus and sulcus (G_and_S_cingul-Ant-deep), (8) superficial anterior part of the cingulate gyrus and sulcus (G_and_S_cingul-Ant-superficial), (9) right superior part of the precentral sulcus (R S_precentral-sup-part), (10) right superior temporal sulcus (R S_temporal_sup), (11) right orbital gyri (R G_orbital), (12) posterior-ventral part of the cingulate gyrus (G_cingul-Post-ventral) near the calcarine sulcus, (13) lingual gyrus (G_oc-temp_med-Lingual), (14) right parieto-occipital sulcus (R S_parieto_occipital) and (15) left cuneus (L G_cuneus). For detailed locations and surface area of these ROIs, see Fig. 6 and Table III.

Scatter plots were made (Fig. 7) to examine the distributions of average participation coefficient of each subject in three ROIs (G_and_S_cingul-Ant-superficial (left: (-8, 56, 3), right: (9, 55, 2)),

G_cingul-Post-ventral (left: (-8, -52, 3), right: (12, -53, 5)) and R S_parieto_occipital (18, -81, 38)). These three ROIs were representative of all 15 ROIs analyzed (see table IV for the complete list of the ROI analysis results). Similar to the trends observed in global and node-specific network measures, the TBI I cohort, on average, had lower participation coefficients ($p_{\text{uncorr}} < 0.05$) than the controls on the initial scans, yielding up to 15 (36.6%) relatively ‘abnormal’ TBI patients. (Fig. 7a-c *left panel*). Such group differences resolved at the time of the follow-up scans (Fig. 7a-c *right panel*). In the TBI I cohort, 8 of the 15 ROIs had statistically significant group differences after Bonferroni correction for multiple comparisons ($p < 0.0033$).

Subsequently, without free parameters with regard to ROI selection, we used the TBI II cohort as a validation dataset to test the hypotheses generated with the TBI I cohort. On the initial scans, in the three ROIs, relative ‘abnormality’ patterns in the TBI II cohort were less striking than those in the TBI I cohort, yielding up to 3 (9.6%) TBI patients with relatively ‘abnormal’ participation coefficients (Fig. 7d-f *left panels*). Table IV indicates that the number of TBI patients from the TBI II cohort with relatively ‘abnormal’ ROI-specific participation coefficients on the initial scans was greater than the expected number by chance (0 above and 0 below). Relatively abnormal participation coefficient on the initial scans in TBI patients from the TBI II cohort were identified in all ROIs except in the G_front_sup-*medial* and L G_cuneus. However, there were fewer TBI patients with relatively abnormal participation coefficient over the ROIs in the TBI II cohort compared with the TBI I cohort (Fig. 7 and Table IV). None of the ROIs in the TBI II cohort showed statistically significant group differences at $\alpha = 0.05$ on either initial or follow-up scans.

Turning to multiple ROI single-subject analyses, we counted the number of relatively ‘abnormal’ ROIs in each individual TBI patient and tested if this observed distribution of ‘abnormal’ ROIs differed from the distribution expected by chance (Fig. 8). On the initial scans, the observed numbers of TBI patients with more than two ‘abnormal’ ROIs were markedly different from those expected by chance, and these differences were statistically significant at $\alpha < 0.05$ in both datasets (27/47 observed versus 2/47 expected in the TBI I cohort, $p < 0.0001$, one-sided z -test; 8/31 observed versus 1/31 expected in the TBI II cohort, $p = 0.006$, one-sided z -test). As expected considering the nature of these analyses, the proportion of TBI patients from the TBI II cohort with more than two relatively ‘abnormal’ ROIs was lower than those from the TBI I cohort: 44.9% reduction from the TBI I cohort to TBI II cohort on the initial scans (i.e., 57.4% = 27/47 versus 25.8% = 8/31).

On the follow-up scans, the proportion of patients in the TBI I cohort with more than two ‘abnormal’ ROIs was marginally statistically significantly different than expected by chance ($p = 0.044$). The proportion of patients in the TBI II cohort with more than two ‘abnormal’ ROIs on follow-up scans was not statistically significant ($p = 0.276$).

Multivariate analysis aggregating all 15 ROIs after dimensionality reduction via probabilistic principal component analysis (Fig. 9) demonstrated a similar reduction in the proportion of the TBI patients with relatively ‘abnormal’ ROIs from the TBI I cohort to the TBI II cohort. Specifically, 31/47 (66.0%) of the patients from the TBI I cohort (Fig. 9a) and 9/31 (29.0%) of the patients from the TBI II cohort (Fig. 9b) were deemed to be relatively ‘abnormal’ across the 15 ROIs on the initial scans. On the follow-up scans, 4/37 (10.8%) of the patients from the TBI I

cohort (Fig 8c) and 1/27 (3.7%) of the patients from the TBI II cohort (Fig 9d) were found to be ‘abnormal’ using this multivariate analysis.

3.7 Control analysis results

3.7.1 Assessment of the effects of subtle head motion

Recently, the effects of subtle motion have been found to substantially influence resting-state functional connectivity MRI findings (Power et al., 2012; Satterthwaite et al., 2012; van Dijk et al., 2012). Our motion analysis (Fig. S5) revealed that there were not statistically significant group differences in average frame-to-frame movement in the analyzed data, after censoring and exclusion of scans with excessive motion (table I). There were no associations between average participation coefficient and head motion (Fig. S6) in any of the groups. Furthermore, there was no relationship between the number of ‘abnormal’ ROIs and head motion (Fig. S7).

3.7.2 Assessment of the effects of network connectivity thresholds

The differences between TBI subjects and controls in the number of regions on interest with ‘abnormal’ participation coefficient were replicated at 2 additional threshold levels for connectivity matrices (Figs. S8, S9 for 2% and 1.5% tie densities, respectively).

3.7.3 Effects of global signal regression

Analyses of the number of regions of interest with abnormal participation coefficient in TBI patients vs. controls based on connectivity matrices created without global signal regression (Fig. S10) essentially replicated the results with global signal regression (Fig. 8). The only exception

was that the number of TBI I patients with relatively ‘abnormal’ ROI values on the follow-up scans was not quite statistically significant at $\alpha = 0.05$.

3.7.4 Effects of region of interest size

To explore the effect of ROI size, we re-analyzed the data using all nodes within 20 mm rather than 15 mm geodesic distance of the local peaks of participation coefficient difference between groups as the ROIs (Fig. S11). The analysis of the number of regions of interest with abnormal participation coefficient in TBI patients versus controls using 20 mm geodesic distance ROIs (Fig. S12) again essentially replicate the results with 15 mm geodesic distance ROIs (Fig. 8).

DISCUSSION

In summary, we found disrupted community organization of resting-state functional connectivity in a subset of U.S. military personnel following concussive bTBI using module-based graph theoretic analysis. Of the module-based graph theoretical measures studied, participation coefficient, a measure of between-module connectivity, showed the most pronounced disruptions in the TBI patients relative to the controls. There were spatially localized ‘abnormalities’ over multiple brain regions in the TBI patients. Importantly, these abnormalities were detected in comparison with US military controls that had blast-exposures but no clinical diagnosis of TBI. At the time of the initial scans, the distribution of the number of the ‘abnormal’ regions was different from the expected distribution by chance. Multivariate analysis aggregating the 15 ROI values of between-module connectivity consistently demonstrated the substantial portion of TBI patients had relatively ‘abnormal’ between-module connectivity. Abnormalities had largely resolved at the time of the follow-up scans. In an independent group of concussive bTBI patients, we were able to partially replicate these results with no free parameters.

4.1 Technological innovations effectively analyze heterogeneous concussive bTBI patients at the single subject level.

The single-subject analyses performed in this study were useful to effectively analyze a heterogeneous group of bTBI patients in this report. Scatter plots (Figs. 3, 7) illustrate skewed distribution of the network measures in the TBI patients. The distributions of the TBI patients with multiple ‘abnormal’ regions (Fig. 8) were consistently different from those expected by chance. The multivariate analysis (Fig. 9) also consistently revealed the TBI patients with

relatively ‘abnormal’ regions over the two independent cohorts. Thus, we suggest that single-subject analysis should be considered along with group analysis for the identification of ‘abnormalities’ in heterogeneous subject populations such as concussive bTBI patients. Obviously, single-subject analyses have greater potential clinical applicability than group analyses.

We adopted a surface-based approach to reduce between-subject variability arising from brain anatomy. An advantage of the surface-based approach is an increase in sensitivity by (1) matching sulcus-to-sulcus and gyrus-to-gyrus of cortical surface across subjects to circumvent the issues of improper registration and (2) utilizing spatial smoothing on the cortical surface rather than the voxel space (Jo et al., 2007, 2008; Tucholka et al., 2012). On the other hand, a disadvantage of the surface-based approach is that it does not represent the whole brain. The surface based approach does not assess cerebellum and subcortical regions such as basal ganglia and thalamus due to technical limitations.

Complex network analysis using the graph theory is advantageous in bTBI populations with heterogeneous injury mechanisms since it does not make assumptions regarding networks or regions of interest. Thus, our data-driven approach may provide more ‘comprehensive’ view than hypothesis-driven approaches do in the studies of heterogeneous TBI populations. Disrupted between-module connectivity in the TBI patients over multiple regions (Figs. 4b, 5c, 7-9, Table IV) indicates that multiple regions or networks should be included to detect ‘abnormalities’ in TBI patients if hypothesis-driven approaches are adopted.

In contrast to other graph theoretic analyses on TBI populations (Castellanos et al., 2011; Nakamura et al., 2009), we exploited the spatial resolution of fMRI by defining each vertex of the cortical surface as a node. Network analyses with higher spatial resolution of nodes are beneficial over region-based network analyses in identifying network properties of interests with greater sensitivity and specificity and visualizing spatially localized network properties of interest (Hayasaka and Laurienti, 2010). Thus, we attempted to use a vertex as a node considering that the spatial extent of ‘abnormalities’ in concussive bTBI populations measured by the graph theoretic analysis in fMRI was unknown. Indeed, the utilization of high spatial resolution of fMRI allowed us to identify localized ‘abnormalities’ in the TBI patients in greater detail, which would be missed if a node was defined from coarse parcellations. However, a vertex itself is arguably less biologically meaningful than a functional brain region in the context of graph theoretic analysis (Wig et al., 2011). Unfortunately our currently understanding of the functional subdivisions of the human brain is not yet sufficient for optimal prespecified ROI analyses.

4.2 Findings in relation to prior literature

4.2.1 Multiple regions with disrupted between-module connectivity as potential candidates for hypothesis-driven network-specific approaches

Previous functional connectivity studies in fMRI on civilian TBI patients (Arenivas et al., 2012; Bonnelle et al., 2011; Caeyenberghs et al., 2012; Kasahara et al., 2010; Marquez de la Plata et al., 2011; Mayer et al., 2011; Sharp et al., 2011; Slobounov et al., 2011; Tang et al., 2011) used hypothesis-driven approaches within the default mode (Greicius et al., 2002; Raichle et al., 2001), executive control (Seeley et al., 2007; Vincent et al., 2008), motor (Biswal et al., 1995), thalamic

(Zhang et al., 2008) and hippocampal (Rombouts et al., 2003) networks. However, to our knowledge, there are no current fMRI studies of resting-state functional connectivity in concussive bTBI patients using these networks. In this regard, future work based on the identified ‘abnormal’ regions in Figs. 4-7 could involve assessment of within-network and between-network connectivity in these specific resting-state networks.

4.2.2 Transient change of module-based organizations following concussive bTBI

A prevailing view on the plasticity of TBI patients based on functional neuroimaging studies (Castellanos et al., 2010, 2011; Mayer et al., 2011; Nakamura et al., 2009; Sponheim et al., 2011) is that the recovery of functional network at the chronic stage is incomplete. Even after 7 to 12 months of active rehabilitation treatments, it has been reported that many TBI patients had incomplete recovery of the graph-theory measures, associated with the incomplete reestablishment of cognitive function (Castellanos et al., 2011). Furthermore, concussive bTBI patients with 32 months of mean post-injury time demonstrated relatively reduced inter-hemispheric connectivity in lateral frontal lobe despite no observed deficits in neuropsychological measures (Sponheim et al., 2011).

In contrast, in our study at the global and node- and region-specific levels (Figs. 3-5, 7-9), most of the relative alterations in module-based connectivity of the TBI patients observed on the initial scans had resolved at the follow-up scan 6-12 months later. This transient change in module-based connectivity supports the utility of early scanning (if feasible) on bTBI patients to identify localized modular disruptions in brain networks. However, resolved alterations in between-module connectivity of the TBI patients at the follow-ups do not necessarily mean complete restoration of their network architectures to baseline.

4.2.3 Marginally perturbed within-module connectivity, but markedly unbalanced between-module connectivity with increased modularity

Node-specific analysis of the module-based network measures (Figs. 4, 5) demonstrates that the TBI patients had disrupted between-module connectivity with marginal change in within-module connectivity relative to the controls. Disrupted between-module connectivity in the TBI patients indicate that the blast-related injuries may interfere with integration across functional brain networks, as between-module connectivity may be necessary for complex tasks spanning multiple modules. In healthy normal subjects, modules in the spontaneous brain network are closely associated with auditory, visual, somatosensory/motor, attention, sub-cortical and default mode networks (He et al., 2009). Though we did not directly assess in this study, traumatic axonal injuries in long range fibers mediating connections with multiple modules may lead to disruptions in between-module connectivity. In TBI patients, disrupted white matter integrity in the splenium of the corpus callosum has been correlated with PCC functional connectivity in the default mode network (Sharp et al., 2011). Our previous DTI study showed disrupted white matter integrity in the TBI I cohort relative to the controls (Mac Donald et al., 2011). However, it is too early to interpret the association of altered white matter integrity reported in Mac Donald et al. (2011) with disrupted between-module functional connectivity following bTBI without direct investigation of structural white matter connectivity at a subject by subject level. Since strong functional connectivity between regions is often maintained without monosynaptic connections between these regions (Honey et al. 2009), direct comparisons of functional and structural connectivity are not straightforward. Therefore, further studies on the association between structural and functional connectivity on these concussive bTBI patients are needed to

understand the underlying mechanisms of disrupted between-module connectivity following bTBI. This will require further investigations that are beyond the scope of the current manuscript.

4.3 Technical Limitations

The present study has several limitations due to data quality. First, our analysis results were from a subset (75% of all subjects' data; 62%, 76%, 81% of the controls, TBI I cohort and TBI II cohort, respectively) of the subjects' data to ensure data quality. Our study results may be more representative if more subjects' data had passed the quality assurance procedure. The exclusion of a part of the subjects' data for data quality assurance may not be surprising to neuroimaging researchers, particularly in fMRI, considering difference in subjects' conditions between clinical populations and healthy subjects. However, this is an important consideration clinically as it may not be feasible to collect reliable data from every patient to be used as early indicators of injury, disease, or for non-invasive monitoring of rehabilitation progress.

Second, moderate data quality of the T_1 -weight MRI due to subject motion was not sufficient for Freesurfer to reconstruct cortical surfaces in fully automated fashion. Thus, following the well-documented instructions, a substantial amount of time was required for manual intervention during cortical surface reconstruction to compensate MRI data quality of our study. Cortical surface reconstruction would be more reliable (and require less manual intervention) if we increased signal-to-noise ratio of the T_1 -weighted MRI by acquiring two or more images as the Freesurfer instructions suggest. However, a practical limitation of studies of relatively acutely injured subjects is that time in the scanner must be kept relatively short for patient comfort and safety.

Third, we were not able to include much of the orbitofrontal cortex and inferior temporal cortex in our analysis due to signal loss by fMRI susceptibility artifacts (Ojemann et al., 1997) and low signal to noise due to distance from the MR receiver coils. Particularly, orbitofrontal cortex was of interest based on a previous simulation study on the effect of blasts on the brain (Taylor and Ford, 2009) and our previous DTI study (Mac Donald et al., 2011) involving the TBI I cohort. An optimized pulse sequence to account for susceptibility artifacts (Domsch et al., 2012) would be beneficial in this regard for future studies.

Finally, we did not make direct comparison of the initial and follow-up scans even though we acquired MRI data at two time points. Instead, we performed only a cross-sectional study at two time points and observed change of modular organization of the TBI patients relative to the controls at each time point. Lack of quantification on the effects of the two different MRI scanners, medications between the time of the initial and follow-up scans and sleep deprivation at the time of the initial scans prevented us from directly analyzing our data in a subject-by-subject longitudinal fashion.

4.4 Interpretations

The underlying biological mechanisms and consequences of the findings in this study are not yet clear. Possible explanations for the relatively disrupted between-module functional connectivity in the TBI cohorts on initial scans may be related to white matter injury. This hypothesis is based on previous combined DTI and fMRI connectivity studies on TBI populations (Bonnelle et al., 2012; Mayer et al., 2011; Sharp et al., 2011). Another possibility is unmeasured pathophysiology following TBI in the gray matter, for example, changes in cerebral blood flow (hypo- and hyperperfusion), impairment of cerebrovascular autoregulation, imbalance of cerebral

oxygenation and/or cerebral metabolic dysfunction (see Werner and Engelhard, (2007) for review).

The biological mechanisms for apparent resolution of between-module functional connectivity in the TBI patients on the follow-up scans are not known. One possibility is that the TBI patients could have been subjected to more sleep deprivation at the time of initial scans; sleep deprivation has been shown to affect BOLD signal (Gujar et al., 2010). Medications used by TBI patients at the acute stage and during rehabilitation could also be partially accountable.

There are several alternative explanations for our findings:

1) It is possible that some of these results may have occurred by chance as group differences at the node- and region-specific level were not statistically significant after correction for multiple comparisons ($q_{\text{FDR}} < 0.05$). We do not think that this is likely to be the case for all of our results since the analysis of the TBI II cohort was performed with no free parameters after we obtained the analysis results of the TBI I cohort. In other words, the TBI II cohort served as a validation dataset. Thus, the single-subject analyses of the initial scan (Figs. 7-9) should be regarded as the most solid.

2) Unmeasured systematic differences in the time spent in the scanner with eyes open versus closed or awake versus asleep could also be confounding factors. It has been reported that functional connectivity strength in the default mode network and attention network with eyes closed is decreased over network connectivity with eyes opened (van Dijk et al., 2010). Functional connectivity in the default mode, attention, executive control, motor, visual and auditory network is retained (Larson-Prior et al., 2009) during light sleep, but functional connectivity in the default mode network is partially changed during deep sleep (Horovitz et al.,

2009). We were not able to control the extent of eyes-open vs. eyes closed time, nor assess sleep in the scanner due to the logistical challenges of obtaining scans in acutely injured US military personnel.

3) The effects of analgesic medications could be another confounding factor. To our knowledge, immediate effects of analgesics on resting-state functional connectivity in fMRI are unknown, but alterations in regional synchrony of resting-state functional connectivity in fMRI in the right anterior cingulate cortex and left precentral frontal gyrus in chronic ketamine users has been reported (Liao et al., 2012).

4) Other, unmeasured differences in pre- and post-injury characteristics among three groups could also provide alternative explanations for our findings. The initial scan data of the controls and TBI I cohort were acquired in 2008-2009 while the TBI II cohort in 2010-2011. During this period, the pace of the wars was changed and rehabilitation strategies and treatments may have improved (See van Wingen et al. (2012) for the effects of combat stress on functional connectivity). All these characteristics were unmeasured. Thus, it is unclear whether reduction in the proportion of TBI patients with relatively 'abnormal' participation coefficient across ROIs (Figs. 7-9) from the TBI I cohort to the TBI II cohort was solely due to different detection performance of the multivariate analysis over the two datasets or due to intrinsic difference between the subjects in the 2 TBI cohorts.

5) Biases due to incomplete blinding during the manual portions of the Freesurfer analysis could also affect our results though the associated effects are not likely to be substantial considering the difference in spatial resolutions: 4^3 mm^3 in fMRI versus 1 mm^3 in structural MRI.

6) Test-retest reliability of our findings is still unknown. Two previous reports, one indicating moderately good reliability (Braun et al., 2012) and another indicating relatively low

test-retest reliability for many graph theoretical measures (Wang et al., 2011) used coarser parcellation and less aggressive motion scrubbing than the current work.

4.4 Future Directions

The most important future direction for this line of investigation is an assessment of the relationship between these graph-theoretically derived neuroimaging variables and clinical outcomes in these cohorts. This will be the topic of future communications. Further studies will be required to address the technical concerns discussed above and assess the mechanisms underlying these observed network properties.

CONCLUSIONS

In conclusion, we demonstrated disrupted modular organization of resting-state cortical functional network in U.S. military personnel with concussive bTBI. Module-based graph theoretic analysis revealed altered between-module connectivity in the TBI patients relative to the controls who had blast exposures without a diagnosis of TBI. Single-subject multivariate analysis fairly consistently detected the TBI patients with relatively ‘abnormal’ ROIs over two independent cohorts. Our single-subject analysis approach may be useful for heterogeneous populations and potentially complement hypothesis-driven approaches for these populations in future resting-state fMRI studies. Further studies are required to explain the underlying mechanisms and consequences of these phenomena.

ACKNOWLEDGMENTS

First of all, we would like to thank all participants, their families, the commanding officers and the clinical care providers that supported this study. Our thanks also go to Dr. Nico U.

Dosenbach and Dr. Steven E. Petersen for their helpful comments on the earlier version of this manuscript. This work has been supported by Department of Defense CDMRP grants PT075299 and PT090444 to DLB. We also would like to thank the facilities of the Washington University Center for High Performance Computing, which were partially provided through grant NCRR 1S10RR022984-01A1 for providing computational resource for conducting this study.

REFERENCES

- Achard, S., R. Salvador, B. Whitcher, J. Suckling, and E. T. Bullmore. 2006. "A Resilient, Low-Frequency, Small-World Human Brain Functional Network with Highly Connected Association Cortical Hubs." *J Neurosci* 26: 63–72. <http://dx.plos.org/10.1371/journal.pcbi.0030017>
- Anderson, J. S., T. J. Druzgal, M. Lopez-Larson, E. Jeong, K. Desai, and D. Yurgelun-Todd. 2011. "Network Anticorrelations, Global Regression, and Phase-shifted Soft Tissue Correction." *Hum Brain Mapp* 32: 919–934. <http://www.ncbi.nlm.nih.gov/pubmed/20533557>
- Arenivas, A., R. Diaz-Arrastia, J. Spence, C. M. Cullum, K. Krishnan, C. Bosworth, C. Culver, B. Kennard, and C. Marquez de la Plata. 2012. "Three Approaches to Investigating Functional Compromise to the Default Mode Network After Traumatic Axonal Injury." *Brain Imaging Behav* (in press). <http://www.springerlink.com/index/10.1007/s11682-012-9191-2>
- Argall, B. D., Z. S. Saad, and M. S. Beauchamp. 2006. "Simplified Intersubject Averaging on the Cortical Surface Using SUMA." *Hum Brain Mapp* 27: 14–27. <http://doi.wiley.com/10.1002/hbm.20158>
- Biswal, B., F. Z. Yetkin, V. M. Haughton, and J. S. Hyde. 1995. "Functional Connectivity in the Motor Cortex of Resting Human Brain Using Echo-planar MRI." *Magn Reson Med* 34: 537–541.
- Blondel, V. D., J. Guillaume, R. Lambiotte, and E. Lefebvre. 2008. "Fast Unfolding of Communities in Large Networks." *J Stat Mech: Theory and Exp* 2008: P10008. <http://stacks.iop.org/1742-5468/2008/i=10/a=P10008?key=crossref.46968f6ec61eb8f907a760be1c5ace52>
- Bonnelle, V., R. Leech, K. M. Kinnunen, T. E. Ham, C. F. Beckmann, X. de Boissezon, R. J. Greenwood, and D. J. Sharp. 2011. "Default Mode Network Connectivity Predicts Sustained Attention Deficits After Traumatic Brain Injury." *J Neurosci* 31: 13442–13451. <http://www.jneurosci.org/cgi/doi/10.1523/JNEUROSCI.1163-11.2011>
- Bonnelle, V., T. E. Ham, R. Leech, K. M. Kinnunen, M. A. Mehta, R. J. Greenwood, and D. J. Sharp. 2012. "Salience Network Integrity Predicts Default Mode Network Function After Traumatic Brain Injury." *Proc Natl Acad Sci USA* 109: 4690–4695. doi:10.1073/pnas.1113455109. <http://www.pnas.org/cgi/doi/10.1073/pnas.1113455109>.
- Braun, Urs, M. M. Plichta, C. Esslinger, C. Sauer, L. Haddad, O. Grimm, D. Mier, et al. 2012. "Test-retest Reliability of Resting-state Connectivity Network Characteristics Using fMRI and Graph Theoretical Measures." *Neuroimage* 59: 1404–1412. <http://dx.doi.org/10.1016/j.neuroimage.2011.08.044>.
- Bullmore, E.T., and O. Sporns. 2009. "Complex Brain Networks: Graph Theoretical Analysis of Structural and Functional Systems." *Nat Rev Neurosci* 10: 186–198. <http://www.nature.com/doi/10.1038/nrn2575>
- Caeyenberghs, K., A. Leemans, M. H. Heitger, I. Leunissen, T. Dhollander, S. Sunaert, P. Dupont, and S. P. Swinnen. 2012. "Graph Analysis of Functional Brain Networks for Cognitive Control of Action in Traumatic Brain Injury." *Brain* 135: 1293–1307. <http://www.brain.oxfordjournals.org/cgi/doi/10.1093/brain/aws048>
- Casscells, S. W. 2007. "Traumatic Brain Injury: Definition and Reporting". Washington, DC: Department of Defense. (memorandum) (<http://mhs.osd.mil/Content/docs/pdfs/policies/2007/07-030.pdf>.)
- Castellanos, N. P., N. Paul, V. E. Ordonez, O. Demuynck, R. Bajo, P. Campo, A. Bilbao, T. Ortiz, F. del-Pozo, and F. Maestu. 2010. "Reorganization of Functional Connectivity as a Correlate of Cognitive Recovery in Acquired Brain Injury." *Brain* 133: 2365–2381. <http://www.brain.oxfordjournals.org/cgi/doi/10.1093/brain/awq174>

- Castellanos, N. P., I. Leyva, J. M. Buldu, R. Bajo, N. Paul, P. Cuesta, V. E. Ordonez, et al. 2011. "Principles of Recovery from Traumatic Brain Injury: Reorganization of Functional Networks." *Neuroimage* 55: 1189–1199. <http://linkinghub.elsevier.com/retrieve/pii/S1053811910016320>
- Chai, X. J., A. N. Castanon, D. Ongur, and S. Whitfield-Gabrieli. 2012. "Anticorrelations in Resting State Networks Without Global Signal Regression." *Neuroimage* 59: 1420–1428. <http://www.ncbi.nlm.nih.gov/pubmed/21889994>
- Chang, C., and G. H. Glover. 2009. "Effects of Model-based Physiological Noise Correction on Default Mode Network Anti-correlations and Correlations." *Neuroimage* 47: 1448–1459. <http://linkinghub.elsevier.com/retrieve/pii/S1053811909005126>
- Chen, Z. J., Y. He, P. Rosa-Neto, J. Germann, and A. C. Evans. 2008. "Revealing Modular Architecture of Human Brain Structural Networks by Using Cortical Thickness from MRI." *Cereb Cortex* 18: 2374–2381. <http://dx.doi.org/10.1093/cercor/bhn003>.
- Cordes, D., V. M. Haughton, K. Arfanakis, G. J. Wendt, P. A. Turski, C. H. Moritz, M. A. Quigley, and M. E. Meyerand. 2000. "Mapping Functionally Related Regions of Brain with Functional Connectivity MR Imaging." *AJNR. Am J Neuroradiol* 21: 1636–1644. <http://www.ncbi.nlm.nih.gov/pubmed/11039342>.
- Cordes, D., V. M. Haughton, K. Arfanakis, J. D. Carew, P. A. Turski, C. H. Moritz, M. A. Quigley, and M. E. Meyerand. 2001. "Frequencies Contributing to Functional Connectivity in the Cerebral Cortex in 'Resting-state' Data." *AJNR. Am J Neuroradiol* 22: 1326–1333. <http://www.ncbi.nlm.nih.gov/pubmed/11498421>
- Cox, R. W. 1996. "AFNI: Software for Analysis and Visualization of Functional Magnetic Resonance Neuroimages." *Comput Biomed Res* 29: 162–173. <http://www.sciencedirect.com/science/article/pii/S0010480996900142>
- Dale, A. M., and M. I. Sereno. 1993. "Improved Localization of Cortical Activity by Combining EEG and MEG with MRI Cortical Surface Reconstruction: a Linear Approach." *J Cogn Neurosci* 5: 162–176. <http://www.mitpressjournals.org/doi/abs/10.1162/jocn.1993.5.2.162>
- Dale, A. M., B. Fischl, and M. I. Sereno. 1999. "Cortical Surface-based Analysis. I. Segmentation and Surface Reconstruction." *Neuroimage* 9: 179–194. <http://www.sciencedirect.com/science/article/pii/S1053811998903950>
- de Haan, W., W. M. van der Flier, T. Koene, L. L. Smits, P. Scheltens, and C.J. Stam. 2012. "Disrupted Modular Brain Dynamics Reflect Cognitive Dysfunction in Alzheimer's Disease." *Neuroimage* 59: 3085–3093. <http://linkinghub.elsevier.com/retrieve/pii/S1053811911013371>
- Dempsey, K. E., W. C. Dorlac, K. Martin, R. Fang, C. Fox, B. Bennett, K. Williams, and S. Flaherty. 2009. "Landstuhl Regional Medical Center: Traumatic Brain Injury Screening Program." *J Trauma Nurs* 16: 6–12. <http://www.ncbi.nlm.nih.gov/pubmed/19305293>
- Destrieux, C., B. Fischl, A. M. Dale, and E. Halgren. 2010. "Automatic Parcellation of Human Cortical Gyri and Sulci Using Standard Anatomical Nomenclature." *Neuroimage* 53: 1–15. <http://linkinghub.elsevier.com/retrieve/pii/S1053811910008542>
- Domsch, S., J. Linke, P. M. Heiler, A. Kroll, H. Flor, M. Wessa, and L. R. Schad. 2012. "Increased BOLD Sensitivity in the Orbitofrontal Cortex Using Slice-dependent Echo Times at 3 T." *Mag Reson Imaging* (in press). <http://linkinghub.elsevier.com/retrieve/pii/S0730725X12002305>
- Doppenberg, E. M. R., and R. Bullock. 1997. "Clinical Neuro-Protection Trials in Severe Traumatic Brain Injury: Lessons from Previous Studies." *J Neurotrauma* 14: 71–80. <http://www.liebertonline.com/doi/abs/10.1089/neu.1997.14.71>
- Duda, R. O., P. E. Hart, and D. G. Stork. 2001. *Pattern Classification*. 2nd ed. Wiley.

- Evans, A. C., D. L. Collins, S. R. Mills, E. D. Brown, R. L. Kelly, and T. M. Peters. 1993. "3D Statistical Neuroanatomical Models from 305 MRI Volumes." In *Proc IEEE Nucl Sci Symp Med Imaging Conf*, 1813–1817. IEEE. <http://dx.doi.org/10.1109/NSSMIC.1993.373602>.
- Finkel, M. F. 2006. "The Neurological Consequences of Explosives." *J Neurol Sci* 249: 63–67. <http://dx.doi.org/10.1016/j.jns.2006.06.005>.
- Fischl, B., M. I. Sereno, and A. M. Dale. 1999a. "Cortical Surface-Based Analysis: II: Inflation, Flattening, and a Surface-Based Coordinate System." *Neuroimage* 9: 195 – 207. <http://www.sciencedirect.com/science/article/pii/S1053811998903962>
- Fischl, B., M. I. Sereno, R. B. H. Tootell, and A. M. Dale. 1999b. "High-resolution Intersubject Averaging and a Coordinate System for the Cortical Surface." *Hum Brain Mapp* 8: 272–284. [http://dx.doi.org/10.1002/\(SICI\)1097-0193\(1999\)8:4<272::AID-HBM10>3.0.CO;2-4](http://dx.doi.org/10.1002/(SICI)1097-0193(1999)8:4<272::AID-HBM10>3.0.CO;2-4)
- Fischl, B., A. Liu, and A. M. Dale. 2001. "Automated Manifold Surgery: Constructing Geometrically Accurate and Topologically Correct Models of the Human Cerebral Cortex." *IEEE Trans Med Imaging* 20: 70–80. <http://ieeexplore.ieee.org/xpl/articleDetails.jsp?arnumber=906426>
- Fischl, B., D. H. Salat, E. Busa, M. Albert, M. Dieterich, C. Haselgrove, A. J. W. van der Kouwe, et al. 2002. "Whole Brain Segmentation: Automated Labeling of Neuroanatomical Structures in the Human Brain." *Neuron* 33: 341–355. <http://www.sciencedirect.com/science/article/pii/S089662730200569X>
- Fischl, B., A. J. W. van der Kouwe, C. Destrieux, E. Halgren, F. Segonne, D. H. Salat, E. Busa, et al. 2004a. "Automatically Parcellating the Human Cerebral Cortex." *Cereb Cortex* 14: 11–22. <http://cercor.oxfordjournals.org/content/14/1/11.abstract>
- Fischl, B., D. H. Salat, A. J. W. van der Kouwe, N. Makris, F. Segonne, B. T. Quinn, and A. M. Dale. 2004b. "Sequence-independent Segmentation of Magnetic Resonance Images." *Neuroimage* 23: S69 – S84. <http://www.sciencedirect.com/science/article/B6WNP-4DCMGVT-2/2/7eee26326dc63f931b826eac33becc8b>
- Fox, M. D., A. Z. Snyder, J. L. Vincent, M. Corbetta, D. C. van Essen, and M. E. Raichle. 2005. "From The Cover: The Human Brain Is Intrinsically Organized into Dynamic, Anticorrelated Functional Networks." *Proc Natl Acad Sci USA* 102: 9673–9678. <http://www.pnas.org/cgi/doi/10.1073/pnas.0504136102>
- Fox, M. D., D. Zhang, A. Z. Snyder, and M. E. Raichle. 2009. "The Global Signal and Observed Anticorrelated Resting State Brain Networks." *J Neurophysiol* 101: 3270–3283. <http://jn.physiology.org/cgi/doi/10.1152/jn.90777.2008>
- Genovese, C. R., N. A. Lazar, and T. E. Nichols. 2002. "Thresholding of Statistical Maps in Functional Neuroimaging Using the False Discovery Rate." *NeuroImage* 15: 870–878. <http://www.sciencedirect.com/science/article/pii/S1053811901910377>
- Greicius, M. D., B. Krasnow, A. L. Reiss, and V. Menon. 2002. "Functional Connectivity in the Resting Brain: A Network Analysis of the Default Mode Hypothesis." *Proc Natl Acad Sci U S A* 100: 253–258. <http://www.pnas.org/cgi/doi/10.1073/pnas.0135058100>
- Guimera, R., and L. A. N. Amaral. 2005. "Functional Cartography of Complex Metabolic Networks." *Nature* 433: 895–900. <http://www.nature.com/doi/10.1038/nature03288>
- Gujar, N., S. Yoo, P. Hu, and M. P. Walker. 2010. "The Unrested Resting Brain: Sleep Deprivation Alters Activity Within the Default-mode Network." *J Cog Neurosci* 22: 1637–1648. <http://www.mitpressjournals.org/doi/abs/10.1162/jocn.2009.21331>
- Hagler, D. J., A. P. Saygin, and M. I. Sereno. 2006. "Smoothing and Cluster Thresholding for Cortical Surface-based Group Analysis of fMRI Data." *Neuroimage* 33: 1093–1103. <http://dx.doi.org/10.1016/j.neuroimage.2006.07.036>.

- Hagmann, P., L. Cammoun, X. Gigandet, R. Meuli, C. J. Honey, V. J. Wedeen, and O. Sporns. 2008. "Mapping the Structural Core of Human Cerebral Cortex." *PLoS Biol* 6: e159. <http://biology.plosjournals.org/perlserv/?request=get-document&doi=10.1371%2Fjournal.pbio.0060159>
- Hayasaka, S., and P. J. Laurienti. 2010. "Comparison of Characteristics Between Region-and Voxel-based Network Analyses in Resting-state fMRI Data." *Neuroimage* 50: 499–508. <http://dx.doi.org/10.1016/j.neuroimage.2009.12.051>.
- He, Y., Z. J. Chen, and A. C. Evans. 2007. "Small-World Anatomical Networks in the Human Brain Revealed by Cortical Thickness from MRI." *Cereb Cortex* 17: 2407–2419. <http://dx.doi.org/10.1093/cercor/bhl149>.
- He, Y., J. Wang, L. Wang, Z. J. Chen, C. Yan, H. Yang, H. Tang, et al. 2009. "Uncovering Intrinsic Modular Organization of Spontaneous Brain Activity in Humans." *PLoS ONE* 4: e5226. <http://dx.doi.org/10.1371/journal.pone.0005226>.
- Honey, C. J., O. Sporns, L. Cammoun, X. Gigandet, J. P. Thiran, R. Meuli, and P. Hagmann. 2009. "Predicting Human Resting-state Functional Connectivity from Structural Connectivity." *Proc Natl Acad Sci USA* 106: 2035–2040. <http://dx.doi.org/10.1073/pnas.0811168106>.
- Horowitz, S. G., A. R. Braun, W. S. Carr, D. Picchioni, T. J. Balkin, M. Fukunaga, and J. H. Duyn. 2009. "Decoupling of the Brain's Default Mode Network During Deep Sleep." *Proc Natl Acad Sci USA* 106: 11376–11381. .
- Jo, H. J., J. Lee, J. Kim, C. Choi, B. Gu, D. Kang, J. Ku, J. S. Kwon, and S. I. Kim. 2008. "Artificial Shifting of fMRI Activation Localized by Volume- and Surface-based Analyses." *Neuroimage* 40: 1077–1089. <http://dx.doi.org/10.1016/j.neuroimage.2007.12.036>.
- Jo, H. J., J. Lee, J. Kim, Y. Shin, I. Kim, J. S. Kwon, and S. I. Kim. 2007. "Spatial Accuracy of fMRI Activation Influenced by Volume- and Surface-based Spatial Smoothing Techniques." *Neuroimage* 34: 550–564. <http://dx.doi.org/10.1016/j.neuroimage.2006.09.047>.
- Johnstone, T., K. S. O. Walsh, L. L. Greischar, A. L. Alexander, A. S. Fox, R. J. Davidson, and T. R. Oakes. 2006. "Motion Correction and the Use of Motion Covariates in Multiple-subject Fmri Analysis." *Hum Brain Mapp* 27: 779–788. <http://dx.doi.org/10.1002/hbm.20219>.
- Jovicich, J., S. Czanner, D. Greve, Elizabeth Haley, A. J. W. van der Kouwe, R. Gollub, D. Kennedy, et al. 2006. "Reliability in Multi-site Structural MRI Studies: Effects of Gradient Non-linearity Correction on Phantom and Human Data." *Neuroimage* 30: 436 – 443. <http://dx.doi.org/10.1016/j.neuroimage.2009.02.010>.
- Kasahara, M., D. K. Menon, C. H. Salmond, J. G. Outtrim, J. V. Taylor Tavares, T. A. Carpenter, J. D. Pickard, B. J. Sahakian, and E. A. Stamatakis. 2010. "Altered Functional Connectivity in the Motor Network After Traumatic Brain Injury." *Neurology* 75: 168–176. <http://dx.doi.org/10.1212/WNL.0b013e3181e7ca58>.
- Larson-Prior, L. J., J. M. Zempel, T. S. Nolan, F. W. Prior, A. Z. Snyder, and M. E. Raichle. 2009. "Cortical Network Functional Connectivity in the Descent to Sleep." *Proc Natl Acad Sci USA* 106: 4489–4494. .
- Latora, V., and M. Marchiori. 2001. "Efficient Behavior of Small-World Networks." *Phys Rev Lett* 87: 198701. <http://dx.doi.org/10.1103/PhysRevLett.87.198701>.
- Levin, H. S., E. A. Wilde, M. Troyanskaya, N. J. Petersen, R. Scheibel, M. Newsome, M. Radaideh, et al. 2010. "Diffusion Tensor Imaging of Mild to Moderate Blast-Related Traumatic Brain Injury and Its Sequelae." *J Neurotrauma* 27: 683–694. <http://dx.doi.org/10.1089/neu.2009.1073>.

- Liang, X., Q. Zou, Y. He, and Y. Yang. 2013. "Coupling of Functional Connectivity and Regional Cerebral Blood Flow Reveals a Physiological Basis for Network Hubs of the Human Brain." *Proc Natl Acad Sci* 110: 1929–1934. <http://dx.doi.org/10.1073/pnas.1214900110>.
- Liao, Y., J. Tang, A. Fornito, T. Liu, X. Chen, H. Chen, X. Xiang, X. Wang, and W. Hao. 2012. "Alterations in Regional Homogeneity of Resting-state Brain Activity in Ketamine Addicts." *Neurosci Lett* 522: 36–40. <http://dx.doi.org/10.1016/j.neulet.2012.06.009>.
- Lowe, M.J., B.J. Mock, and J.A. Sorenson. 1998. "Functional Connectivity in Single and Multislice Echoplanar Imaging Using Resting-State Fluctuations." *NeuroImage* 7: 119–132. <http://dx.doi.org/10.1006/nimg.1997.0315>.
- Mac Donald, C. L., A. M. Johnson, D. Cooper, E. C. Nelson, N. J. Werner, J. S. Shimony, A. Z. Snyder, et al. 2011. "Detection of Blast-related Traumatic Brain Injury in U.S. Military Personnel." *N Engl J Med* 364: 2091–2100. <http://dx.doi.org/10.1056/NEJMoa1008069>.
- Marquez de la Plata, C. D., J. Garces, E. S. Kojori, J. Grinnan, K. Krishnan, R. Pidikiti, J. Spence, et al. 2011. "Deficits in Functional Connectivity of Hippocampal and Frontal Lobe Circuits After Traumatic Axonal Injury." *Arch Neurol* 68: 74–84. <http://dx.doi.org/10.1001/archneurol.2010.342>.
- Mayer, A. R., M. V. Mannell, J. Ling, C. Gasparovic, and R. A. Yeo. 2011. "Functional Connectivity in Mild Traumatic Brain Injury." *Hum Brain Mapp* 32: 1825–1835. <http://dx.doi.org/10.1002/hbm.21151>.
- Meunier, D., S. Achard, A. Morcom, and E. T. Bullmore. 2009a. "Age-related Changes in Modular Organization of Human Brain Functional Networks." *Neuroimage* 44: 715–723. <http://dx.doi.org/10.1016/j.neuroimage.2008.09.062>.
- Meunier, D., R. Lambiotte, A. Fornito, K. D. Ersche, and E. T. Bullmore. 2009b. "Hierarchical Modularity in Human Brain Functional Networks." *Front Neuroinform* 3: 37. <http://dx.doi.org/10.3389/neuro.11.037.2009>.
- Micheloyannis, S., E. Pachou, C. J. Stam, M. Breakspear, P. Bitsios, M. Vourkas, S. Erimaki, and M. Zervakis. 2006. "Small-world Networks and Disturbed Functional Connectivity in Schizophrenia." *Schizophr Res* 87: 60–66. <http://dx.doi.org/10.1016/j.schres.2006.06.028>.
- Minka, T., "Automatic Choice of Dimensionality for PCA," Massachusetts Inst. Technol., Cambridge, Tech. Rep. 514, 2000.
- Murphy, K., R. M. Birn, D. A. Handwerker, T. B. Jones, and P. A. Bandettini. 2009. "The Impact of Global Signal Regression on Resting State Correlations: Are Anti-correlated Networks Introduced?" *Neuroimage* 44: 893–905. <http://dx.doi.org/10.1016/j.neuroimage.2008.09.036>.
- Nakamura, T., F. G. Hillary, and B. B. Biswal. 2009. "Resting Network Plasticity Following Brain Injury." *PLoS ONE* 4: e8220. <http://dx.doi.org/10.1371/journal.pone.0008220>.
- Newman, M. E. J. 2004. "Fast Algorithm for Detecting Community Structure in Networks." *Phys Rev E* 69: 066133. <http://dx.doi.org/10.1103/PhysRevE.69.066133>.
- Newman, M., and M. Girvan. 2004. "Finding and Evaluating Community Structure in Networks." *Phys Rev E* 69: 026113. <http://dx.doi.org/10.1103/PhysRevE.69.026113>.
- Nichols, T. E., and A. P. Holmes. 2001. "Nonparametric Permutation Tests for Functional Neuroimaging: A Primer with Examples." *Hum Brain Mapp* 15: 1–25. <http://dx.doi.org/10.1002/hbm.1058>.
- Niogi, S. N., P. Mukherjee, J. Ghajar, C. E. Johnson, R. Kolster, H. Lee, M. Suh, R. D. Zimmerman, G. T. Manley, and B. D. McCandliss. 2008. "Structural Dissociation of Attentional Control and Memory in Adults with and without Mild Traumatic Brain Injury." *Brain* 131: 3209–3221. <http://dx.doi.org/10.1093/brain/awn247>.

- Niogi, S. N., and P. Mukherjee. 2010. "Diffusion Tensor Imaging of Mild Traumatic Brain Injury." *J Head Trauma Rehabil* 25: 241–255. <http://dx.doi.org/10.1097/HTR.0b013e3181e52c2a>.
- Ojemann, J. G., E. Akbudak, A. Z. Snyder, R. C. McKinstry, M. E. Raichle, and T. E. Conturo. 1997. "Anatomic Localization and Quantitative Analysis of Gradient Refocused Echo-planar fMRI Susceptibility Artifacts." *Neuroimage* 6: 156–167. <http://dx.doi.org/10.1006/nimg.1997.0289>
- Okie, Susan. 2006. "Reconstructing Lives — A Tale of Two Soldiers." *N Engl J Med* 355: 2609–2615. <http://dx.doi.org/10.1056/NEJMp068235>.
- Ponten, S. C., F. Bartolomei, and C. J. Stam. 2007. "Small-world Networks and Epilepsy: Graph Theoretical Analysis of Intracerebrally Recorded Mesial Temporal Lobe Seizures." *Clin Neurophysiol* 118: 918–927. <http://dx.doi.org/10.1016/j.clinph.2006.12.002>.
- Power, J. D., A. L. Cohen, S. M. Nelson, G. S. Wig, K. A. Barnes, J. A. Church, A. C. Vogel, et al. 2011. "Functional Network Organization of the Human Brain." *Neuron* 72: 665–678. <http://dx.doi.org/10.1016/j.neuron.2011.09.006>.
- Power, J. D., K. A. Barnes, A. Z. Snyder, B. L. Schlaggar, and S. E. Petersen. 2012. "Spurious but Systematic Correlations in Functional Connectivity MRI Networks Arise from Subject Motion." *Neuroimage* 59: 2142–2154. <http://dx.doi.org/10.1016/j.neuroimage.2011.10.018>.
- Raichle, M. E., A. M. MacLeod, A. Z. Snyder, W. J. Powers, D. A. Gusnard, and G. L. Shulman. 2001. "A Default Mode of Brain Function." *Proc Natl Acad Sci USA* 98: 676–682. <http://dx.doi.org/10.1073/pnas.98.2.676>.
- Rombouts, S. A. R. B., C. J. Stam, J. P. A. Kuijter, Ph. Scheltens, and F. Barkhof. 2003. "Identifying Confounds to Increase Specificity During a 'no Task Condition': Evidence for hippocampal connectivity using fMRI." *Neuroimage* 20: 1236–1245. [http://dx.doi.org/10.1016/S1053-8119\(03\)00386-0](http://dx.doi.org/10.1016/S1053-8119(03)00386-0).
- Rosvall, M., and C. T. Bergstrom. 2008. "Maps of Random Walks on Complex Networks Reveal Community Structure." *Proc Natl Acad Sci* 105: 1118–1123. <http://dx.doi.org/10.1073/pnas.0706851105>.
- Rubinov, M., and O. Sporns. 2010. "Complex Network Measures of Brain Connectivity: Uses and Interpretations." *Neuroimage* 52: 1059–1069. <http://dx.doi.org/10.1016/j.neuroimage.2009.10.003>.
- Saad Z. S., Reynolds R. C., Argall B., Japee S., Cox R. W. (2004) SUMA: an interface for surface-based intra- and inter-subject analysis with AFNI. 2004 2nd IEEE International Symposium on Biomedical Imaging: From Nano to Macro, Vols 1 and 2. pp 1510–1513. <http://dx.doi.org/10.1109/ISBI.2004.1398837>.
- Saad, Z. S., S. J. Gotts, K. Murphy, G. Chen, H. J. Jo, A. Martin, and R. W. Cox. 2012. "Trouble at Rest: How Correlation Patterns and Group Differences Become Distorted After Global Signal Regression." *Brain Connect* 2: 25–32. <http://dx.doi.org/10.1089/brain.2012.0080>.
- Saatman, K. E., A. Duhaime, R. Bullock, A. I. R. Mass, A. Valadka, G. T. Manley, and Workshop scientific team and advisory panel members. 2008. "Classification of Traumatic Brain Injury for Targeted Therapies." *J Neurotrauma* 25: 719–738. <http://dx.doi.org/10.1089/neu.2008.0586>.
- Salvador, R., J. Suckling, M. R. Coleman, J. D. Pickard, D. Menon, and E. T. Bullmore. 2005. "Neurophysiological Architecture of Functional Magnetic Resonance Images of Human Brain." *Cereb Cortex* 15: 1332–1342. <http://dx.doi.org/10.1093/cercor/bhi016>.
- Satterthwaite, T. D., D. H. Wolf, J. Loughhead, K. Ruparel, M. A. Elliott, H. Hakonarson, R. C. Gur, and R. E. Gur. 2012. "Impact of In-scanner Head Motion on Multiple Measures of Functional Connectivity: Relevance for Studies of Neurodevelopment in Youth." *Neuroimage* 60: 623–632. <http://dx.doi.org/10.1016/j.neuroimage.2011.12.063>.

- Scheibel, R. S., M. R. Newsome, M. Troyanskaya, X. Lin, J. L. Steinberg, M. Radaideh, and H. S. Levin. 2012. "Altered Brain Activation in Military Personnel with One or More Traumatic Brain Injuries Following Blast." *J Int Neuropsychol Soc* 18: 89–100. <http://dx.doi.org/10.1017/S1355617711001433>.
- Seeley, W. W., V. Menon, A. F. Schatzberg, J. Keller, G. H. Glover, H. Kenna, A. L. Reiss, and M. D. Greicius. 2007. "Dissociable Intrinsic Connectivity Networks for Salience Processing and Executive Control." *J Neurosci* 27: 2349–2356. <http://dx.doi.org/10.1523/JNEUROSCI.5587-06.2007>.
- Segonne, F., A. M. Dale, E. Busa, M. Glessner, D. H. Salat, H. K. Hahn, and B. Fischl. 2004. "A Hybrid Approach to the Skull Stripping Problem in MRI." *Neuroimage* 22: 1060 – 1075. <http://dx.doi.org/10.1016/j.neuroimage.2004.03.032>.
- Sharp, D. J., C. F. Beckmann, R. Greenwood, K. M. Kinnunen, V. Bonnelle, X. de Boissezon, J. H. Powell, S. J. Counsell, M. C. Patel, and R. Leech. 2011. "Default Mode Network Functional and Structural Connectivity After Traumatic Brain Injury." *Brain* 134: 2233–2247. <http://dx.doi.org/10.1093/brain/awr175>.
- Shenton, M. E., H. M. Hamoda, J. S. Schneiderman, S. Bouix, O. Pasternak, Y. Rathi, M.-A. Vu, et al. 2012. "A Review of Magnetic Resonance Imaging and Diffusion Tensor Imaging Findings in Mild Traumatic Brain Injury." *Brain Imaging and Behav* 6: 137–192. <http://dx.doi.org/10.1007/s11682-012-9156-5>.
- Slobounov, S. M., M. Gay, K. Zhang, B. Johnson, D. Pennell, W. Sebastianelli, S. Horovitz, and M. Hallett. 2011. "Alteration of Brain Functional Network at Rest and in Response to YMCA Physical Stress Test in Concussed Athletes: RsfMRI Study." *Neuroimage* 55: 1716–1727. <http://dx.doi.org/10.1016/j.neuroimage.2011.01.024>.
- Sponheim, S. R., K. A. McGuire, S. S. Kang, N. D. Davenport, S. Aviyente, E. M. Bernat, and K. O. Lim. 2011. "Evidence of Disrupted Functional Connectivity in the Brain After Combat-related Blast Injury." *Neuroimage* 54: S21–S29. <http://dx.doi.org/10.1016/j.neuroimage.2010.09.007>.
- Stam, C., B. Jones, G. Nolte, M. Breakspear, and P. Scheltens. 2006. "Small-World Networks and Functional Connectivity in Alzheimer's Disease." *Cereb Cortex* 17: 92–99. <http://dx.doi.org/10.1093/cercor/bhj127>.
- Tang, L., Y. Ge, D. K. Sodickson, L. Miles, Y. Zhou, J. Reaume, and R. I. Grossman. 2011. "Thalamic Resting-State Functional Networks: Disruption in Patients with Mild Traumatic Brain Injury." *Radiology* 260: 831–840. <http://dx.doi.org/10.1148/radiol.11110014>.
- Taylor, P. A., and C. C. Ford. 2009. "Simulation of Blast-induced Early-time Intracranial Wave Physics Leading to Traumatic Brain Injury." *J Biomech Eng* 131: 061007. <http://dx.doi.org/10.1115/1.3118765>.
- Tucholka, A., V. Fritsch, J. Poline, and B. Thirion. 2012. "An Empirical Comparison of Surface-based and Volume-based Group Studies in Neuroimaging." *Neuroimage* 63: 1443–1453. <http://dx.doi.org/10.1016/j.neuroimage.2012.06.019>.
- Valencia, M., M. A. Pastor, M. A. Fernandez-Seara, J. Artieda, J. Martinerie, and M. Chavez. 2009. "Complex Modular Structure of Large-scale Brain Networks." *Chaos* 19: 023119. <http://dx.doi.org/10.1063/1.3129783>.
- van den Heuvel, M. P., C. J. Stam, M. Boersma, and H. E. Hulshoff Pol. 2008. "Small-world and Scale-free Organization of Voxel-based Resting-state Functional Connectivity in the Human Brain." *Neuroimage* 43: 528–539. <http://dx.doi.org/10.1016/j.neuroimage.2008.08.010>.

- van Dijk, K. R. A., T. Hedden, A. Venkataraman, K. C. Evans, S. W. Lazar, and R. L. Buckner. 2010. "Intrinsic Functional Connectivity as a Tool for Human Connectomics: Theory, Properties, and Optimization." *J Neurophysiol* 103: 297–321. <http://dx.doi.org/10.1152/jn.00783.2009>.
- van Dijk, K. R.A., M. R. Sabuncu, and R. L. Buckner. 2012. "The Influence of Head Motion on Intrinsic Functional Connectivity MRI." *Neuroimage* 59: 431–438. .
- van Essen, D. C., and D. Dierker. 2007. "On Navigating the Human Cerebral Cortex: Response to 'in Praise of Tedious Anatomy'." *Neuroimage* 37: 1050–1054. <http://dx.doi.org/10.1016/j.neuroimage.2007.02.021>.
- van Wingen, G. A., E. Geuze, M. W. A. Caan, T. Kozicz, S. D. Olabarriaga, D. Denys, E. Vermetten, and G. Fernandez. 2012. "Persistent and Reversible Consequences of Combat Stress on the Mesofrontal Circuit and Cognition." *Proc Natl Acad Sci USA* 109: 15508–15513. <http://dx.doi.org/10.1073/pnas.1206330109>.
- Vincent, J. L., I. Kahn, A. Z. Snyder, M. E. Raichle, and R. L. Buckner. 2008. "Evidence for a Frontoparietal Control System Revealed by Intrinsic Functional Connectivity." *J Neurophysiol* 100: 3328–3342. <http://dx.doi.org/10.1152/jn.90355.2008>.
- Wang, J., X. Zuo, S. Gohel, M. P. Milham, B. B. Biswal, and Y. He. 2011. "Graph Theoretical Analysis of Functional Brain Networks: Test-Retest Evaluation on Short- and Long-Term Resting-State Functional MRI Data." *PLoS ONE* 6: e21976. <http://dx.doi.org/10.1371/journal.pone.0021976>.
- Warden, D. L. 2006. "Military TBI During the Iraq and Afghanistan Wars." *J Head Trauma Rehabil* 21: 398–402.
- Watts, D. J., and S. H. Strogatz. 1998. "Collective Dynamics of 'small-world' Networks." *Nature* 393: 440–442. <http://dx.doi.org/10.1038/30918>.
- Werner, C., and K. Engelhard. 2007. "Pathophysiology of Traumatic Brain Injury." *Br J Anaesth* 99: 4–9. <http://dx.doi.org/10.1093/bja/aem131>.
- Wig, G. S., B. L. Schlaggar, and S. E. Petersen. 2011. "Concepts and Principles in the Analysis of Brain Networks." *Ann NY Acad Sci* 1224: 126–146. <http://dx.doi.org/10.1111/j.1749-6632.2010.05947.x>
- Yeo, B. T. T., F. M. Krienen, J. Sepulcre, M. R. Sabuncu, D. Lashkari, M. Hollinshead, J. L. Roffman, et al. 2011. "The Organization of the Human Cerebral Cortex Estimated by Intrinsic Functional Connectivity." *J of Neurophysiol* 106: 1125–1165. <http://dx.doi.org/10.1152/jn.00338.2011>.
- Zhang, D., A. Z. Snyder, M. D. Fox, M. W. Sansbury, J. S. Shimony, and M. E. Raichle. 2008. "Intrinsic Functional Relations Between Human Cerebral Cortex and Thalamus." *J Neurophysiol* 100: 1740–1748. <http://dx.doi.org/10.1152/jn.90463.2008>.

Figures and Legends

Figure 1. An illustration of the analysis procedure. For each subject, with volumetric structural MRI data (**a**), cortical surface (**b**) was reconstructed. Subsequently, the surface underwent the inter-subject alignment and spatial resampling close to the spatial resolution of resting-state BOLD fMRI (**c**) to allow surface-based, node-by-node cross-subject analyses. The preprocessed resting-state BOLD fMRI data (**d**) were converted to surface-based BOLD signal data (**f**) aligned to the individual cortical surface (**e**). BOLD fluctuation correlation coefficients between every pair of nodes in the brain (e.g., the gray square from red and cyan nodes in (**e**)) were obtained to yield a correlation matrix (**g**). A connectivity matrix (**h**) was derived by thresholding the correlation matrix, and a brain network (**i**) was constructed. In this illustration, yellow lines indicate connection between nodes. With the identified modules (three modules delineated by dashed lines in this example) in (**j**), modularity, within-module degree z -score (e.g., five magenta lines for the red-colored node in (**k**)) and participation coefficient (e.g., the distribution of magenta, cyan and olive lines for the red-colored node in (**l**)) were obtained for each node.

Figure 2. Group module assignments of each of the controls and the first TBI (TBI I) cohort. The identified modules from group averaged correlation matrices were color-coded as a function of tie densities (densities of the retained strongest correlations): 3% (**a**), 2% (**b**) and 1.5% (**c**). Only modules of size greater than 1% of total number of nodes were displayed.

Figure 3. Global network properties of the controls and the first TBI (TBI I) cohort. Scatter plots for modularity (**a**) and average participation coefficients over all nodes (**b**). Each symbol represents a single individual's averaged measure across brain regions. The I bars indicate the means and standard deviation for the control, the dotted horizontal bar is two standard deviations from the mean of the control and the solid horizontal bar in the TBI I cohort is the mean of the TBI I cohort. Filled triangles represent TBI patients with relatively 'abnormal' measures, located outside of the dotted horizontal bars. The number of relatively 'abnormal' TBI patients for each measure was labeled in parentheses, and the p -values were obtained from permutation tests (10,000 permutations) on group mean difference.

Figure 4. Node-specific network properties of the controls and TBI I cohort. Group mean comparison maps ($p_{\text{uncorr}} < 0.05$) of within-module degree z -score (**a**) and participation coefficient (**b**), respectively. All color maps were superimposed on the averaged cortical surface from all participants in dataset I. R G_precentral: right precentral gyrus, R G_pariet_inf-Supramar: right supramarginal gyrus, R G_front_inf-Opercular: right opercular part of the inferior frontal gyrus, R G_front_sup-medial: right medial superior frontal gyrus, R G_front_sup-dorsomedial: right dorsomedial superior frontal gyrus.

Figure 5. Count of the TBI patients from the TBI I cohort with 'abnormal' node-specific network properties relative to the controls. Color maps of the number of TBI patients whose measures (within-module degree z -score and participation coefficient, respectively) were outside two standard deviations from the mean of the control. All color maps were superimposed on the averaged cortical surface from all participants in the controls and TBI I cohort.

Figure 6. Regions of interest (ROIs) for participation coefficient. 15 ROIs are colored and labeled (1: central sulcus, 2: left anterior transverse temporal gyrus, 3: right long insular gyrus and central sulcus of the insula, 4: superior frontal sulcus, 5: medial superior frontal gyrus, 6: anterior superior frontal gyrus, 7: deep anterior part of the cingulate gyrus and sulcus, 8: superficial anterior part of the cingulate gyrus and sulcus, 9: right superior part of the precentral sulcus, 10: right superior temporal sulcus, 11: right orbital gyri, 12: posterior-ventral part of the cingulate gyrus, 13: lingual gyrus, 14: right parieto-occipital sulcus and 15: left cuneus). See Table III for the coordinates and areas of these ROIs.

Figure 7. ROI analysis of participation coefficient of the controls and patients with TBI. Scatter plots for averaged participation coefficients within each of three selected ROIs. See Fig. 3 for the details of the scatter plots, Table III for abbreviations and Table IV for results from all ROIs.

Figure 8. Bar graphs for observed and expected ‘abnormal’ ROIs in the patients with TBI relative to the controls. The distribution of expected relatively ‘abnormal’ ROIs was calculated from the binomial distribution with the probability that one region deems ‘abnormal’ by chance (0.0455; the probability that participation coefficient for a TBI patient falls outside two standard deviations from the mean of the controls). The p -values were obtained by the one-sided z -test (TBI I > controls in the number of ‘abnormal’ ROIs).

Figure 9. Scatter plots for multivariate analysis of participation coefficients within the ROIs after dimensionality reduction by probabilistic principal component analysis. Solid triangles represent relatively ‘abnormal’ TBI patients whose values are locating within the lower and upper tail, accounting for 2.5% in each tail, of the estimated multivariate normal distribution from the control. The label in each panel indicates the number of relatively ‘abnormal’ TBI patients and the number of TBI patients on the corresponding scan.

Tables

Table I. Excluded datasets after the quality assurance procedure.

Criteria	Ctrl		TBI I		TBI II		Total
	Initial	Follow-up	Initial	Follow-up	Initial	Follow-up	
Poor T ₁ image quality	0	0	1	0	0	0	1
Brain outside FOV	1	0	1	0	3	1	6
Motion correction failure	1	0	1	0	0	0	2
Lack of frames	0	0	1	0	0	0	1
Intensity distortion	0	0	1	0	0	0	1
Susceptibility artifacts	1	1	0	1	0	0	3
<4 minutes of data after motion scrubbing	5	4	7	9	4	3	32
Fragmented modules	1	1	4	0	2	1	9
Total	9	6	16	10	9	5	55

Note: FOV, field of view; Ctrl, Control; TBI I, TBI I cohort; TBI II, TBI II cohort.

Table II. Demographics of the controls, TBI I cohort and TBI II cohort.

Demographics ^a	Ctrl, all (N=21)	Ctrl, subset ^b (N=14)	TBI I, all (N=63)	TBI I, subset ^b (N=54)	TBI II, all (N=40)	TBI II, subset ^b (N=38)
Age (years) ^c	19-49, 29	20-49, 29	19-57, 25	19-44, 24	19-44, 23	19-44, 23
Gender (males, females)	21,0	14,0	63,0	54,0	37,3 ^e	35,3 ^f
Education (years) ^c	11-17.5, 12.5	11-16, 12	8-17, 12	8-17, 12	9-16, 12	9-16, 12
Post-injury time (days) ^{c,d}	N/A	N/A	0-90, 14	0-90, 14	0-30, 7	0-30, 7

^aDemographics of the controls and TBI I cohort were reproduced from Table I in Mac Donald et al. (2011).

^bSubsets of subjects that were included in graph theoretical analyses of either the initial scans, the follow-up scans, or both.

^cRange and median values were reported.

^dPost-injury time on the day of the initial scan.

^e $p < 0.05$ (chi-square) vs. TBI II, all.

^f $p < 0.05$ (chi-square) vs. TBI II, included subset.

Table III. Regions-of-interest (ROI) for participation coefficient analyses.

Index ^a	ROI name	MNI coordinates (x,y,z) of center ^b		Surface area (mm ²) ^c	
		Left	Right	Left	Right
1(45)	S_central	(-51, -11, 28)	(51, -11, 30)	531.5	616.5
2(33)	L G_temp_sup-G_T_transv	(-41, -20, 4)		419.0	
3(17)	R G_Ins_lg_and_S_cent_ins		(39, -15, 10)		560.4
4(54)	S_front_sup	(-21, 25, 46)	(28, 27, 41)	281.0	310.5
5(16)	G_front_sup-medial	(-5, 39, 31)	(9, 41, 22)	409.3	411.5
6(16)	G_front_sup-anterior	(-8, 63, 25)	(13, 57, 29)	490.9	473.2
7(6)	G_and_S_cingul-Ant-deep	(-4, 37, -8)	(7, 38, -7)	262.3	356.0
8(6)	G_and_S_cingul-Ant-superficial	(-8, 56, 3)	(9, 55, 2)	203.8	338.7
9(69)	R S_precentral-sup-part		(23, -13, 61)		260.7
10(73)	R S_temporal_sup		(55, -20, -12)		291.8
11(24)	R G_orbital		(41, 28, -16)		237.3
12(10)	G_cingul-Post-ventral	(-8, -52, 3)	(12, -53, 5)	300.0	199.5
13(22)	G_oc-temp_med-Lingual	(-14, -60, 1)	(29, -41, -11)	441.9	381.2
14(65)	R S_parieto_occipital		(18, -81, 38)		302.2
15(11)	L G_cuneus	(-2, -85, 14)		465.1	

^aInitial index numbers indicate regions of interest labeled in Figure 6. Numbers in parentheses refer to the corresponding index numbers in Destrieux et al. (2010).

^bMNI coordinates correspond to a mid point between pial surface and white matter surface.

^cSurface area of white matter surface

Note: S_central, central sulcus (Rolando's fissure); L G_temp_sup-G_T_transv, left anterior transverse temporal gyrus (of Heschl); R G_Ins_lg_and_S_cent_ins, right long insular gyrus and central sulcus of the insula, S_front_sup, superior frontal sulcus; G_front_sup-medial, medial superior frontal gyrus (F1); G_front_sup-anterior, anterior superior frontal gyrus (F1); G_and_S_cingul-Ant-deep, deep anterior part of the cingulate gyrus and sulcus; G_and_S_cingul-Ant-superficial, superficial anterior part of the cingulate gyrus and sulcus; R S_precentral-sup-part, right superior part of the precentral sulcus; R S_temporal_sup, right superior temporal sulcus (parallel sulcus); R G_orbital, right orbital gyri; G_cingul-Post-ventral, posterior-ventral part of the cingulate gyrus (vPCC, isthmus of the cingulate gyrus); G_oc-temp_med-Lingual, lingual gyrus, lingual part of the medial occipito-temporal gyrus (O5); R S_parieto_occipital, right parieto-occipital sulcus (or fissure); L G_cuneus, left cuneus (O6); MNI, Montreal Neurological Institute (Evans et al., 1993)

Table IV. ROI analysis results of participation coefficients.

Index	ROI name	TBI I vs. Control				TBI II vs. Control			
		Initial		Follow-up		Initial		Follow-up	
		<i>p</i> -value	'Abnormal' TBI ^a	<i>p</i> -value	'Abnormal' TBI ^a	<i>p</i> -value	'Abnormal' TBI ^a	<i>p</i> -value	'Abnormal' TBI ^a
1(45)	S_central	0.0008	13/0	0.9662	3/0	0.1307	1/0	0.7192	1/1
2(33)	L_G_temp_sup-G_T_transv	0.0103	12/1	0.7192	4/0	0.8152	2/1	0.3153	4/0
3(17)	R_G_Ins_lg_and_S_cent_ins	0.0056	10/1	0.8592	4/3	0.3969	1/1	0.6634	2/1
4(54)	S_front_sup	0.0055	10/0	0.6465	2/1	0.6172	1/0	0.2664	0/1
5(16)	G_front_sup-medial	0.0032	11/0	0.594	1/1	0.4542	0/0	0.3939	0/1
6(16)	G_front_sup-anterior	0.0028	14/0	0.2659	1/3	0.4114	2/0	0.1762	0/1
7(6)	G_and_S_cingul-Ant-deep	0.0042	12/0	0.5598	1/2	0.1805	3/0	0.3045	0/1
8(6)	G_and_S_cingul-Ant-superficial	0.0024	13/0	0.1512	0/2	0.1235	3/0	0.0896	0/1
9(69)	R_S_precentral-sup-part	0.0152	11/0	0.9521	1/0	0.2991	1/0	0.8342	1/1
10(73)	R_S_temporal_sup	0.0056	13/0	0.6993	2/0	0.3637	3/0	0.8812	1/0
11(24)	R_G_orbital	0.0012	15/0	0.5254	2/1	0.3905	1/0	0.4276	0/0
12(10)	G_cingul-Post-ventral	0.0005	13/0	0.1326	1/1	0.0952	3/0	0.0725	0/1
13(22)	G_oc-temp_med-Lingual	0.0002	15/0	0.909	2/0	0.2482	3/1	0.7578	0/1
14(65)	R_S_parieto_occipital	0.0021	15/0	0.5216	1/0	0.1133	3/0	0.6265	0/1
15(11)	L_G_cuneus	0.0046	8/0	0.6474	2/0	0.2018	0/0	0.6863	0/1

^aThe number of TBI patients with 'abnormally' low participation coefficients / the number of TBI patients with 'abnormally' high participation coefficients.

Note: See Table III for the abbreviations of ROI names.

Supplemental Materials

Supplemental Results

1.1 Direction comparisons between the initial scans and the follow-up scans

Additional, direct comparisons between the initial and follow-up scans with subjects who underwent both scans at the single-subject level (Fig. S4a, b) demonstrated large amount of change (both increases and decreases) over time (See discussion for the limitations of this study relevant to this observation). Further, notable group differences in longitudinal changes in these measures were mainly due to ‘abnormal’ TBI patients in terms of the global network properties (Fig. S4a, b *4th column*). Without these ‘abnormal’ TBI patients, group differences in longitudinal changes were not statistically significant at $\alpha = 0.05$.

Supplemental Discussion

4.2.4 Modularity

Higher modularity in the TBI I cohort than in the controls on the initial scans may at first seem counterintuitive. However, higher modularity in the TBI I cohort on the initial may be explained by decreases or losses of functional connectivity from blast injuries over multiple regions in a heterogeneous fashion. By definition, modular organizations are marked by many within-module connections and fewer between-module connections. Thus, losses of the few between-module connections may have more marked impact on modular organizations than losses of many within-module connections. These losses of between-module connections might make the brain network appear more modular. Indeed, modularity of young healthy subjects increases at sparser network density (Braun et al., 2012; He et al., 2009).

Supplementary Figures and Legends

Figure S1. Group statistic maps for seed-based Fisher-Z transformed correlations of the controls and the TBI I cohort. With each subject's data that passed the quality assurance procedure before checking the module assignment results, the seed was placed at the left posterior cingulate cortex (PCC; -7, -55, 27, red spot) including nodes within 6 mm Euclidean distance from the PCC. The colors represent statistical significance of the group means of Fisher-Z transformed correlation coefficients. After ensuring that the Fisher-Z transformed correlations across subjects within each group passed the Shapiro-Wilk test at $\alpha = 0.05$, the t-test on the group means were performed, thresholded ($p_{\text{uncorr}} < 0.001$) and converted to z-score.

Figure S2. Group module assignments of each of the controls and TBI I cohort using the Infomap algorithm. See Fig. 2 for the details of labels.

Figure S3. Single subject comparisons of module assignments between the Louvain and Infomap algorithm at 3% tie density.

Figure S4. Longitudinal changes in modularity (a) and average participation coefficient (b). The first and second columns are scatter plots for the global measures of subjects who had acceptable data quality for both the initial and follow-up scans. Changes in these global measures at each subject are on the third column. Scatter plots on the fourth column are symmetrized percent change, i.e., (follow-up scans – initial scans)/average of initial and follow-up scans. Filled triangles on the third and fourth columns are relatively 'abnormal' TBI patients on the initial scans. Dotted magenta horizontal bars on the TBI I in the fourth column represent the group average values of the TBI patients without these 'abnormal' TBI patients. See Fig. 3 for the other details of the scatter plots.

Figure S5. Average frame-to-frame head movement rate of each subject after censoring. The p -values were obtained from permutation tests (10,000 permutations) on group mean difference. See Fig. 3 for the details of the scatter plots.

Figure S6. Average frame-to-frame head movement rate of each TBI patient after censoring versus average participation coefficient. The ρ -values are the Spearman correlation coefficients.

Figure S7. Number of 'abnormal' ROIs in the TBI I cohort as a function of average frame-to-frame head movement rate.

Figure S8. Bar graphs for observed and expected 'abnormal' ROIs in the patients with TBI relative to the controls at 2% tie density. See Fig. 8 for the details of the bar graphs.

Figure S9. Bar graphs for observed and expected 'abnormal' ROIs in the patients with TBI relative to the controls at 1.5% tie density. See Fig. 8 for the details of the bar graphs.

Figure S10. Bar graphs for observed and expected ‘abnormal’ ROIs in the patients with TBI relative to the controls without global signal regression. See Fig. 8 for the details of the bar graphs.

Figure S11. Larger sized regions of interest (ROIs) for participation coefficient. Regions are nodes within 20 mm geodesic distance from the local peaks. See Fig. 6 for the details of labels.

Figure S12. Bar graphs for observed and expected ‘abnormal’ ROIs in the patients with TBI relative to the controls with ROIs of nodes within 20 mm geodesic distance from the local peaks. See Fig. 8 for the details of the bar graphs.

P28-2 Advanced Magnetic Resonance Imaging in Blast-related Traumatic Brain Injury



Mac Donald, C.L.¹, Cooper, D.¹, Witherow, J.², Snyder, A.³, Shimony, J.³, Raichle, M.^{1,3}, Flaherty, S.², Brody, D.L.¹

1. Dept. of Neurology, Washington University
2. Landstuhl Regional Medical Center, Landstuhl, Germany
3. Mallinckrodt Inst. of Radiology, Washington University



Introduction

Traumatic Brain Injury (TBI) is currently a common injury experienced by US military personnel in Operation Iraqi Freedom (OIF) and Operation Enduring Freedom (OEF). Recent reports estimate 78% of all combat casualties in Iraq and Afghanistan have occurred because of blast injury (Belanger et al, 2009). Like civilian TBI patients, many service members are left functionally impaired following the incident, though the contribution of brain-injury per se vs. PTSD and depression has not been definitively resolved. Furthermore, the structural basis of blast-related TBI itself is unknown. Based on animal studies, we hypothesize that a substantial portion of blast-related TBI is due to axonal injury. Diffusion tensor imaging (DTI) has been shown to be more sensitive to traumatic axonal injury than conventional MRI, which is in turn more sensitive than CT. Therefore, to better explore the possible traumatic axonal injury occurring in the brain following blast-related TBI, we performed DTI in 43 US service members MEDEVAC'd to Landstuhl Region Medical Center in Landstuhl, Germany acutely following blast-related TBI. High resolution conventional MRI was performed for comparison.

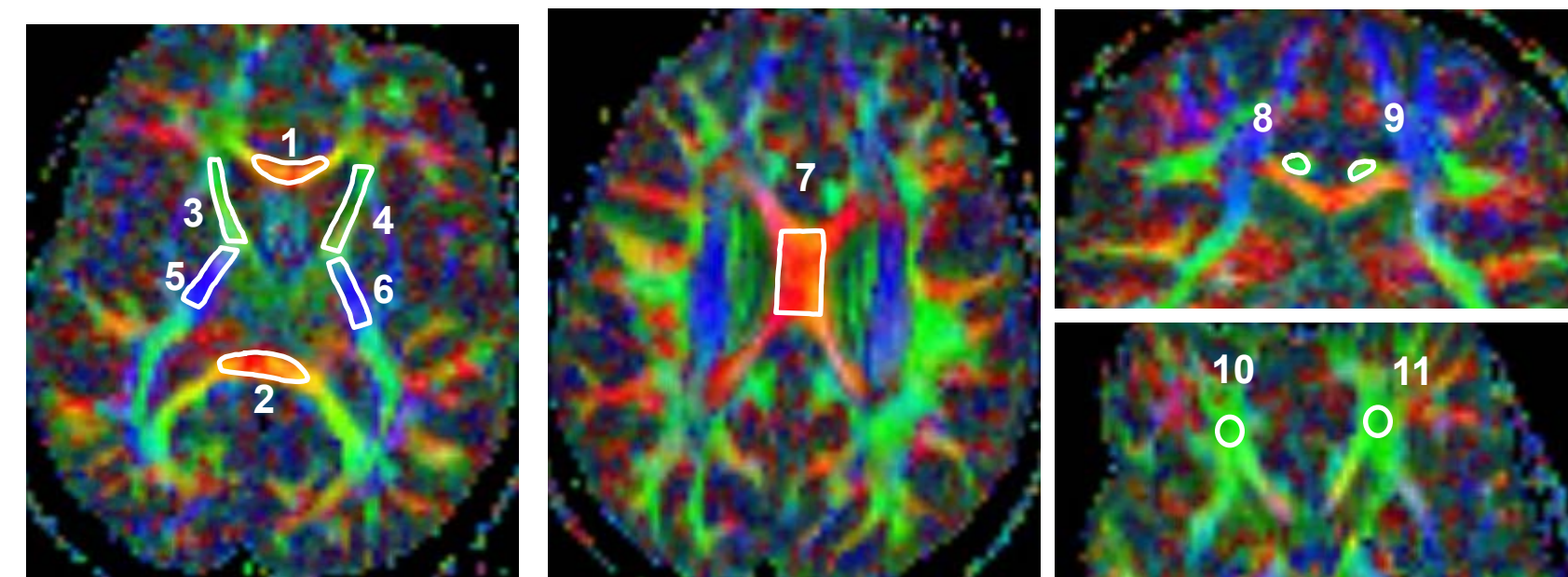
Methods

- 1) 43 blast-related TBI patients and 20 control subjects were enrolled at Landstuhl Region Medical Center (LRMC) Landstuhl, Germany. LRMC is the central triage point for OIF and OEF, and nearly 100% of evacuated patients are screened for TBI.
- 2) Blast-TBI patients were all male, 19-49 year-old active-duty US military personnel who sustained blast-related loss of consciousness, amnesia and/or change in mental status in either OIF or OEF.
- 3) Control subjects were also all male, active duty service members who reported exposure to blast but had no signs or symptoms of brain injury and were MEDEVAC'd to LRMC for other injuries, typically to extremities.
- 4) All subjects were required to provide their own written, informed consent for this study, thus no severe TBI patients were enrolled, and all injuries were considered 'concussive' or 'mild-moderate' by clinical criteria.
- 5) Subjects were scanned with a 1.5 T Avanto MRI scanner (Siemens, Erlangen, Germany) at LRMC.
- 6) Conventional structural imaging included a high-resolution (1x1x1.25 mm) T1 sagittal magnetization-prepared rapid gradient-echo (MP-RAGE), a T2-weighted sagittal fast spin echo, and an axial fluid attenuated inversion recovery (FLAIR) scan. A T2* image was also acquired to rule out the presence of microhemorrhage.
- 7) Diffusion Tensor Imaging was acquired using diffusion weighted images which were sensitized in 25 directions using a locally modified echo planar imaging (EPI) sequence (TR=6400 ms, TE=87 ms, 2 x 2 x 2 mm voxels). DTI was repeated 2x. Total scan time was approximately 1 hour/subject. All conventional images were read by a board certified clinical radiologist on site at LRMC within 24 hours of the MRI scan.
- 8) Data was analyzed offline with custom written scripts (Shimony et al, Cereb Cor. 2006; Fox et al, PNAS, 2005).
- 9) All image sets were re-aligned to a standard atlas using affine transforms and image registration with the T1 image. The standard atlas was previously created from a group of 25 control subjects of the same age range.
- 10) Regions of interest (ROIs) were manually traced using Analyze 6.1 (Mayo Foundation, Rochester, Minn) on individual subject relative anisotropy (RA) images while simultaneously viewing the co-registered MP-RAGE. Thus, the ROIs generated on anatomical images were resampled in register with the DTI data.
- 11) ROIs were also re-sampled onto each additional DTI image data set including ADC, Axial Diffusivity (AD) and Radial Diffusivity (RD) as well as onto each conventional imaging set for comparison.
- 12)

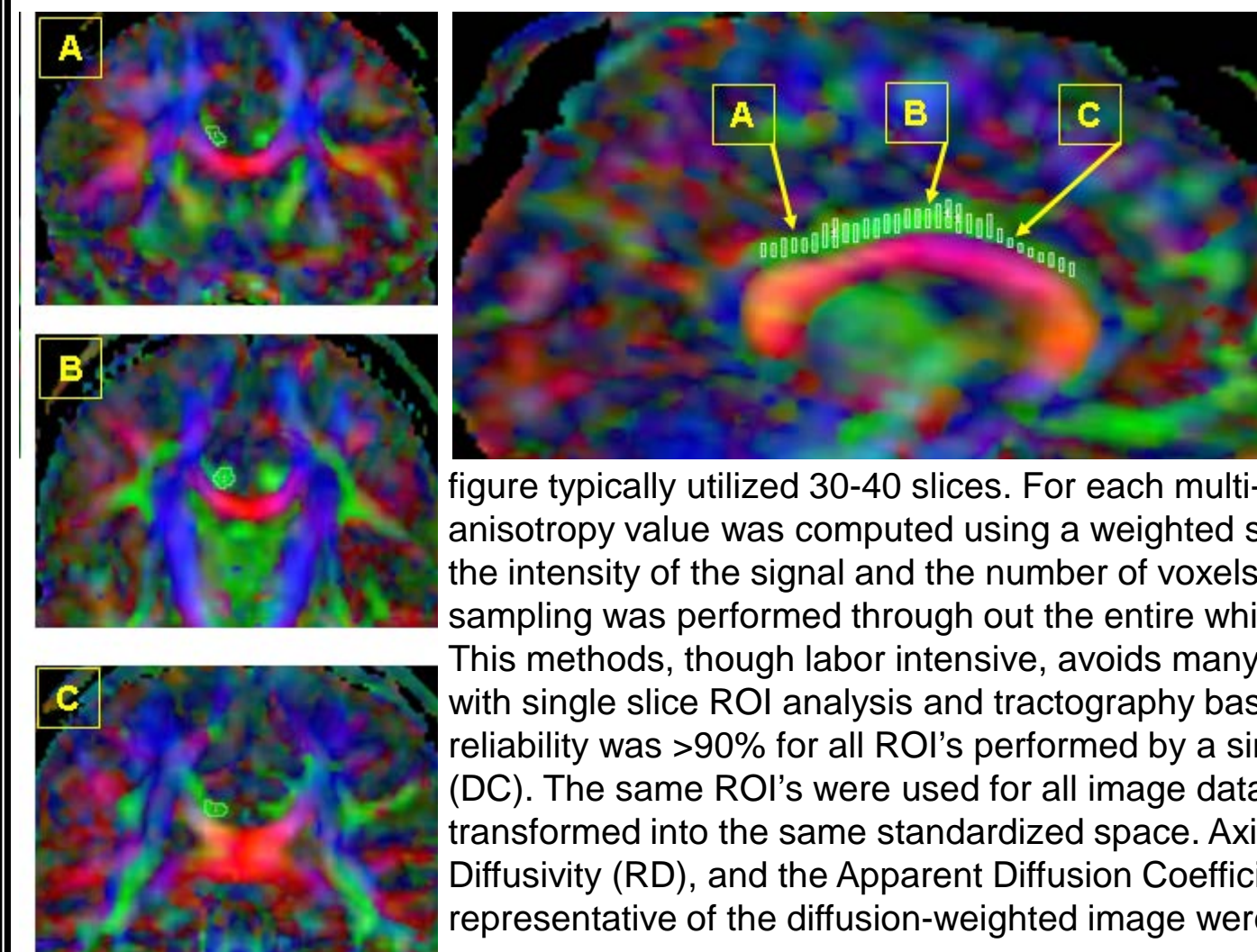
Hypotheses

- 1) Blast-related, concussive TBI primarily causes traumatic axonal injury.
- 2) Quantitative signal abnormalities in injured white matter tracts will be detected on Diffusion Tensor Imaging (DTI) acutely following blast-related TBI.
- 3) These abnormalities may not be detectable with conventional MRI.

Results: Diffusion Tensor Imaging ROI Analysis

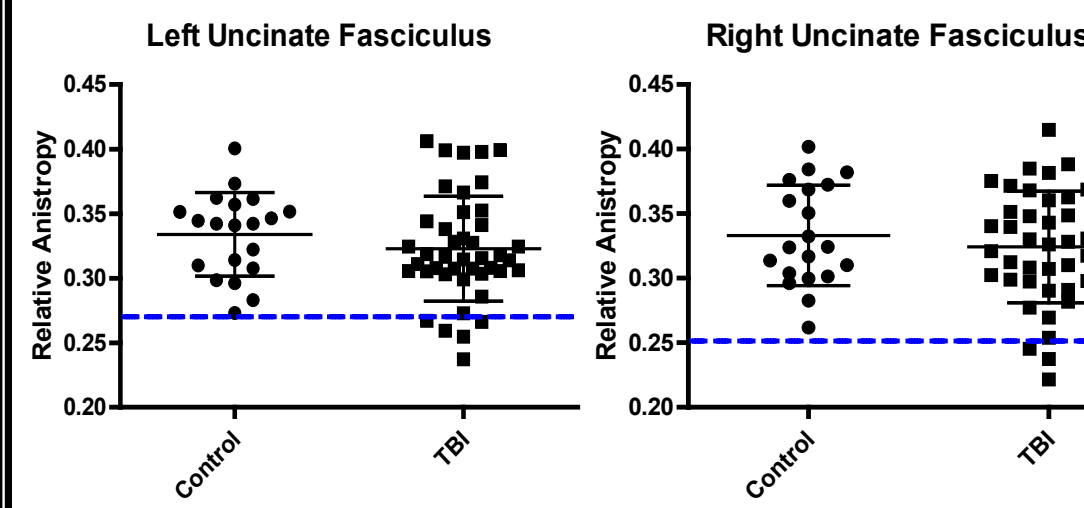


DTI Regions of Interest. Regions of interest included the following 11 white matter tracts: genu of the corpus callosum (1), splenium of the corpus callosum (2), left (3) and right (4) anterior limb of the internal capsule, left (5) and right (6) posterior limb of the internal capsule, body of the corpus callosum (7), left (8) and right (9) cingulum bundle, and left (10) and right (11) uncinate fasciculus. Relative anisotropy RGB images are displayed from 1 control subject. Single slices within each multi-slice ROIs shown for clarity.

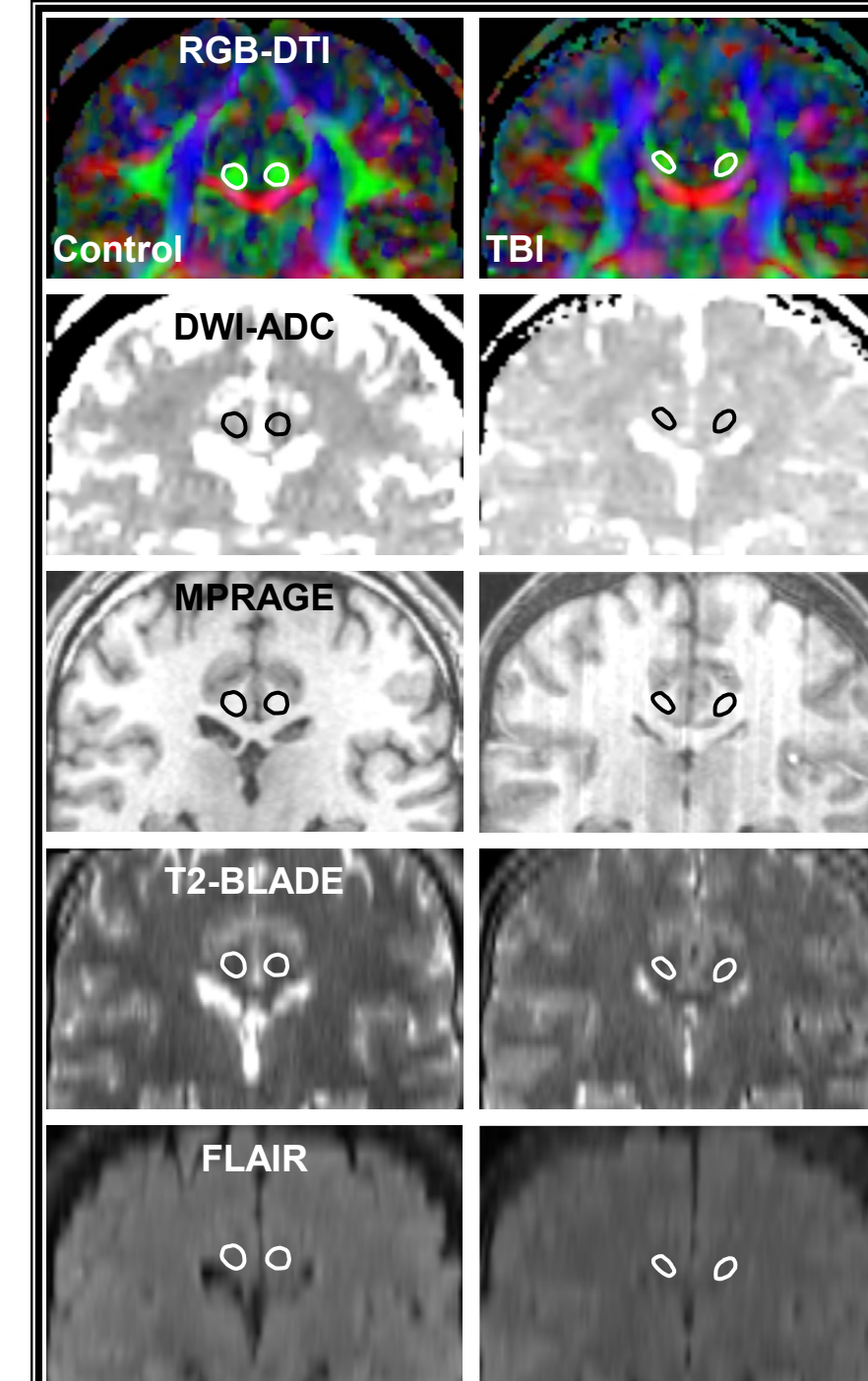


This methods, though labor intensive, avoids many of the pitfalls associated with single slice ROI analysis and tractography based analysis. Intra-rated reliability was >90% for all ROI's performed by a single blinded observer (DC). The same ROI's were used for all image data sets; all images were transformed into the same standardized space. Axial Diffusivity (AD), Radial Diffusivity (RD), and the Apparent Diffusion Coefficient (ADC) representative of the diffusion-weighted image were analyzed quantitatively.

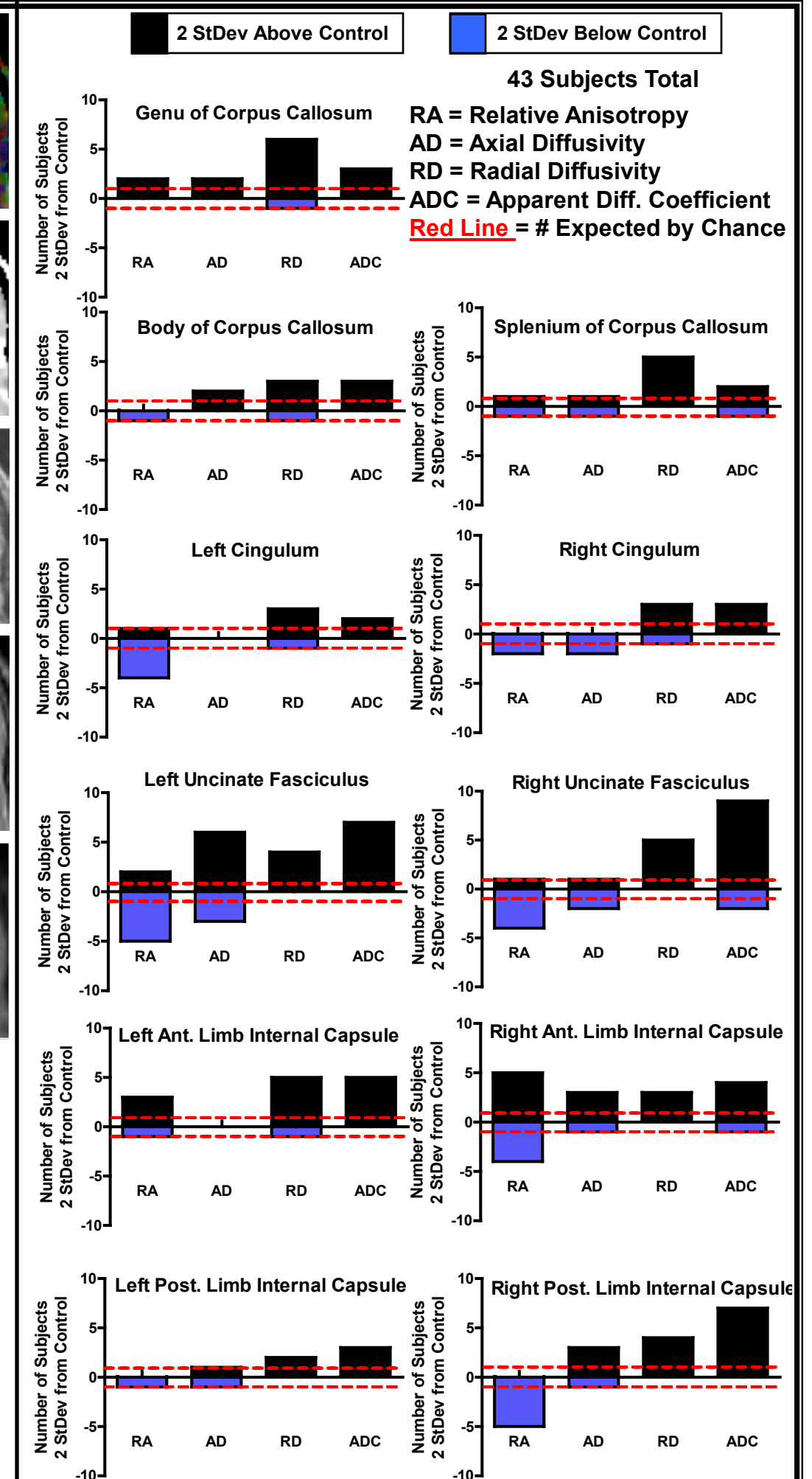
Anisotropy in the Uncinate Fasciculus. Following multi-slice ROI analysis, the anisotropy within the each region was evaluated for each service member in comparison to control. Note the number of service members who fall below two standard deviations (blue dotted line) from the control mean. All participants were found to have no abnormalities within these regions on conventional images acquired during the same imaging session, as read by a board certified radiologist (JW).



Results: DTI – Comparison with Conventional MR Imaging



Diffusion Tensor Imaging Comparison with Conventional Imaging. Conventional image sets consisting of a diffusion weighted image (DWI-ADC), magnetization prepared rapid gradient echo (MP-RAGE), T2-BLADE, fluid attenuated inversion recovery (FLAIR) were acquired at the time for the DTI scan. Figure A shows the comparison of the cingulum bundle in a blast-TBI service member with control for each image set acquired. The subjects cingulum bundles appeared to be of much lower signal intensity indicative of injury on the DTI images however there is no visual evidence of abnormality on the same slice evaluated on the conventional images. This patient endorsed difficulty with short term memory and scored a 23/30 on his MACE (military assessment of concussion exam) missing 1 for attention, 2 for concentration, and 4 for delayed recall/short term memory suggesting that this possible disruption noted with DTI could have functional consequences.



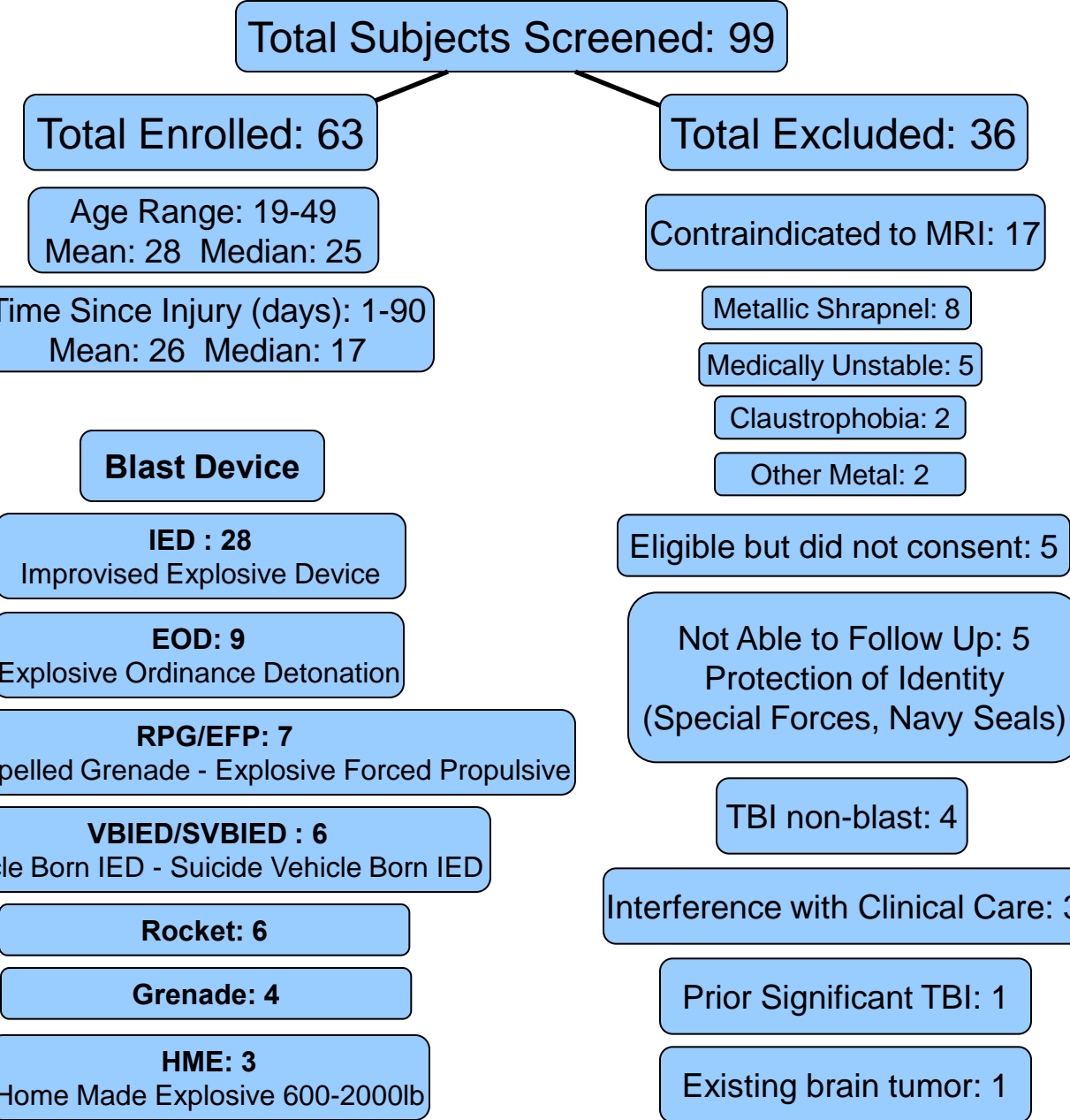
Number of DTI Abnormalities in Each Region of Interest. Each chart graphically displays the number of subjects with abnormalities that are two standard deviations above or below values for the control subjects. The largest number of abnormalities were detected in the uncinate fasciculus. Reduced anisotropy in this region has been correlated with impaired verbal memory in civilian TBI patients (Niogi, Mukherjee, et al Brain 2008). There also were frequent abnormalities suggestive of traumatic axonal injury in the cingulum and internal capsule.

Conclusions, Future Directions, and Impact

- 1) An advanced MRI cohort study of US military personnel with acute blast-related TBI is feasible.
- 2) In a subset of subjects, DTI reveals quantitative abnormalities in white matter tracts which are not readily detectable using conventional MRI.
- 3) Most blast-related TBI subjects, however, have quantitatively normal DTI on these analyses.
- 4) **The key question will be whether the acute imaging findings acutely predict 6-12 month clinical status.** Follow-up clinical evaluations 6-12 months after injury are ongoing.
- 5) **If so, these methods may be useful in assisting triage decisions and guiding rehabilitation.**

Acknowledgements

We greatly appreciate the service and dedication of the men and women in our Armed Forces and kindly thank the MRI Clinic at Landstuhl Region Medical Center for allowing us to scan service members enrolled in this study. Without their support this project would not have been possible.
Funding: Grant W81XWH-08-2-0061 (D. Brody) & the Washington University NeuroImaging Lab.
Correspondence: David Brody: brodyd@neuro.wustl.edu



ADVANCED MR IMAGING OF ACTIVE DUTY MILITARY PERSONNEL FOLLOWING ACUTE BLAST-RELATED TBI



Mac Donald, C.L.¹, Cooper, D.¹, Witherow, J.², Snyder, A.³, Shimony, J.³, Raichle, M.^{1,3}, Flaherty, S.², Brody, D.L.¹

1. Dept. of Neurology, Washington University
2. Landstuhl Regional Medical Center, Landstuhl, Germany
3. Mallinckrodt Inst. of Radiology, Washington University



Introduction

TBI has been called the signature injury of both Operation Iraqi Freedom (OIF) and Operation Enduring Freedom (OEF) and it is currently a common injury experienced by US soldiers. Improved explosive devices (IEDs) are becoming a heavily used weaponry tactic in both OIF and OEF theatres. Recent reports estimate 78% of all combat casualties in Iraq and Afghanistan have occurred because of blast injury (Belanger et al, 2009). Like civilian TBI patients, many service members are left functionally impaired following the incident, though the contribution of brain-injury per se vs. PTSD and depression has not been definitively resolved. Furthermore, the structural basis of blast-related TBI itself is unknown. Based on animal studies, we hypothesize that a substantial portion of blast-related TBI is due to axonal injury. To better explore the possible microstructural changes occurring in the brain following blast-related TBI, diffusion tensor imaging (DTI) was performed in 63 US service members MEDEVAC'd to Landstuhl Region Medical Center in Landstuhl, Germany acutely following injury. High quality conventional MRI was performed for comparison.

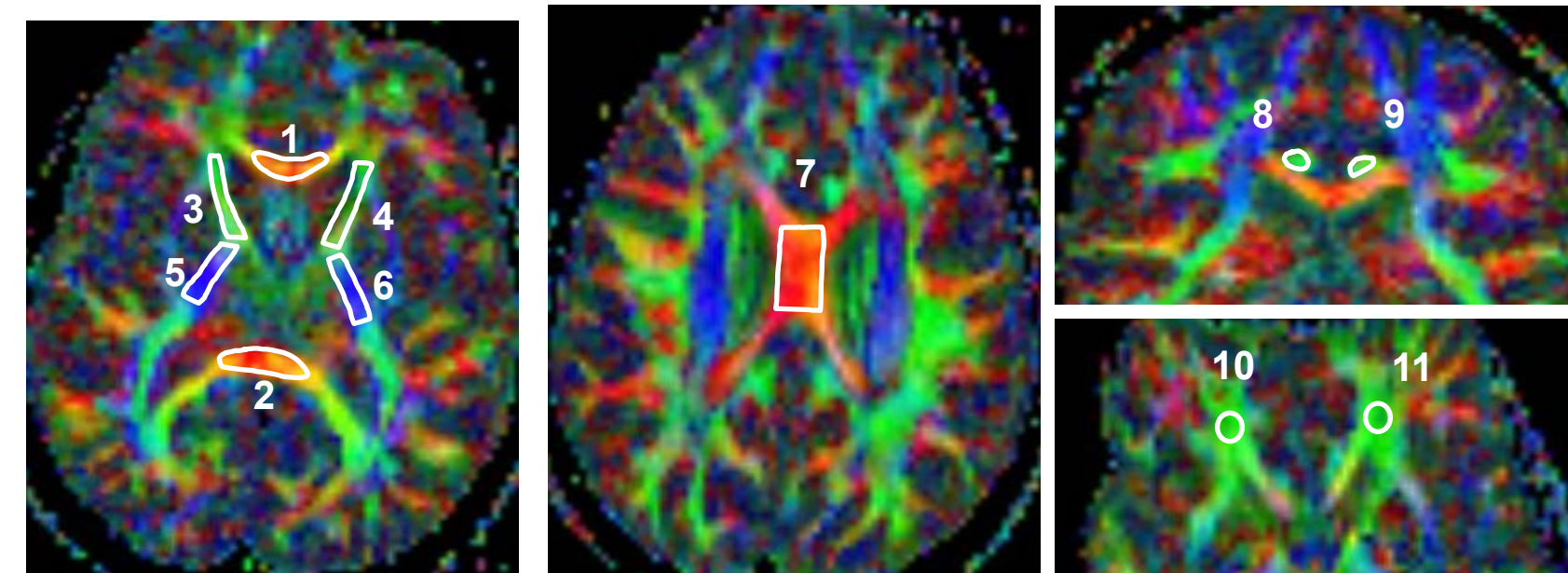
Methods

- 1) 43 blast-related TBI patients and 20 control subjects were enrolled at Landstuhl Region Medical Center (LRMC) Landstuhl, Germany. LRMC is the central triage point for OIF and OEF, and nearly 100% of evacuated patients are screened for TBI.
- 2) Blast-TBI patients were all male, 19-49 year-old active-duty US military personnel who sustained blast-related loss of consciousness, amnesia and/or change in mental status in either OIF or OEF.
- 3) Control subjects were also all male, active duty service members who reported exposure to blast but had no signs or symptoms of brain injury and were MEDEVAC'd to LRMC for other injuries, typically to extremities.
- 4) All subjects were required to provide their own written, informed consent for this study, thus no severe TBI patients were enrolled, and all injuries were considered 'concussive' or 'mild-moderate' by clinical criteria.
- 5) Subjects were scanned with a 1.5 T Avanto MRI scanner (Siemens, Erlangen, Germany) at LRMC.
- 6) Conventional structural imaging included a high-resolution (1x1x1.25 mm) T1 sagittal magnetization-prepared rapid gradient-echo (MP-RAGE), a T2-weighted sagittal fast spin echo, and an axial fluid attenuated inversion recovery (FLAIR) scan. A T2* image was also acquired to rule out the presence of microhemorrhage.
- 7) Diffusion Tensor Imaging was acquired using diffusion weighted images which were sensitized in 25 directions using a locally modified echo planar imaging (EPI) sequence (TR=6400 ms, TE=87 ms, 2 x 2 x 2 mm voxels). DTI was repeated 2x. Total scan time was approximately 1 hour/subject. All conventional images were read by a board certified clinical radiologist on site at LRMC within 24 hours of the MRI scan.
- 9) Data was analyzed offline with custom written scripts (Shimony et al. Cereb Cor. 2006; Fox et al. PNAS, 2005).
- 10) All image sets were re-aligned to a standard atlas using affine transforms and image registration with the T1 image. The standard atlas was previously created from a group of 25 control subjects of the same age range.
- 11) Regions of interest (ROIs) were manually traced using Analyze 6.1 (Mayo Foundation, Rochester, Minn) on individual subject relative anisotropy (RA) images while simultaneously viewing the co-registered MP-RAGE. Thus, the ROIs generated on anatomical images were resampled in register with the DTI data.
- 12) ROIs were also re-sampled onto each additional DTI image data set including ADC, Axial Diffusivity and Radial Diffusivity as well as onto each conventional imaging set for comparison.

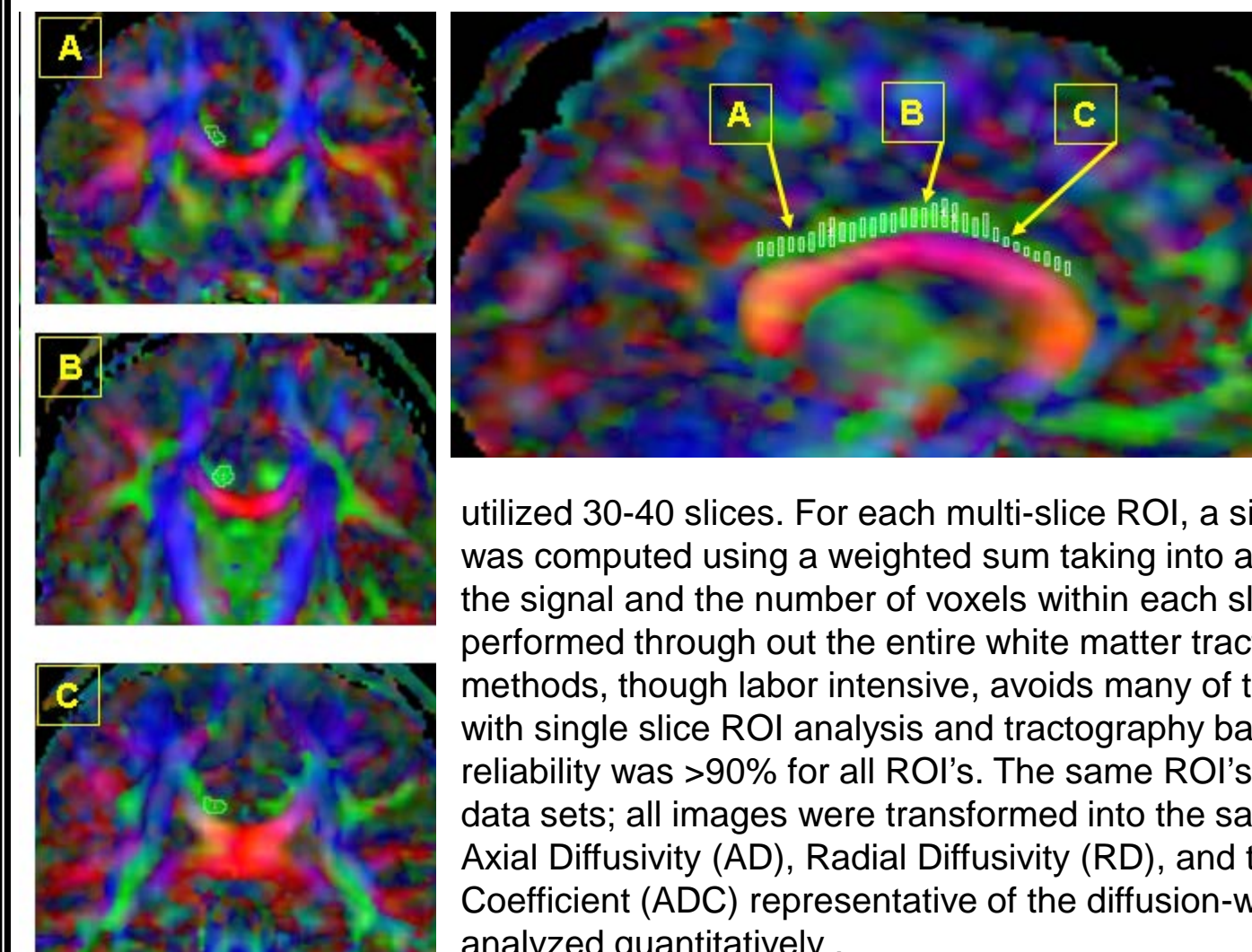
Hypotheses

- 1) Blast-related, concussive TBI primarily causes traumatic axonal injury.
- 2) Quantitative signal abnormalities in injured white matter tracts will be detected on Diffusion Tensor Imaging (DTI) acutely following blast-related TBI.
- 3) These abnormalities may not be detectable with conventional MRI.

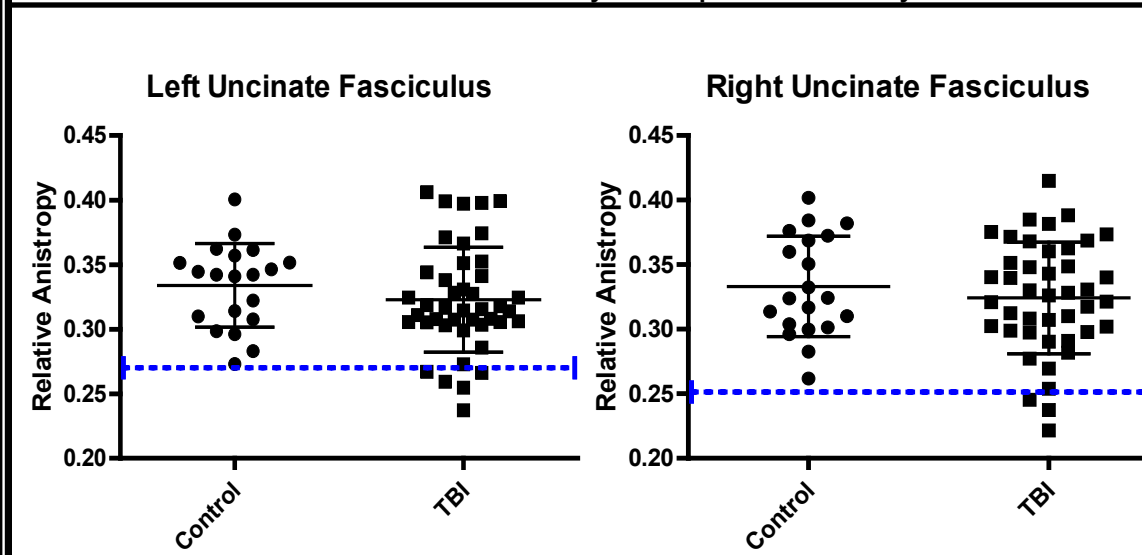
Results: Diffusion Tensor Imaging ROI Analysis



DTI Regions of Interest. Regions of interest included the following 11 white matter tracts: genu of the corpus callosum (1), splenium of the corpus callosum (2), left (3) and right (4) anterior limb of the internal capsule, left (5) and right (6) posterior limb of the internal capsule, body of the corpus callosum (7), left (8) and right (9) cingulum bundle, and left (10) and right (11) uncinate fasciculus. Relative anisotropy RGB images are displayed from 1 control subject. Single slices within each multi-slice ROIs shown for clarity.

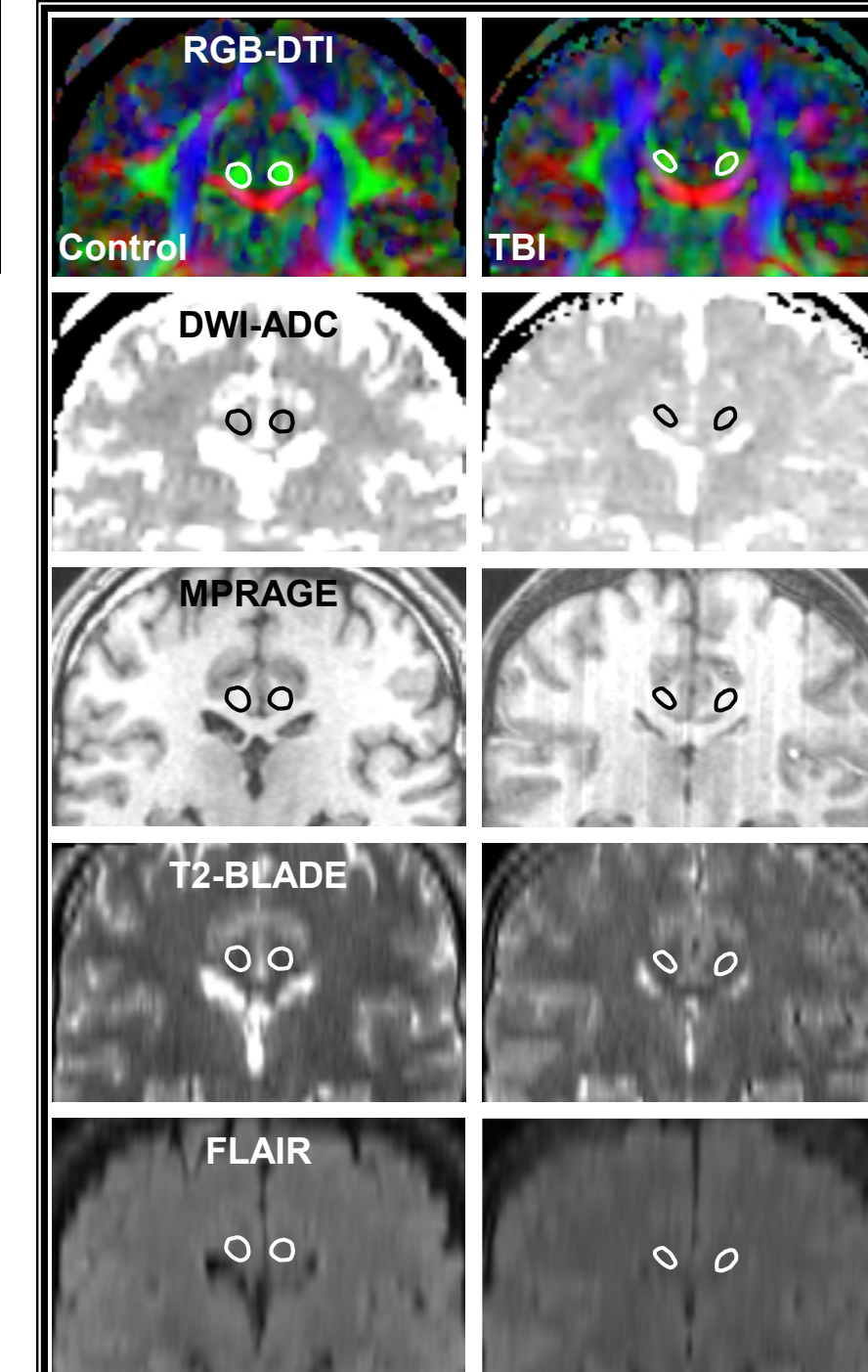


3-Dimensional, Multi-slice Region of Interest Analysis. Each ROI consisted of 9-40 manually traced slices depending on specific white matter tract. The cingulum bundle shown in the figure typically utilized 30-40 slices. For each multi-slice ROI, a single anisotropy value was computed using a weighted sum taking into account the intensity of the signal and the number of voxels within each slice. Thus, sampling was performed throughout the entire white matter tract of interest. This method, though labor intensive, avoids many of the pitfalls associated with single slice ROI analysis and tractography based analysis. Intra-rated reliability was >90% for all ROI's. The same ROI's were used for all image data sets; all images were transformed into the same standardized space. Axial Diffusivity (AD), Radial Diffusivity (RD), and the Apparent Diffusion Coefficient (ADC) representative of the diffusion-weighted image were analyzed quantitatively.

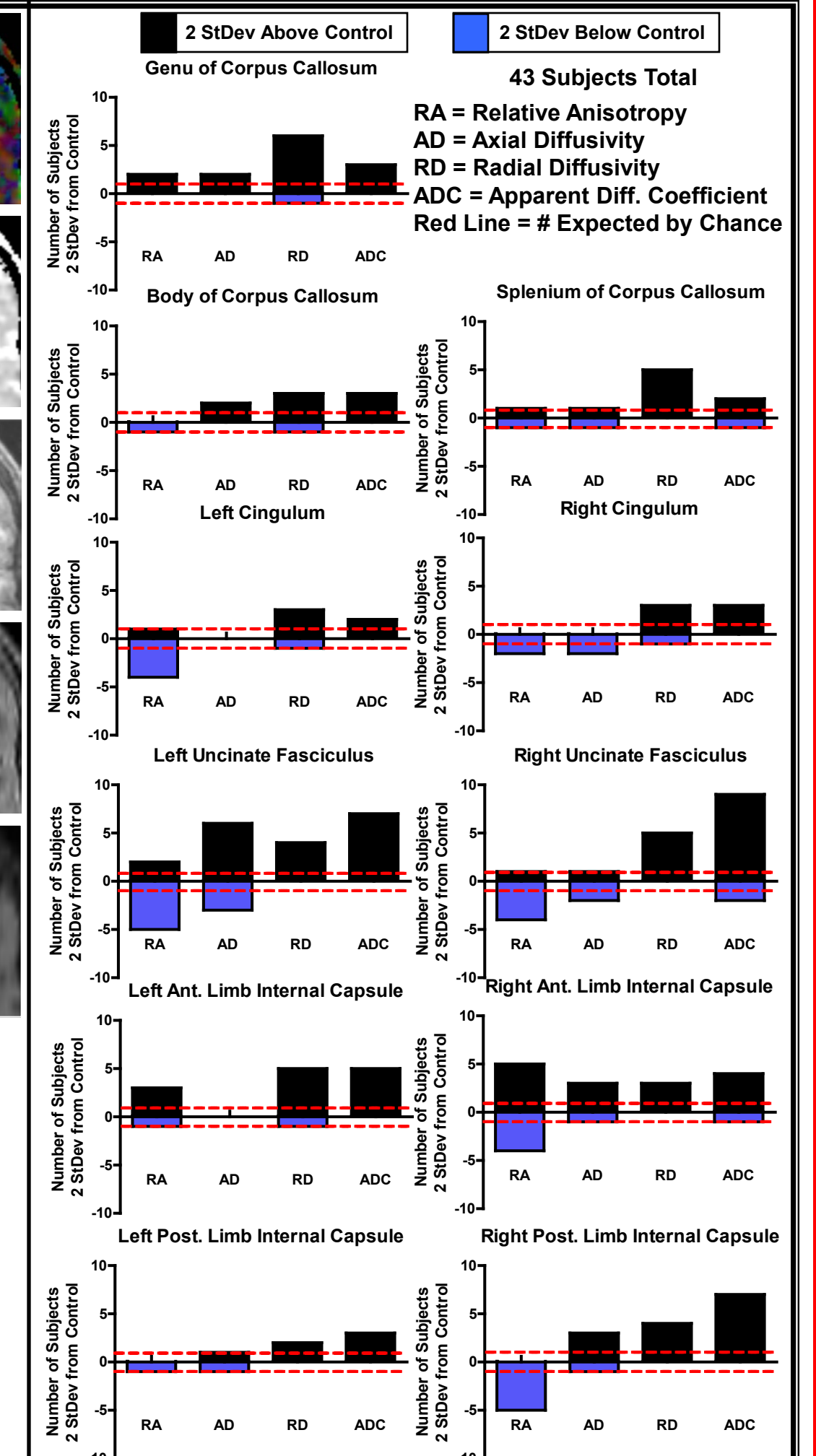


Anisotropy in the Uncinate Fasciculus. Following multi-slice ROI analysis, the anisotropy within the each region was evaluated for each service member in comparison to control. Note the number of service members who fall below two standard deviations (blue dotted line) from the control mean. All participants were found to have no abnormalities within these regions on conventional images acquired during the same imaging session, as read by a board certified radiologist (JW).

Results: DTI – Comparison with Conventional MR Imaging



Diffusion Tensor Imaging Comparison with Conventional Imaging. Conventional image sets consisting of a diffusion weighted image (DWI-ADC), magnetization prepared rapid gradient echo (MP-RAGE), T2-BLADE, fluid attenuated inversion recovery (FLAIR) were acquired at the time for the DTI scan. Figure A shows the comparison of the cingulum bundle in a blast-TBI service member with control for each image set acquired. The subjects cingulum bundles appeared to be of much lower signal intensity indicative of injury on the DTI images however there is no visual evidence of abnormality on the same slice evaluated on the conventional images. This patient endorsed difficulty with short term memory and scored a 23/30 on his MACE (military assessment of concussion exam) missing 1 for attention, 2 for concentration, and 4 for delayed recall/short term memory suggesting that this possible disruption noted with DTI could have functional consequences.



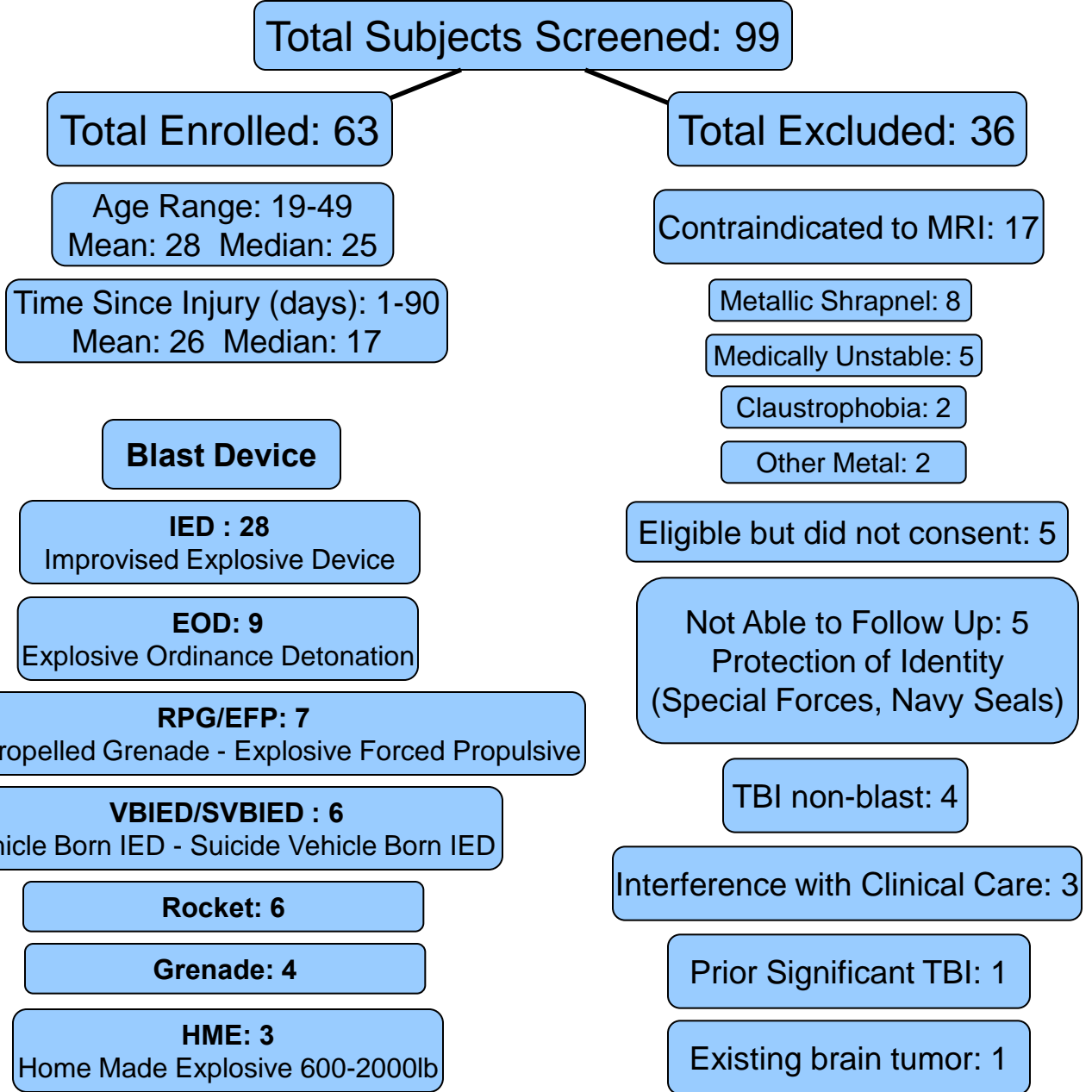
Number of DTI Abnormalities in Each Region of Interest. Each chart graphically displays the number of subjects with abnormalities that are two standard deviations above or below values for the control subjects. The largest number of abnormalities were detected in the uncinate fasciculus. Reduced anisotropy in this region has been correlated with impaired verbal memory in civilian TBI patients (Niogi, Mukherjee, et al Brain 2008). There also were frequent abnormalities suggestive of traumatic axonal injury in the cingulum and internal capsule.

Conclusions and Future Directions

- 1) An advanced MRI study of US military personnel with acute blast-related TBI is feasible.
- 2) In a subset of subjects, DTI reveals quantitative abnormalities in white matter tracts which are not readily detectable using conventional MRI.
- 3) Most blast-related TBI subjects, however, have quantitatively normal DTI on these analyses.
- 4) Follow-up clinical evaluations 6-12 months after injury are ongoing. The key question will be whether the acute imaging findings acutely predict 6-12 month clinical status.
- 5) If so, these methods may be useful in assisting triage decisions and guiding rehabilitation.

Acknowledgements

We greatly appreciate the service and dedication of the men and women in our Armed Forces and kindly thank the MRI Clinic at Landstuhl Region Medical Center for allowing us to scan service members enrolled in this study. Without their support this project would not have been possible.
Funding: Department of Defense grant PT075299 (D. Brody) & the Washington University Neuroimaging Lab.
Correspondence: Christine Mac Donald, PhD macdonaldc@neuro.wustl.edu



Advanced MRI Detection of Blast-Related Traumatic Brain Injury in Active Duty US Military Personnel Assessed at Landstuhl Regional Medical Center

David L. Brody MD PhD¹, Christine Mac Donald PhD¹, Ann Johnson¹, Dana Cooper¹, Elliot Nelson MD¹, Nicole Schwarze Werner PhD¹, Josh Shimony MD PhD¹, Abraham Z. Snyder MD PhD¹, Marcus Raichle MD¹, LTC John Witherow MD², LTC Raymond Fang MD², and COL Stephen Flaherty MD^{2,3}

1. Washington University School of Medicine, St Louis, Missouri
2. Landstuhl Regional Medical Center, Landstuhl, Germany
3. Walter Reed Army Medical Center, Washington DC

Funded by CDMRP W81XWH-08-2-006 (Brody)

OBJECTIVE: To assess the potential of Diffusion Tensor Imaging (DTI), an advanced magnetic resonance imaging (MRI) method, to assess mild traumatic brain injury (mTBI) in combat casualties.

BACKGROUND: Blast-related traumatic brain injury (TBI) is a common cause of morbidity for combat casualties injured in support of Operations IRAQI and ENDURING FREEDOM (OIF/OEF). These injuries are most commonly “concussive” or “mild” and do not reveal intracranial pathology on computed tomography (CT) or conventional MRI (cMRI) of the brain. We hypothesized that traumatic axonal injury is a primary pathological process underlying blast-related TBI. DTI is a sensitive technique to detect traumatic axonal injury in brain white matter compared to other neuroimaging modalities and thus may aid in the diagnosis and assessment of blast-related TBI.

METHODS: This prospective study was reviewed and approved by Institutional Review Boards at both involved institutions. The study group was enrolled from casualties evacuated to Landstuhl Regional Medical Center (LRMC) with signs and/or symptoms of blast-related TBI. The control group consisted of personnel evacuated with blast-exposure but injuries other than TBI. All subjects provided signed informed consent prior to participation. None had detectible intracranial pathology on CT. All participants underwent cMRI/DTI imaging on a Siemens Avanto 1.5T scanner. In each subject, 14 distinct brain regions were assessed and 9 of these 14 regions that were statistically independent of each other in this cohort were analyzed in detail. Patients were scheduled for follow-up 6-12 months after injury.

RESULTS: Sixty three patients were enrolled in the study group and 21 in the control group. The mean age was 28 years (range 19-49). All patients were male. All available clinical histories in study group participants indicated blast injury plus another mechanism of head injury such as a fall, motor vehicle indecent, or being struck by a blunt object. The median time from TBI occurrence to study enrollment was 14 days (range 1-90 days). Forty-eight percent were injured in Iraq and 52% in Afghanistan. 94% were enlisted and 6% were officers. Scan time for cMRI/DTI required 21 minutes per patient.

Seventeen of 63 mTBI patients (27%) showed white matter abnormalities on DTI consistent with traumatic axonal injury. Specifically, relative anisotropy, a DTI marker of white matter integrity, was abnormal in 2 or more brain regions in each of these 17 subjects. Relative anisotropy abnormalities were defined as values more than 2 standard deviations below the control group mean. By chance, no more than 1 of 63 normal subjects would be expected to have 2 or more such abnormalities in 9 independent regions ($p < 0.0001$, Chi-Squared). None had detectible intracranial TBI-related pathology on cMRI.

As a group, statistically significant DTI abnormalities consistent with traumatic axonal injury were found in the study group as compared to the control group in 5 of the 9 statistically independent brain regions analyzed: the bilateral cingulum bundles ($p = 0.0015$, t-test), bilateral uncinate fasciculi ($p = 0.02$), bilateral middle cerebellar peduncles ($p = 0.0003$), left anterior limb of the internal capsule ($p = 0.02$), and right posterior limb of the internal capsule ($p = 0.05$). The middle cerebellar peduncles are not commonly injured in civilian mTBI. However, recent computer simulation models predict especially high mechanical stresses in this area of the brain independent of the orientation of the head relative to the blast.

Follow-up patient assessments are ongoing. To date, 77% (43/56) of patients report impairments their professional and/or personal lives. While neuropsychological testing has not detected substantial deficits, 48% have met Clinician-Administered PTSD Scale (CAPS) criteria for post-traumatic stress disorder (PTSD) and 48% have met Montgomery-Asberg Rating Scale criteria for moderate to severe depression. None had pre-existing major psychiatric disorders. While the prevalence of PTSD and depression did not differ between the study and control groups, the severity of PTSD was greater in the study group ($p = 0.007$, Mann Whitney U-test).

CONCLUSIONS: Statistically significant differences in relative anisotropy existed between the study and control groups. We interpret this difference as evidence that traumatic axonal injury plays a role in blast-related mTBI. Thus, DTI may offer improved diagnostic sensitivity in blast-exposed US military personnel for mTBI. Additional research is required using independent cohorts to validate these findings and to prospectively evaluate the clinical utility of DTI-based assessments and management for mTBI.

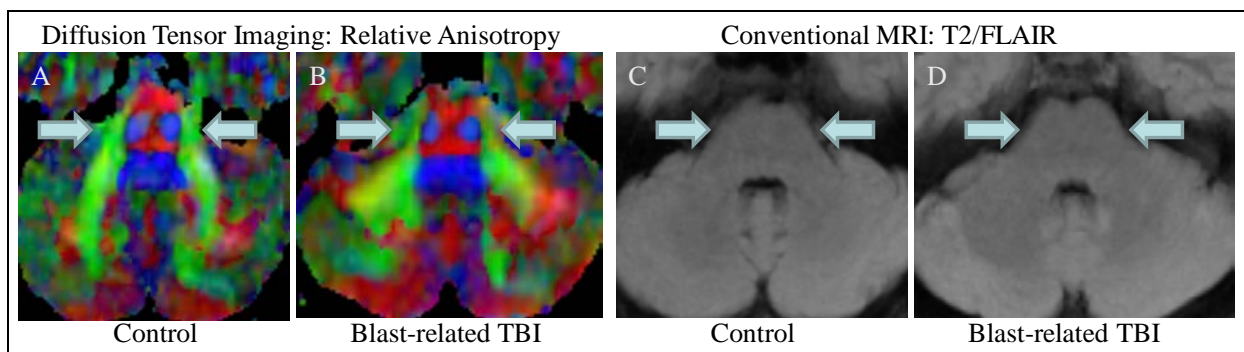


Figure 1: DTI reveals abnormalities after blast-related TBI that are not apparent on conventional MRI. **A-B** DTI from a control subject (**A**) and a blast-related TBI patient (**B**). Middle cerebellar peduncles indicated by arrows; note the reduced intensity of yellow-green regions. **C-D**. Conventional MRI from an anatomically matched regions in the same two subjects: no abnormalities detected.

Advanced MRI Detection of Blast-Related Traumatic Brain Injury in Active Duty US Military Personnel



David L. Brody¹, Christine Mac Donald¹, Ann Johnson¹, Dana Cooper¹, Elliot Nelson¹, Nicole Werner¹, Josh Shimony¹, Abraham Z. Snyder¹, Marcus Raichle¹, John Witherow², Raymond Fang², and Stephen Flaherty^{2,3}
¹Washington University, St Louis MO, ²Landstuhl Regional Medical Center, Landstuhl, Germany, ³Walter Reed Army Medical Center, Washington DC



Introduction

- In the current wars in Iraq and Afghanistan, as many as 320,000 US military personnel have sustained blast-related **traumatic brain injury (TBI)**.
- Most of these injuries are categorized as uncomplicated “mild” or “concussive” TBI based on clinical criteria and the absence of intracranial pathology on CT or conventional MRI
- However, little is known about these “mild” injuries and the relationship between TBI and outcomes remains controversial.
- **Diffusion Tensor Imaging (DTI)** is an advanced MRI method that has been shown to be more sensitive to traumatic axonal injury than conventional MRI.
- In civilian TBI, DTI has shown many abnormalities not apparent on CT or conventional MRI.
- However, no DTI studies of acute blast-related TBI have been published, and the role of axonal injury in blast-related TBI is not known.
- Computer simulations of the effects of blast-induced pressure waves on the brain suggest that the orbitofrontal regions and the posterior fossa (cerebellum and brainstem) may sustain intense stresses independently of the subject’s head orientation relative to the blast.

Hypotheses

- We hypothesized that traumatic axonal injury, detectable with DTI but not apparent with conventional neuroimaging, is a primary pathophysiological process underlying blast-related TBI.
- We hypothesized that major orbitofrontal and posterior fossa white matter tracts would be affected prominently in blast-related TBI.

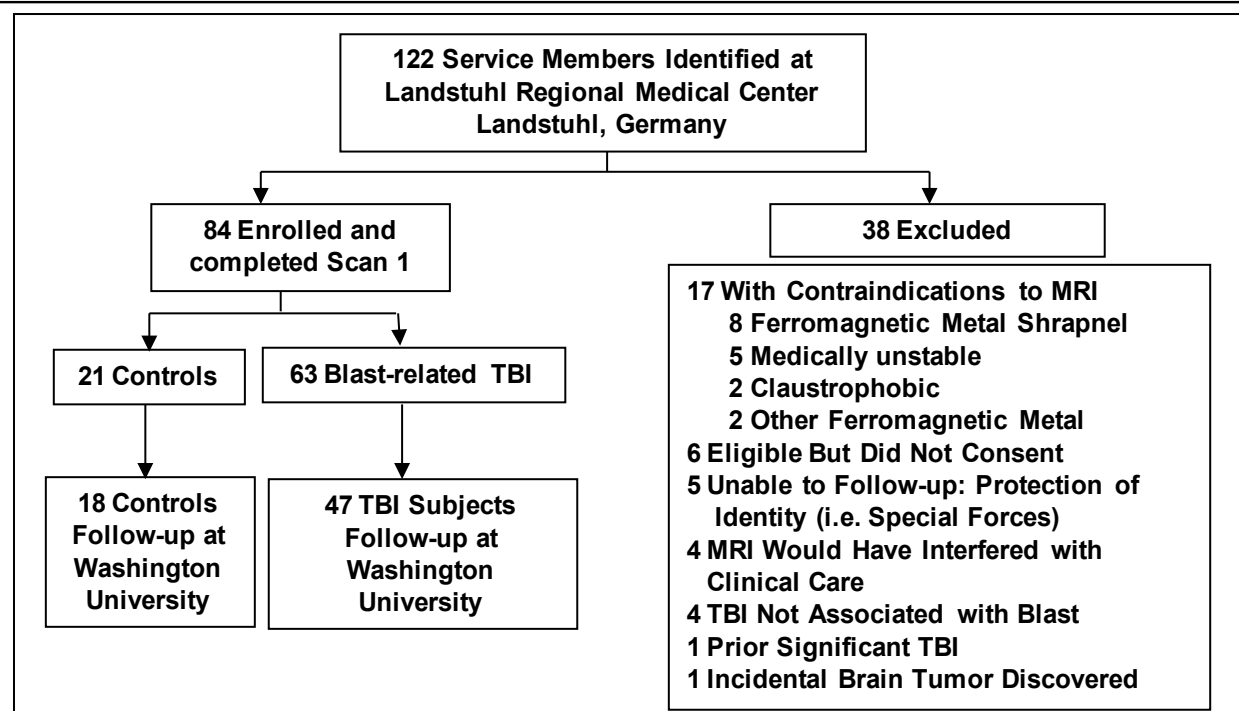
Methods

Blast-related TBI Subjects: A cross-sectional cohort of 63 active-duty US military personnel who presented to Landstuhl Regional Medical Center (LRMC) with signs and/or symptoms of blast-related TBI from 2008-2009. All provided written informed consent.

Controls: 21 US military personnel presenting to LRMC with blast exposure and other injuries but no TBI based on clinical criteria.

Scans: Subjects were scanned at LRMC in the first 90 days after injury on a 1.5T Siemens Avanto MRI scanner. DTI protocol comprised two acquisitions at 2.5 x 2.5 x 2.5 mm resolution with 23 diffusion directions. Scans were repeated 6-12 months later at Washington University.

Fig. 1: Enrollment and exclusion characteristics of the study participants.



Results

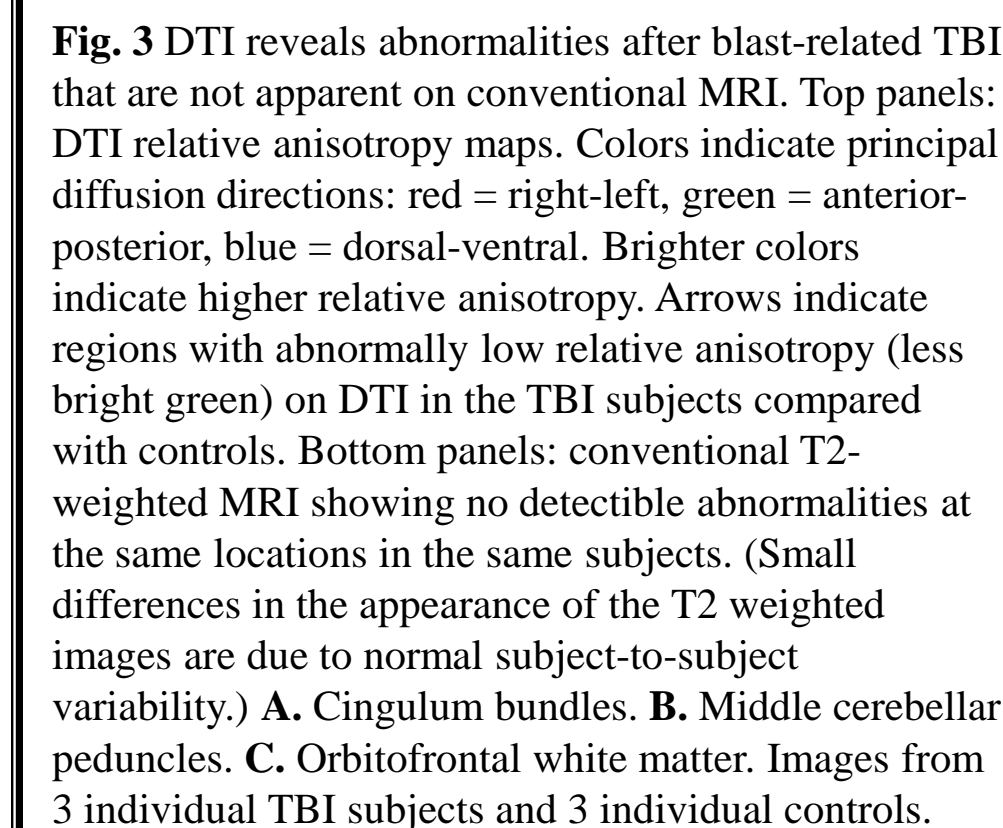
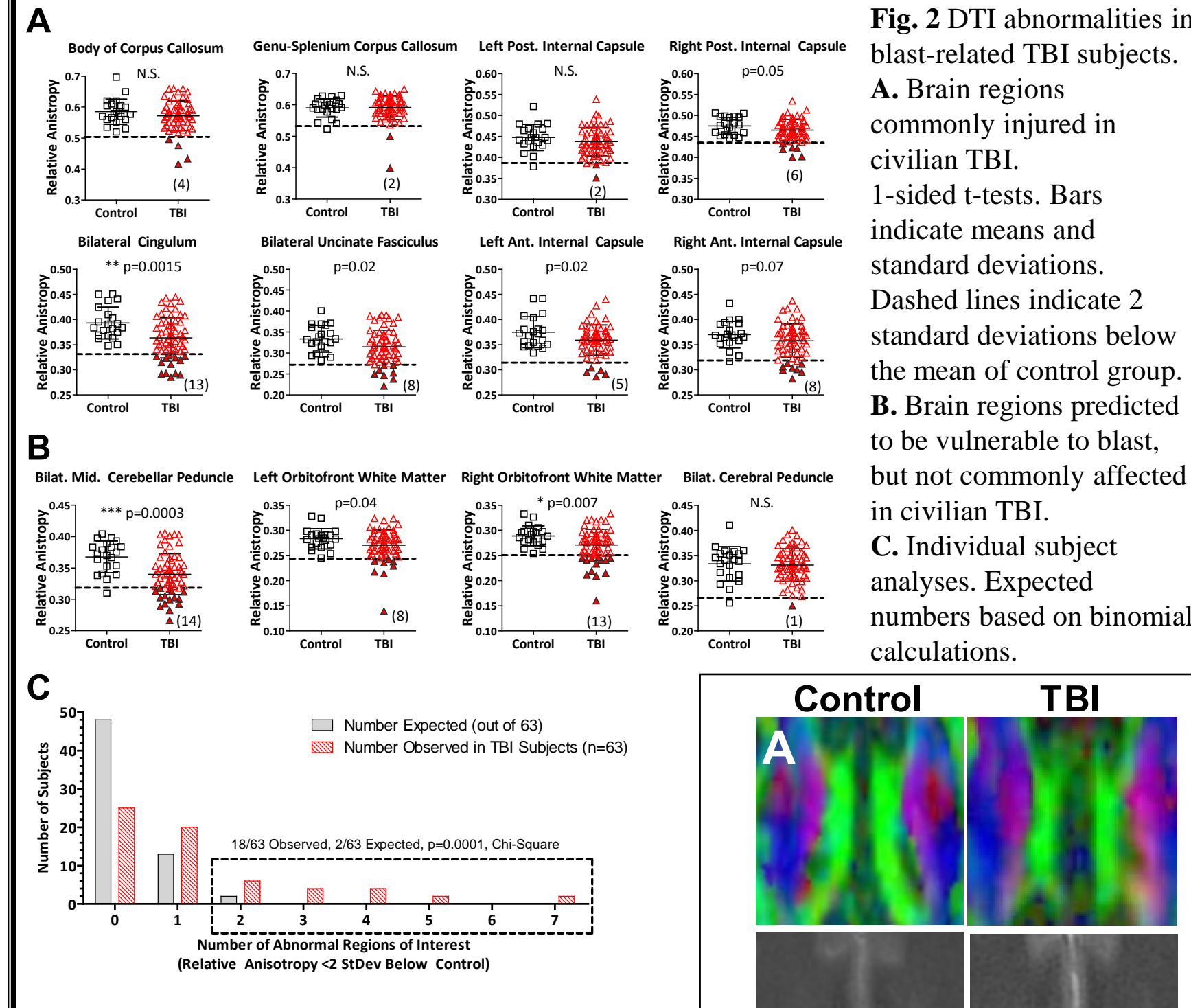
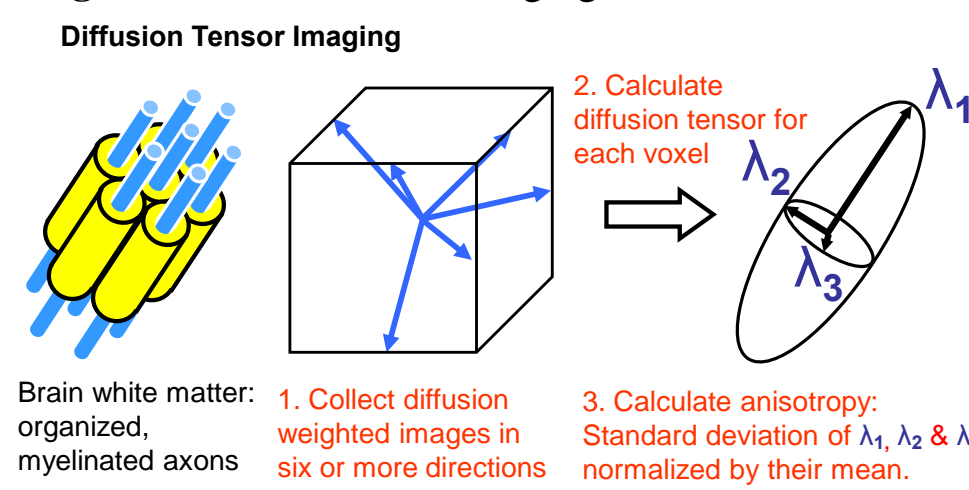
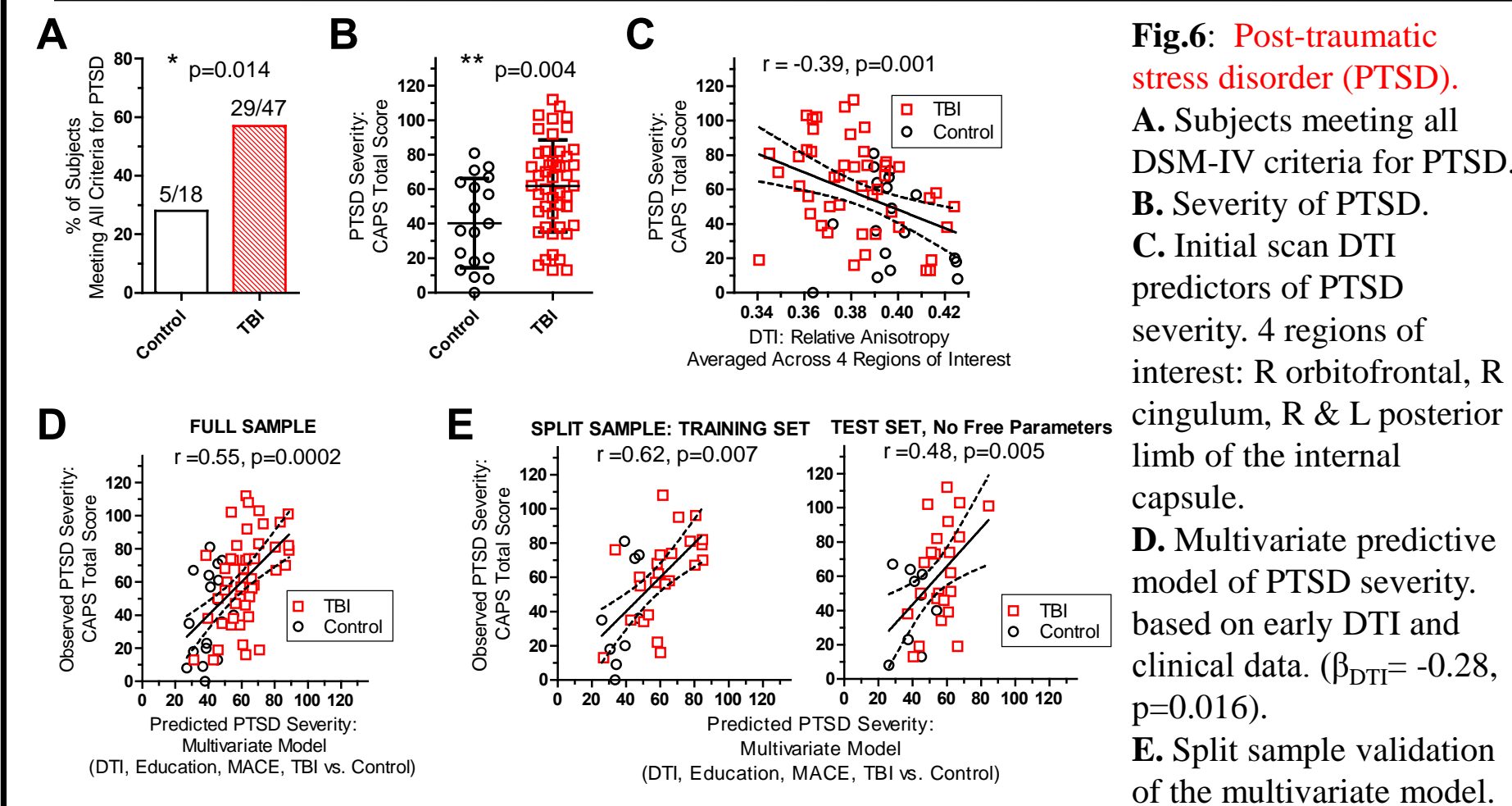
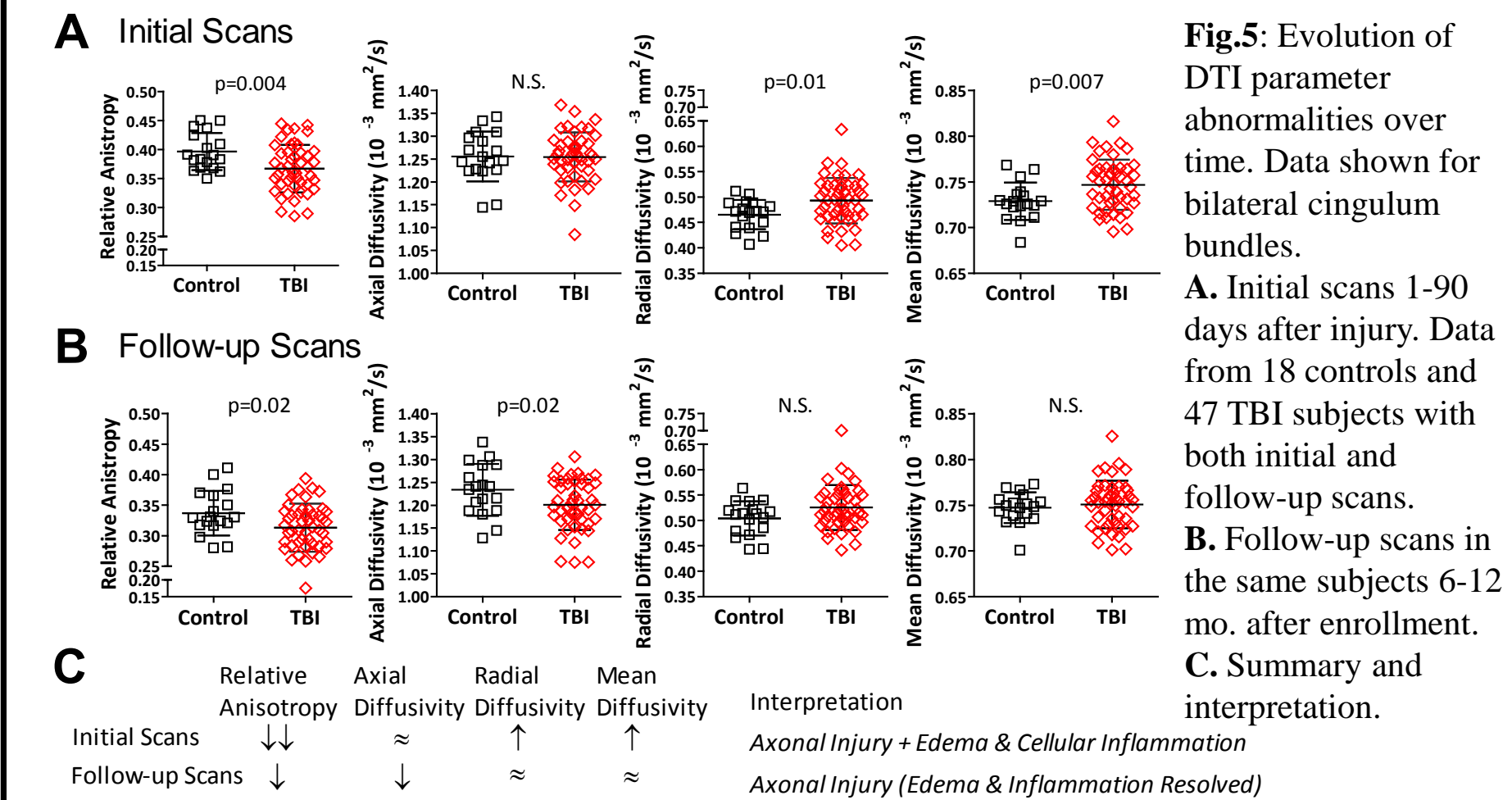


Fig. 4: Diffusion Tensor Imaging.



Results



Conclusions and Future Directions

- DTI findings in US military personnel support the hypothesis that blast-related mild TBI can involve axonal injury which is not detected on conventional MRI.
- The distribution of affected brain regions suggested an admixture of blast effects and other mechanisms.
- However, many TBI subjects did not have DTI abnormalities, and TBI remains a clinical diagnosis
- The relationship between specific DTI abnormalities and post-traumatic stress disorder severity is intriguing and will require validation in an independent cohort.

Acknowledgements

Funding: CDMRP W81XWH-08-2-006 **Correspondence:** brodyd@neuro.wustl.edu

Early Prediction of Post-traumatic Stress Disorder Severity Following Blast-related Traumatic Brain Injury Using Advanced MRI-based Methods



ATACCC 2011: POSTER SESSION 2
 David L. Brody¹, Christine Mac Donald¹, Ann Johnson¹, Dana Cooper¹, Elliot Nelson¹, Nicole Werner¹, Benjamin J. Shannon¹,
 Josh Shimony¹, Abraham Z. Snyder¹, Marcus Raichle¹, COL (ret) Stephen Flaherty^{2,3}, and Lt. Col Raymond Fang²
¹Washington University, St Louis MO, ²Landstuhl Regional Medical Center, Landstuhl, Germany, ³Cape Fear Valley Medical Center, Fayetteville, NC



Introduction

- In the current wars in Iraq and Afghanistan, as many as 320,000 US military personnel have sustained blast-related **traumatic brain injury (TBI)**.
- Most of these injuries are categorized as uncomplicated “mild” or “concussive” TBI based on clinical criteria and the absence of intracranial pathology on CT or conventional MRI
- However, little is known about these “mild” injuries and the relationship between TBI and **Post-traumatic Stress Disorder (PTSD)** remains controversial.
- We recently reported that **Diffusion Tensor Imaging (DTI)**, an advanced MRI-based method, reveals abnormalities consistent with traumatic axonal injury in a subset of US military personnel with blast-related mild TBI. (Mac Donald et al NEJM 2011)
- Abnormalities were found prominently in orbitofrontal cortex, a brain region hypothesized to be involved in emotional regulation and extinction of fearful memories in animal models of PTSD. This led to the hypotheses tested here.

Hypotheses

- We hypothesized that injuries to specific brain regions predispose US military personnel to develop PTSD symptoms of greater severity.
- Operationally, we hypothesized that advanced MRI results using methods sensitive to mild TBI would allow early prediction of the severity of PTSD as assessed 6-12 months after injury.

Methods

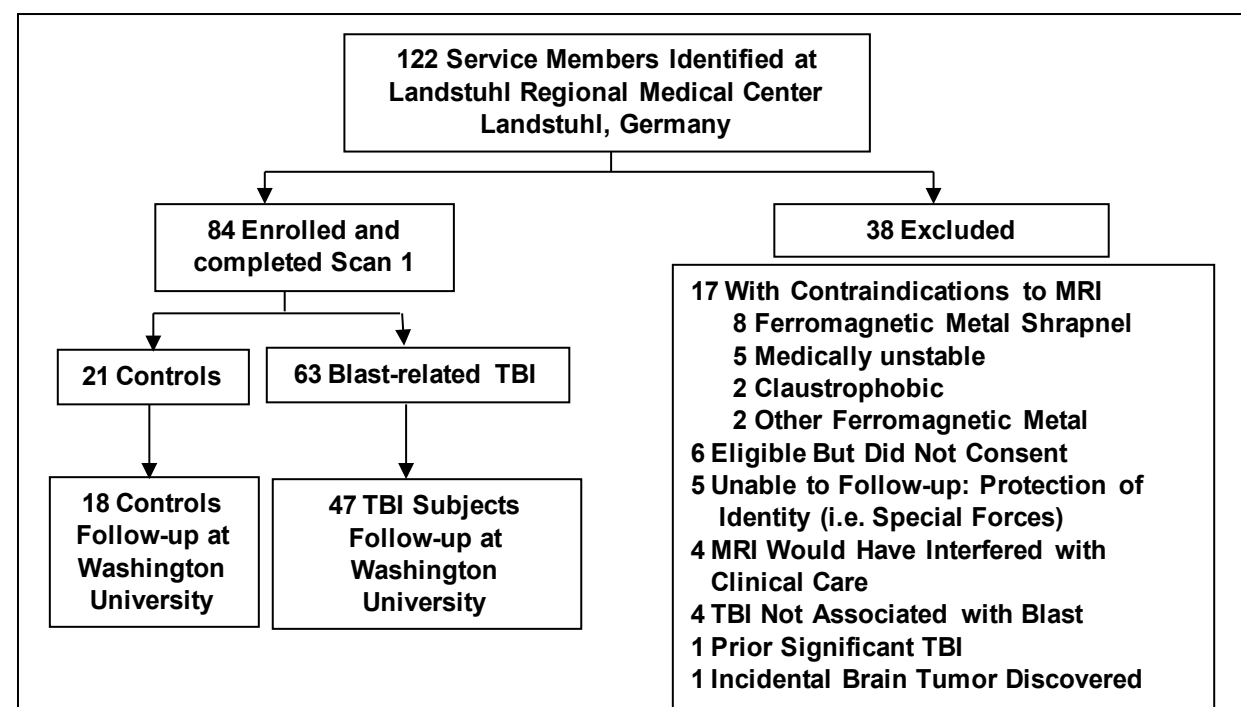
Blast-related TBI Subjects: A cross-sectional cohort of 63 active-duty US military personnel who presented to **Landstuhl Regional Medical Center (LRMC)** with signs and/or symptoms of blast-related TBI from 2008-2009. All provided written informed consent.

Controls: 21 US military personnel presenting to LRMC with other illnesses or injuries and a history of blast exposure but no TBI based on clinical criteria.

Scans: Subjects were scanned at LRMC in the first 90 days after injury on a 1.5T Siemens Avanto MRI scanner. DTI protocol comprised two acquisitions at 2.5 x 2.5 x 2.5 mm resolution with 23 diffusion directions. Resting state **functional connectivity MRI (fcMRI)** protocol consisted of three 7 minute blood oxygen level dependent (BOLD) runs with 1 whole brain acquisition every 2 seconds and 4 x 4 x 4 mm spatial resolution.

Clinical Assessments: Blinded raters performed **Clinician Administered PTSD Scale (CAPS)** ratings on 47 TBI subjects and 18 controls who came to follow-up 6-12 months after injury.

Fig. 1: Enrollment and exclusion characteristics of the study participants. (Mac Donald et al NEJM 2011)



Results

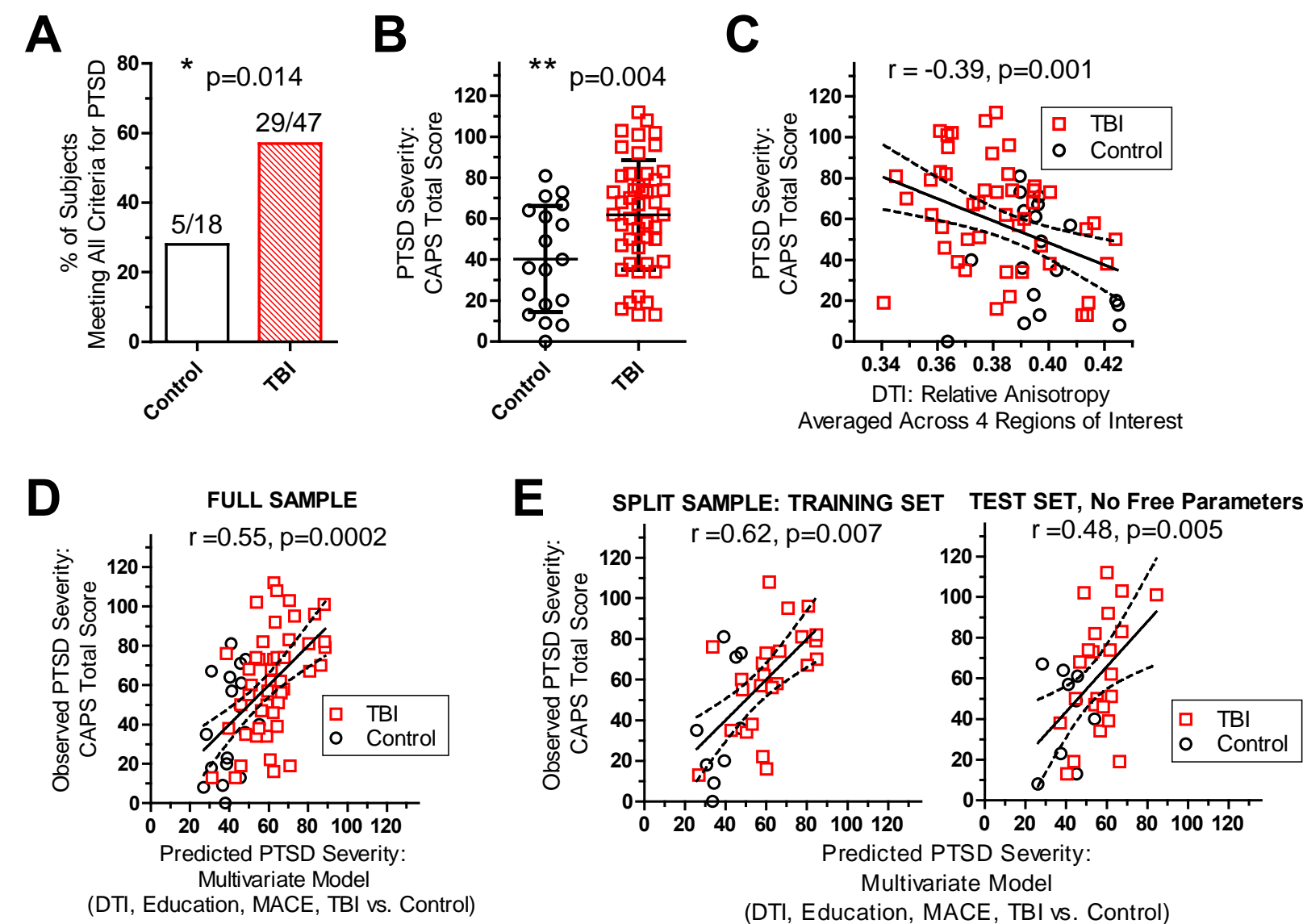


Fig. 2 Post-traumatic Stress Disorder (PTSD): DTI and clinical predictors
A. Subjects meeting all DSM-IV criteria for PTSD. **B.** Severity of PTSD.
C. Initial scan DTI predictors of PTSD severity. 4 regions of interest: right orbitofrontal, right cingulum, right & left posterior limb of the internal capsule.
D. Multivariate predictive model of PTSD severity based on early DTI and clinical data. ($\beta_{DTI} = -0.28$, $p=0.016$). **E.** Split sample validation of the multivariate model.

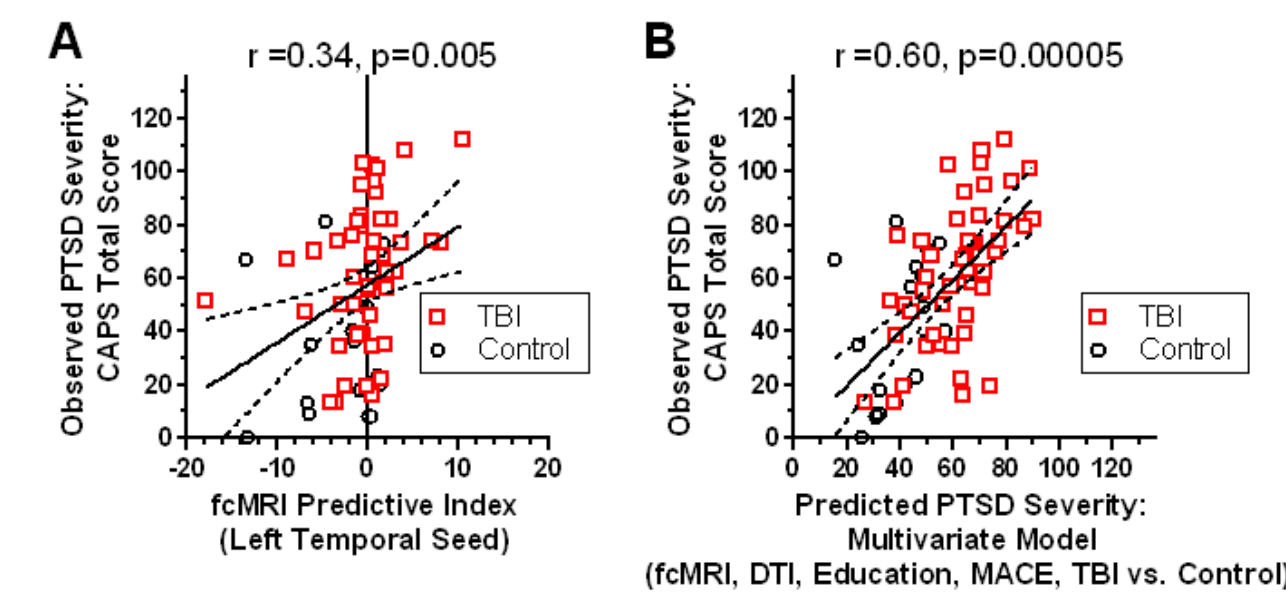
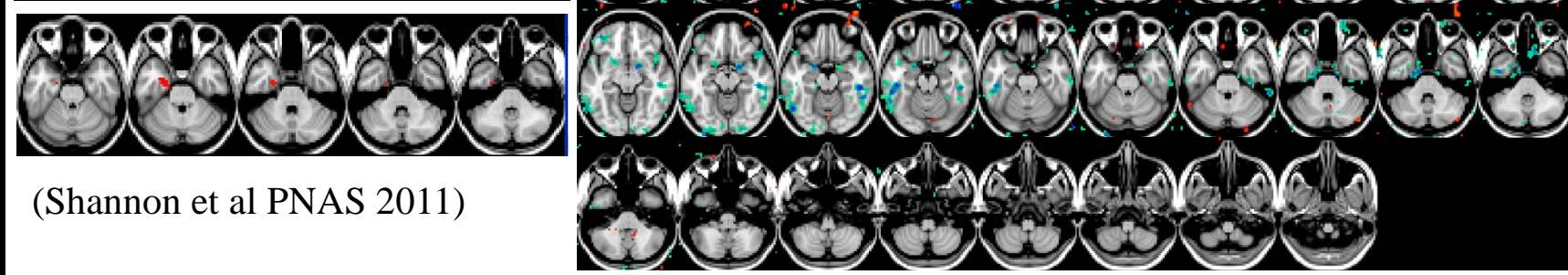


Fig. 3 PTSD: fcMRI predictors
A. Early fcMRI predictor based on correlations of left temporal cortex with bilateral frontal cortex.
B. Multivariate model as in Fig 2D with added fcMRI predictive index

Fig. 4 fcMRI predictors
Below. Left temporal cortex seed region. **Right:** Bilateral frontal cortex regions. Darker blue indicates regions where impaired functional connectivity with left temporal cortex most strongly predicts PTSD severity.



(Shannon et al PNAS 2011)

Results

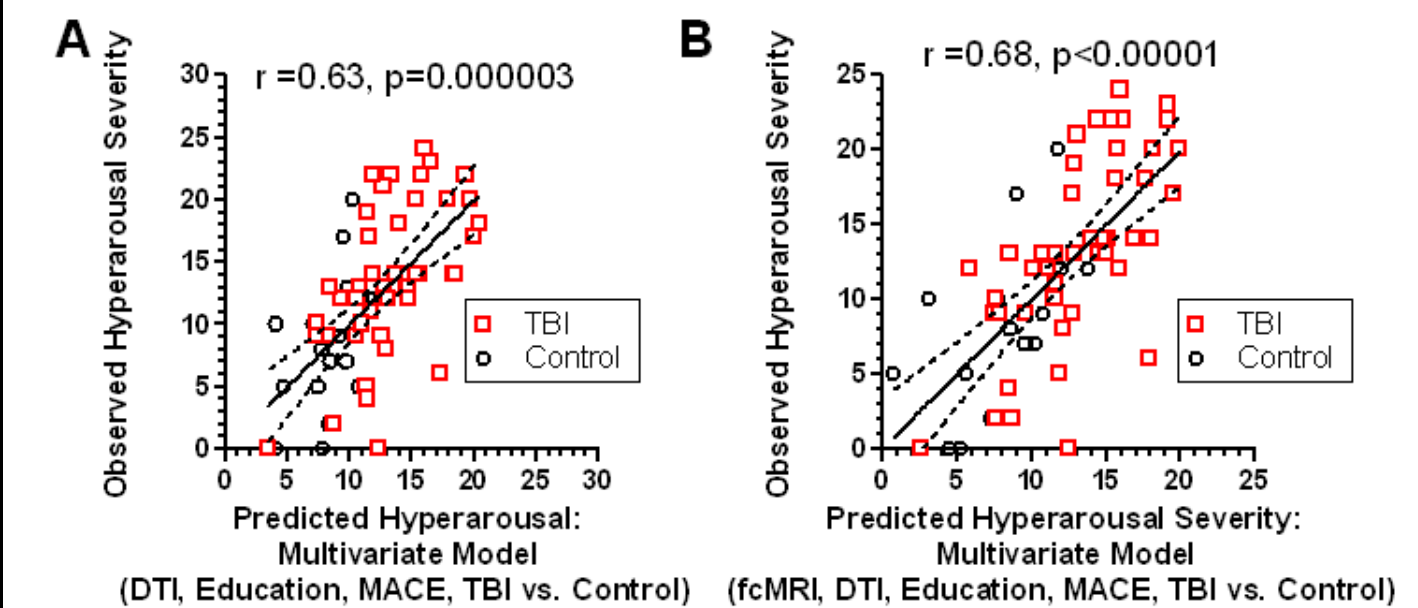


Fig. 5: Hyperarousal component of PTSD: Advanced MRI and clinical predictors.
A. Multivariate predictive model of hyperarousal severity, based on early DTI and clinical data ($\beta_{DTI} = -0.41$, $p=0.00026$). DTI regions of interest included 5 regions: right orbitofrontal, left and right posterior limbs of the internal capsule, bilateral uncinate fasciculus, and left anterior limb of the internal capsule. **B.** Multivariate model as in Fig. 5A with added fcMRI predictive index. ($\beta_{DTI} = -0.43$, $p=0.000074$), ($\beta_{fcMRI} = 0.29$, $p=0.005$).

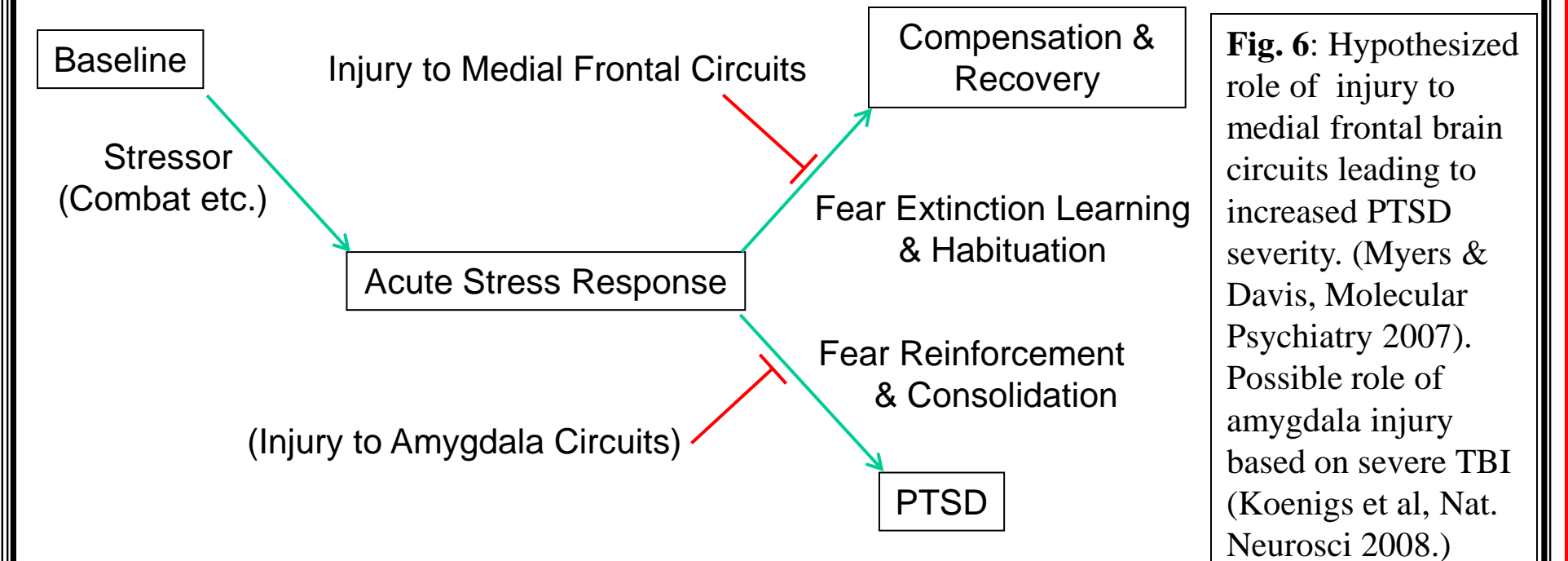


Fig. 6: Hypothesized role of injury to medial frontal brain circuits leading to increased PTSD severity. (Myers & Davis, Molecular Psychiatry 2007). Possible role of amygdala injury based on severe TBI (Koenigs et al, Nat. Neurosci 2008.)

Conclusions and Future Directions

- PTSD was more common and more severe in TBI subjects than controls.
- DTI and fcMRI abnormalities contributed to early prediction of PTSD severity.
- Hyperarousal could be more strongly predicted than overall PTSD severity. *There may be multiple components of PTSD with separable biological substrates.*
- Brain regions with abnormalities that predicted PTSD severity were consistent with known emotional regulation circuitry in animals. *Failure to extinguish fearful memories due to medial frontal network dysfunction may be involved.*
- Prediction of PTSD severity was moderate; a great deal of the variance in PTSD severity was not explained by any of the imaging or clinical factors assessed. *Genetic factors, early life experiences, combat intensity and other comorbid conditions may play important roles but were not addressed in this study.*
- Validation in an independent cohort of US military personnel is ongoing.

Acknowledgements

Funding: CDMRP W81XWH-08-2-006 Correspondence: brodyd@neuro.wustl.edu

Advanced MRI Detection of Blast-Related Traumatic Brain Injury in US Military Personnel

Christine L. Mac Donald PhD¹, Ann M. Johnson¹, Dana Cooper¹, Elliot C. Nelson MD¹, Nicole J. Werner PhD¹, Joshua S. Shimony MD PhD¹, Abraham Z. Snyder MD PhD¹, Marcus E. Raichle MD¹, LTC John R. Witherow MD², LTC Raymond Fang MD², COL Stephen F. Flaherty MD^{2, 3} and David L. Brody MD PhD¹

1. Washington University School of Medicine, St Louis, Missouri
2. Landstuhl Regional Medical Center, Landstuhl, Germany
3. Walter Reed Army Medical Center, Washington DC

ABSTRACT

Background: Blast-related traumatic brain injury (TBI) has been common in the wars in Iraq and Afghanistan, but fundamental questions about these injuries remain unanswered.

Methods: We tested the hypothesis that blast-related TBI causes traumatic axonal injury using Diffusion Tensor Imaging (DTI), an advanced MRI method sensitive to axonal injury. Participants were 63 US military personnel evacuated to Landstuhl Regional Medical Center, clinically diagnosed with mild uncomplicated TBI, and scanned 1-90 days after injury. All had primary blast exposure plus another blast-related mechanism of injury (e.g. struck by a blunt object, fall, motor vehicle crash). Controls were 21 similar personnel with blast exposure and other injuries but no clinical diagnosis of TBI.

Results: DTI revealed abnormalities consistent with traumatic axonal injury in many TBI subjects. None had detectable intracranial injury on CT. DTI was markedly abnormal in the middle cerebellar peduncles ($p < 0.001$), cingulum bundles ($p = 0.002$), and right orbitofrontal white matter ($p = 0.007$). In 18/63 individual TBI subjects, there were significantly more DTI abnormalities than expected by chance ($p < 0.001$). Follow-up scans performed 6-12 months later in 47 TBI subjects demonstrated persistent DTI abnormalities consistent with evolving injuries.

Conclusions: DTI findings in US military personnel support the hypothesis that blast-related mild TBI can involve axonal injury. However, the contributions of primary blast exposure vs. other types of injury could not be resolved directly, as no subject had isolated primary blast injury. Furthermore, many TBI subjects did not have DTI abnormalities, and TBI remains a clinical diagnosis.

MRI Evaluation of Blast-Related TBI

David L. Brody, MD PhD

Washington University in St Louis

Collaborators Christine Mac Donald¹, Ann Johnson¹, Dana Cooper¹, Elliot Nelson¹, Nicole Werner¹, Josh Shimony¹, Abraham Z. Snyder¹, Marcus Raichle¹, John Witherow², Raymond Fang², & Stephen Flaherty^{2,3}

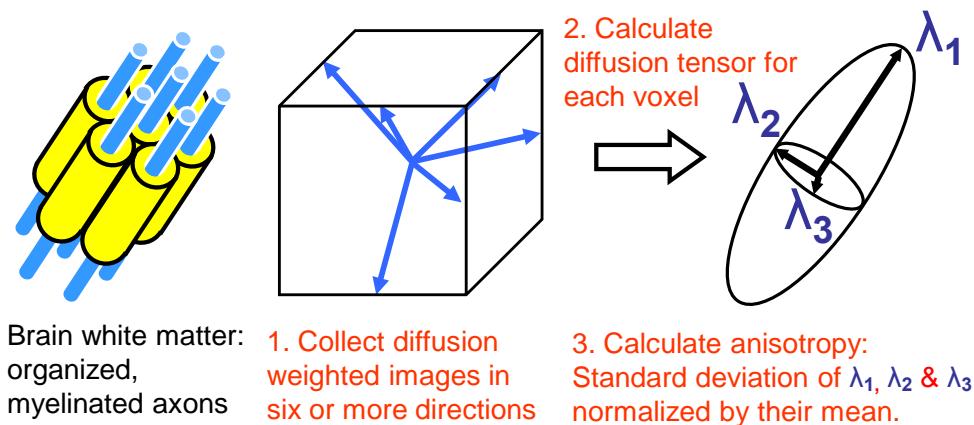
¹Washington University, St Louis MO, ²Landstuhl Regional Medical Center, Landstuhl, Germany, ³Walter Reed Army Medical Center, Washington DC

Overview: The goal of this presentation is to demonstrate the use of several MRI methods in Blast-related traumatic brain injury. The focus will be on both clinical and logistical aspects of our experiences.

Background:

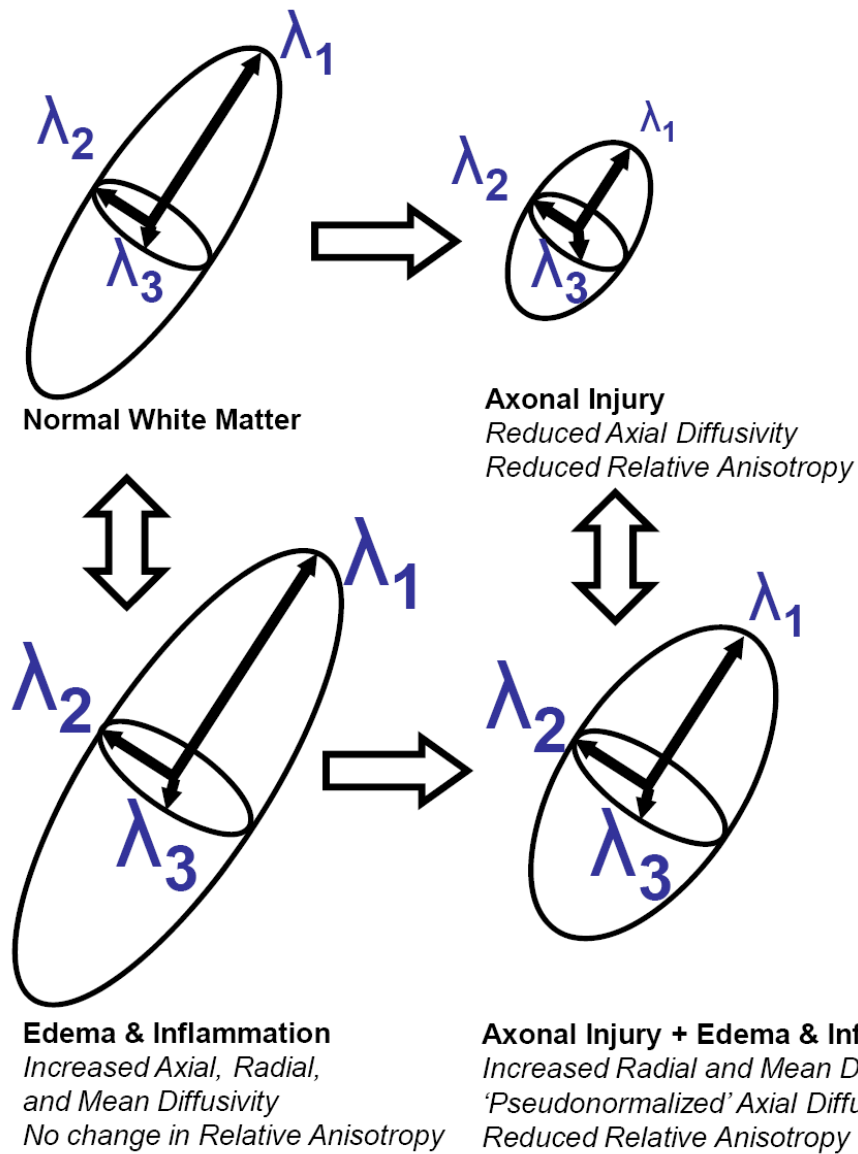
- In the current wars in Iraq and Afghanistan, as many as 320,000 US military personnel have sustained blast-related traumatic brain injury (TBI).
- Most of these injuries are categorized as uncomplicated “mild” or “concussive” TBI based on clinical criteria and the absence of intracranial pathology on CT or conventional MRI
- However, little is known about these “mild” injuries and the relationship between TBI and outcomes remains controversial.
- Diffusion Tensor Imaging (DTI) is an advanced MRI method that has been shown to be more sensitive to traumatic axonal injury than conventional MRI.

Diffusion Tensor Imaging



- In civilian TBI, DTI has shown many abnormalities not apparent on CT or conventional MRI.

- However, no DTI studies of acute blast-related TBI have been published, and the role of axonal injury in blast-related TBI is not known.



- Computer simulations of the effects of blast-induced pressure waves on the brain suggest that the orbitofrontal regions and the posterior fossa (cerebellum and brainstem) may sustain intense stresses independently of the subject's head orientation relative to the blast.

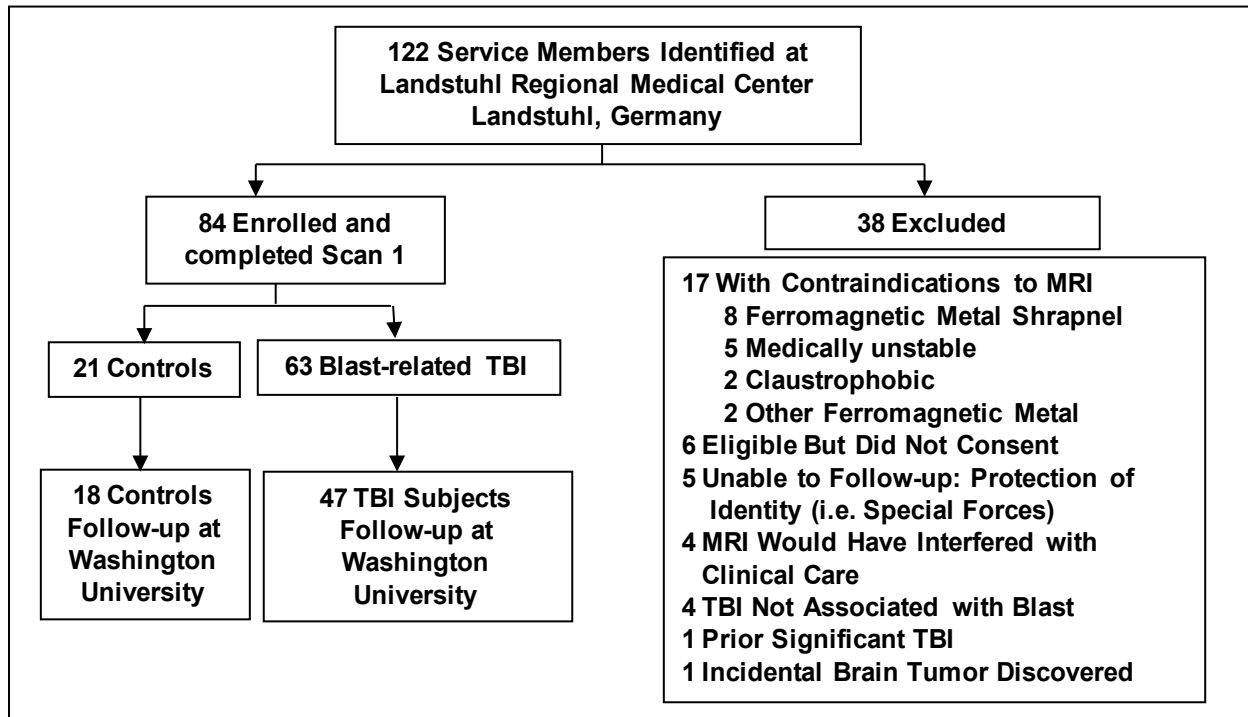
Methods:

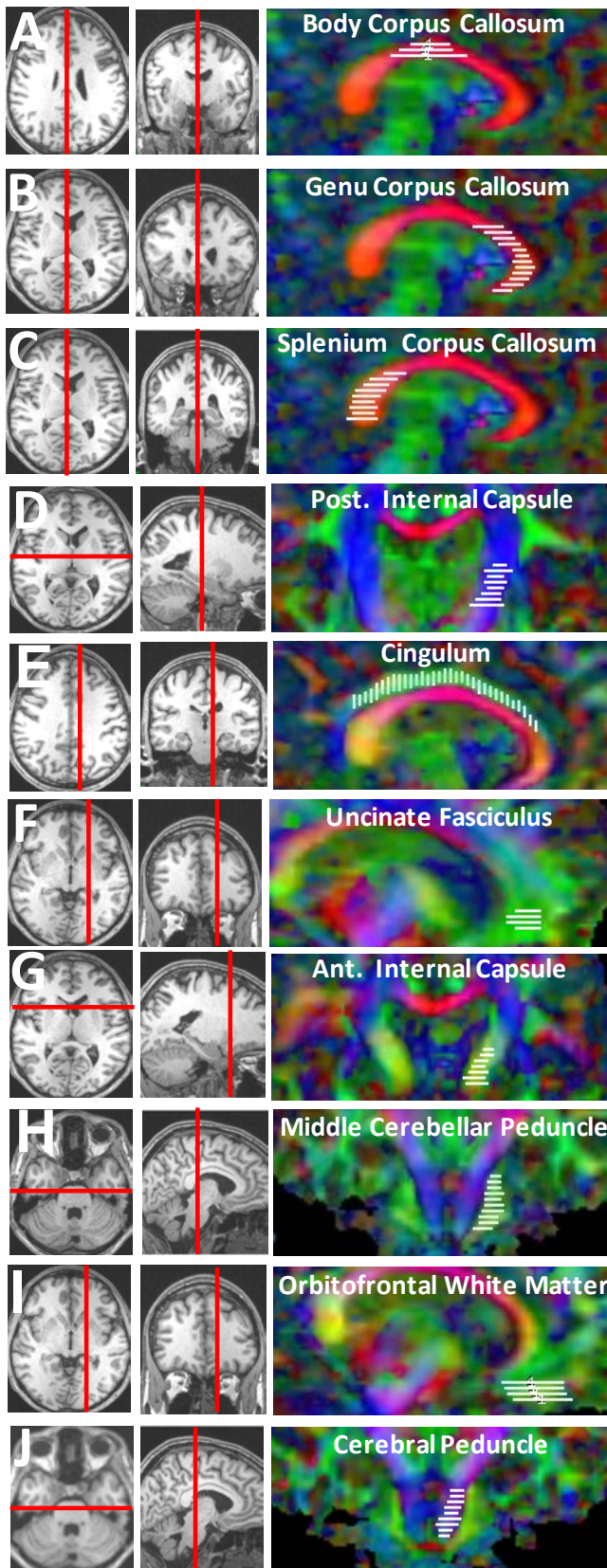
Blast-related TBI Subjects: A cross-sectional cohort of 63 active-duty US military personnel who presented to Landstuhl Regional Medical Center (LRMC) with signs and/or symptoms of blast-related TBI from 2008-2009. All provided written informed consent. Subjects were scanned 1-90 days after injury. All had blast exposure plus another mechanism of injury (e.g. fall, motor vehicle crash, struck by a blunt object).

Controls : 21 US military personnel presenting to LRMC with blast exposure and other injuries but no TBI based on clinical criteria.

Scans: Subjects were scanned at LRMC in the first 90 days after injury on a 1.5T Siemens Avanto MRI scanner. DTI protocol comprised two acquisitions at 2.5 x 2.5 x 2.5 mm resolution with 23 diffusion directions. Scans were repeated 6-12 months later at Washington University.

Safety and Data Monitoring: Subjects were screened using a hand-held metal detector for objects such as shrapnel that would contraindicate MRI scanning. All x-rays and CT scans acquired for clinical purposes were also reviewed for metallic objects. A standard clinical checklist for MRI contraindications was filled out by each subject prior to each scan. The subjects tolerated MRI scans well with no safety concerns arising.





3-D Region of Interest Analysis Brain regions of interest for DTI analysis. Left and center panels: conventional (T1 weighted) MRI for anatomical localization. Right panels: DTI relative anisotropy maps. White bars indicate locations and orientation of slices analyzed for multi-slice regions of interest. **A.** Body of the corpus callosum DTI on a sagittal section, running right-left between the lateral ventricles. **B.** Genu of the corpus callosum DTI on a sagittal section, running right-left anterior to the lateral ventricles. **C.** Splenium of the corpus callosum DTI on a sagittal section, running right-left posterior to the lateral ventricles. **D.** Posterior limb of the internal capsule DTI on a coronal section, running dorsal-ventral and right-left between the putamen and thalamus. **E.** Cingulum bundle DTI on a sagittal section, running anterior-posterior dorsal to the corpus callosum. **F.** Uncinate fasciculus DTI on a sagittal section, running anterior-posterior in the anterior frontal lobe. **G.** Anterior limb of the internal capsule DTI on a coronal section, running anterior-posterior and right-left between the caudate and putamen. **H.** Middle cerebellar peduncle DTI on a coronal section, running anterior-posterior in the dorsal brainstem and cerebellum. **I.** Orbitofrontal white matter DTI on a sagittal section, running anterior-posterior in the ventral frontal lobe, ventral and posterior to the uncinate fasciculus. **J.** Cerebral peduncle DTI on a coronal section, running dorsal-ventral in the midbrain and pons, medial to the middle cerebellar peduncle.

Results: DTI revealed abnormalities consistent with traumatic axonal injury in many TBI subjects. None had detectible intracranial injury on CT. DTI was markedly abnormal in the middle cerebellar peduncles and orbitofrontal white matter— regions predicted to be especially vulnerable to blast but not typically affected in mild civilian TBI. Several regions frequently affected in civilian TBI were also abnormal. In 18/63 individual TBI subjects, there were significantly more DTI abnormalities than expected by chance ($p=0.0001$). Follow-up scans performed 6-12 months later in 47 TBI subjects demonstrated persistent DTI abnormalities consistent with evolving injuries.

Conclusions: DTI findings in US military personnel support the hypothesis that blast-related mild TBI can involve axonal injury. The distribution of affected brain regions suggested an admixture of blast effects and other mechanisms. However, many TBI subjects did not have DTI abnormalities, and TBI remains a clinical diagnosis.

Funding: CDMRP W81XWH-08-2-006

Correspondence: brodyd@neuro.wustl.edu